Cellular determinants of Herpes simplex virus 1 (HSV-1) invasion in human skin:

Unravelling conditions that allow HSV-1 to reach its receptor and internalize

Inaugural-Dissertation

zur

Erlangung des Doktorgrades

der Mathematisch-Naturwissenschaftlichen Fakultät

der Universität zu Köln

vorgelegt von

Nydia Camille De La Cruz

aus Parañaque, Metro Manila Luzon

Republika ng Pilipinas

Veröffentlichung in **Köln, 2023**

Berichterstatter (Gutachter):	Prof. Dr. Dagmar Mörsdorf
	Prof. Dr. Niels Gehring
Prüfungsvorsitzender:	Prof. Dr. Siegfried Roth
Tag der mündlichen Prüfung:	06 März 2023

Abstract

Herpes simplex virus 1 (HSV-1), which is among the most prevalent of human pathogens, targets mucosa, skin or cornea. The overall aim of this thesis was to explore how HSV-1 is able to invade the highly-protected tissue structure of the human skin, access its cellular receptors on target skin cells for entry, and initiate infection in the epithelium. On the cellular level, the focus was on elucidating the impact of cellular entry mechanisms in successful infection. Previous studies have demonstrated that HSV-1 exploits dual modes of uptake—direct fusion at the plasma membrane and endocytic internalization—to gain entry in keratinocytes, however, attributing the contribution of either pathway is still open. Here, infection of human keratinocytes at low temperature (7°C) was used as a tool to selectively block energy-requiring endocytic processes while permitting plasma membrane fusion. Although the uptake of the endocytic markers was inhibited at low temperature, ultrastructural analyses revealed the presence of free capsids in the cytoplasm as well as enveloped virus particles in vesicles after infection at 7°C. In addition to virus particles undergoing direct fusion at the plasma membrane, characterization of virus-containing vesicles revealed the release of capsids from vesicles by fusion with vesicle membranes. These results strengthen the role of endocytic internalization in successful infection.

At the tissue level, the emphasis was on elucidating how HSV-1 overcomes the highly protective barrier function of the human skin to engage a cellular receptor for entry. To gain insights on the early entry events during HSV-1 invasion, *ex vivo* infection studies using human skin explants were implemented. As expected, the barrier function of full-thickness skin prevented HSV-1 invasion from the apical skin surface. Once the epidermis was separated from the underlying dermis, HSV-1 efficiently infected basal keratinocytes and later gained access to the suprabasal layers. Viral replication inhibitor experiments as well as uptake of labelled latex beads (500 nm) demonstrated the role of virus-induced tissue damage in enabling HSV-1 access to all epidermal layers. In contrast, only single infected cells were detected in the most apical part of the papillary dermis demonstrating that the extracellular matrix acts as a barrier against HSV-1 invasion. Strikingly, while partly open skin lesions of wounded full-thickness skin allowed the enhanced uptake of latex beads, nearly no infected cells were identified at the sites of wounds. Intriguingly, when wounds reached through the dermis, HSV-1 infected epidermal keratinocytes via the damaged dermal layer. To further elucidate the impact of epidermal barrier function in restricting HSV-1 invasion, pathological skin conditions characterized by impaired epidermal barriers were explored. As *ex vivo* infection of lesional atopic

dermatitis (AD) demonstrated viral penetration from the skin surface, Th2 cytokines interleukin (IL)-4 and IL-13 were employed to induce AD-like phenotypes in skin without pre-existing barrier defects. Indeed, infected cells in the epidermis of IL-stimulated skin were found indicating that Th2 cytokine-driven inflammatory responses induced modifications that facilitate HSV-1 invasion via the skin surface.

Overcoming epidermal barriers must be accompanied by viral engagement of a cellular receptor to initiate infection in the skin. Thus, the distribution of nectin-1, the major receptor on keratinocytes was investigated. To dissect how barrier formation correlated with receptor accessibility, a human epidermal equivalent (HEE) based on primary human keratinocytes was adopted. In undifferentiated keratinocytes, nectin-1 is readily accessible at apical and basolateral surfaces correlating with a high susceptibility to HSV-1. In fully differentiated HEEs, nectin-1 is expressed at the lateral membranes of most epidermal layers although accessibility to the receptor is restricted by functional tight junctions (TJs) in the upper granular layer thus correlating with no infection. Intriguingly, while IL-4/IL-13 stimulation of HEEs resulted in redistributed nectin-1 and TJ components, the IL-induced modifications had very minor effects on facilitated HSV-1 invasion in fully differentiated epidermal equivalents in contrast to human skin explants where IL-stimulation allowed HSV-1 invasion. Moreover, redistributed TJ components in IL-4/IL-13-stimulated skin and AD skin, both of which promote HSV-1 invasion, support the role of TJ barrier defects in the facilitated access of HSV-1 to nectin-1.

Zusammenfassung

Herpes simplex Virus 1 (HSV-1), das zu den häufigsten Humanpathogenen zählt, dringt über die Mukosa, Haut und Kornea in seinen Wirt ein. Das Ziel dieser Dissertation war zu verstehen, wie HSV-1 in die schützende Gewebestruktur der humanen Haut eindringen kann, um seine Rezeptoren auf den Zielzellen zu erreichen und die Infektion im Epithel zu initiieren. Auf zellulärer Ebene lag der Fokus auf dem Einfluss zellulärer Eintrittsmechanismen, die für eine produktive Infektion verantwortlich sind. Bisherige Studien zeigten, dass HSV-1 zwei Aufnahmemodi nutzt – die direkte Fusion mit der Plasmamembran und die endozytische Internalisierung –, um in Keratinozyten einzudringen. Welcher Aufnahmeweg zu einer produktiven Infektion beiträgt, blieb bisher offen. Hier wurden Infektionsstudien in menschlichen Keratinozyten bei niedriger Temperatur (7 °C) durchgeführt, um energieverbrauchende endozytotische Prozesse selektiv zu blockieren und gleichzeitig die Plasmamembranfusion zu ermöglichen. Obwohl die endozytotische Aufnahme von Markermolekülen bei niedrigen Temperaturen gehemmt wurde, zeigten Ultrastrukturanalysen nach der Infektion bei 7 °C sowohl freie Kapside im Zytoplasma als auch umhüllte Viruspartikel in Vesikeln. Neben der Fusion mit der Plasmamembran, ergab die Charakterisierung virushaltiger Vesikel, dass die Hülle der Viruspartikel auch mit Vesikelmembranen fusionieren konnte. Diese Ergebnisse verdeutlichen, dass die endozytische Internalisierung eine Rolle bei einer erfolgreichen HSV-1-Infektion spielt.

Auf der Ebene des Gewebes wurde untersucht, wie HSV-1 die schützende Barrierefunktion der menschlichen Haut überwinden kann, um seine zellulären Rezeptoren zu erreichen. Dazu wurden Ex-vivo-Infektionsstudien mit humanen Hautexplantaten durchgeführt, um Einblick in die frühen Infektionsereignisse zu gewinnen. Wie erwartet, verhinderte die Barrierefunktion intakter Haut die Invasion von HSV-1 über die apikale Hautoberfläche. Sobald die Epidermis von der darunter liegenden Dermis abgetrennt wurde, infizierte HSV-1 effizient basale Keratinozyten und erreichte auch suprabasale Schichten. Experimente mit viralen Replikationsinhibitoren sowie die Aufnahme markierter Latexkugeln (500 nm) verdeutlichen, dass virus-induzierte Gewebeschäden HSV-1 den Zugang zu allen Epidermisschichten ermöglichte. Im Gegensatz dazu wurden nach Infektion der Dermis nur einzelne infizierte Zellen in der apikalen papillären Dermis nachgewiesen, was zeigt, dass die extrazelluläre Matrix eine Barriere für die HSV-1-Invasion darstellt. Interessanterweise, wurden nach Verwundung der Hautproben Latexkugeln über die Hautläsionen aufgenommen, es waren jedoch kaum infizierte Zellen nachweisbar. Wenn allerdings die Verwundungen auch die Dermis verletzten, konnte HSV-1 die epidermalen Keratinozyten über die Hautläsionen der Dermis erreichen.

Um die Bedeutung der epidermalen Barrierefunktion auf die HSV-1-Invasion näher zu charakterisieren, wurde ein pathologisches Hautmodell untersucht, das durch defekte epidermale Barrieren gekennzeichnet ist. So führte die ex-vivo-Infektion von läsionalen Hautproben atopischer Dermatitis (AD) Patienten zu einer viralen Penetration über die Hautoberfläche. Zur weiteren Charakterisierung wurden AD-ähnliche Phänotypen induziert, indem Hautproben ohne Barrieredefekte mit den Th2-Zytokinen Interleukin (IL)-4 und IL-13 behandelt wurden. Tatsächlich waren infizierte Zellen in der Epidermis von IL-stimulierter Haut nachweisbar, was darauf hindeutet, dass Th2-Zytokin-gesteuerte Entzündungsreaktionen Modifikationen induzierten, die eine HSV-1-Invasion über die Hautoberfläche ermöglichten.

Die Überwindung epidermaler Barrieren bedeutet, dass das Virus seinen zellulären Rezeptor erreichen kann, um eine Infektion auszulösen. Um zu analysieren, wie die Bildung der Barrieren mit der Erreichbarkeit des Rezeptors korreliert, wurde die Lokalisierung des Hauptrezeptors auf Keratinozyten, Nektin-1, untersucht. Dazu wurde ein humanes epidermales Äquivalent etabliert, das auf primären Keratinozyten basierte. In undifferenzierten Keratinozyten lokalisierte Nektin-1 an apikalen und basolateralen Oberflächen, was mit einer hohen Infizierbarkeit korrelierte. In ausdifferenzierten epidermalen Äquivalenten wurde Nektin-1 an den lateralen Membranen in den meisten Epidermisschichten nachgewiesen. Funktionelle tight junctions (TJs) in der obersten granulären Schicht können allerdings den viralen Zugang zu Nektin-1 verhindern, so dass keine Infektion zustande kommt. Interessanterweise führte die IL-4/IL-13-Stimulation von ausdifferenzierten epidermalen Äquivalenten zwar zu einer Umverteilung von Nektin-1- und TJ-Komponenten, die IL-induzierten Modifikationen hatten jedoch nur eine sehr geringe Auswirkung auf eine erleichterte Infizierbarkeit durch HSV-1. Dieser Befund war im Gegensatz zu humanen Hautexplantaten, wo die IL-Stimulation eine HSV-1 Invasion ermöglichte. Die Umverteilung der TJ-Komponenten in IL-4/IL-13-stimulierter und atopischer Dermatitis Haut, die mit einer HSV-1-Invasion korrelierte, lässt allerdings die Schlussfolgerung zu, dass defekte TJ-Barrieren den erleichterten Zugang von HSV-1 zu Nektin-1 ermöglichen können.

Table of Contents

Figures

Introduction

1.1 Herpes Simplex Virus 1 (HSV-1)

Herpes simplex virus (HSV) is a large, double-stranded DNA virus belonging to the *Alphaherpesvirinae* subfamily of the *Herpesviridae* family. HSV is categorized into two serotypes identified as HSV-1 and HSV-2 and are among the most prevalent of human pathogens although HSV-1, which in most cases rapidly acquired during early childhood, is more widespread than HSV-2 infections (Smith and Robinson, 2002). During primary infection, the virus replicates in the human host's epithelial cells and, via retrograde transport, establishes lifelong, latent infection in sensory neurons (Roizman and Whitley, 2013). Upon a variety of external stimuli, such as ultraviolet (UV) light exposure, the virus is reactivated, replicates in the neurons and, via anterograde transport, initiates a secondary infection at or near the site of initial entry. Clinical manifestations are variable but are often only mild mucocutaneous infections. However, in extreme cases this can lead to more severe complications such as encephalitis, keratitis, corneal blindness, and disseminated multi-organ infections especially in immunocompromised hosts (Brady and Bernstein, 2004; Fatahzadeh and Schwartz, 2007). While HSV-1 is mostly associated with orofacial infections (*Herpes labialis*) transmitted through oral-to-oral contact and HSV-2 with genital infections (*Herpes genitalis*) transmitted sexually, HSV infections can occur at any site of the body especially after the virus comes into contact with mucosal surfaces or skin abrasions (Whitley et al., 1998). While *in vivo* HSV infections mostly target neurons and epithelial cells as preferred cell types, most mammalian cell lines are susceptible to HSV *in vitro*.

The structure of HSV-1 is divided into four distinct morphological units consisting of (1) the linear, double-stranded DNA (approximately 152 kbp in length encoding for approximately 85 viral proteins) enclosed in (2) the capsid, an icosahedral shell composed of four structural proteins, mainly the major capsid protein VP5 (Heming et al., 2017), (3) a surrounding proteinaceous layer termed the tegument which is enclosed by (4) a lipid bilayer envelope containing surface proteins (Fig. 1) (Roizman and Sears, 1993; Pilling et al., 1999; Grünewald et al., 2003). There are at least 15 surface proteins encoded by HSV-1. Of these, 12 are glycosylated (denoted as glycoproteins) of which only four—glycoprotein B (gB), gD, gH and

gL—are deemed essential for successful cellular entry (Karasneh and Shukla, 2011; Hilterbrand and Heldwein, 2019).

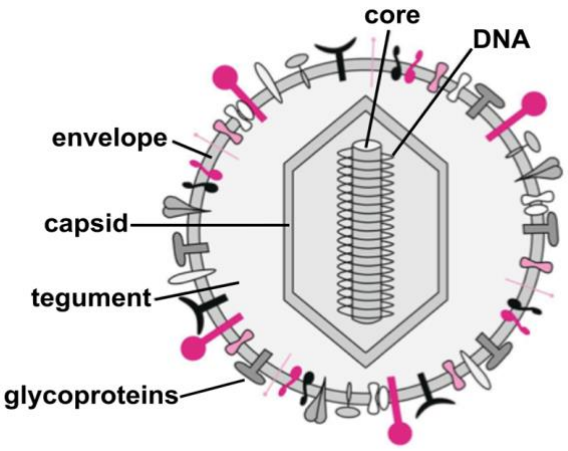

Figure 1. Schematic representing the structure of HSV-1.
The major structural components of HSV-1 include a core containing the linear, double-stranded DNA enclosed in an icosahedral capsid (161 capsomeres made up of 150 hexons and 11 pentons). The capsid is surrounded by a tegument layer of proteins and further enclosed by the envelope, a lipid bilayer containing glycoproteins. As a relatively large virus, HSV-1 measures between 150 to 200 nm in diameter (modified from Modrow et al., 1997).

1.2 Cellular entry of HSV-1

Cellular entry of HSV-1 into its target cells is a multi-step, regulated process which involves the interaction between factors of the host cellular membrane and viral glycoproteins. In brief, the entry process can be separated into distinct steps which include cellular attachment, binding to a specific cellular receptor, an optional and/or cell type-specific vesicle uptake mechanism and, finally, fusion with a cellular membrane (Krummenacher et al., 2013; Connolly et al., 2021) (Fig 2). Of these, receptor-binding and fusion with a cellular membrane are absolutely necessary for viral capsid release, which signifies successful HSV-1 cellular entry, and the subsequent transport and delivery of the viral genome to the host cell nucleus for the expression of viral genes.

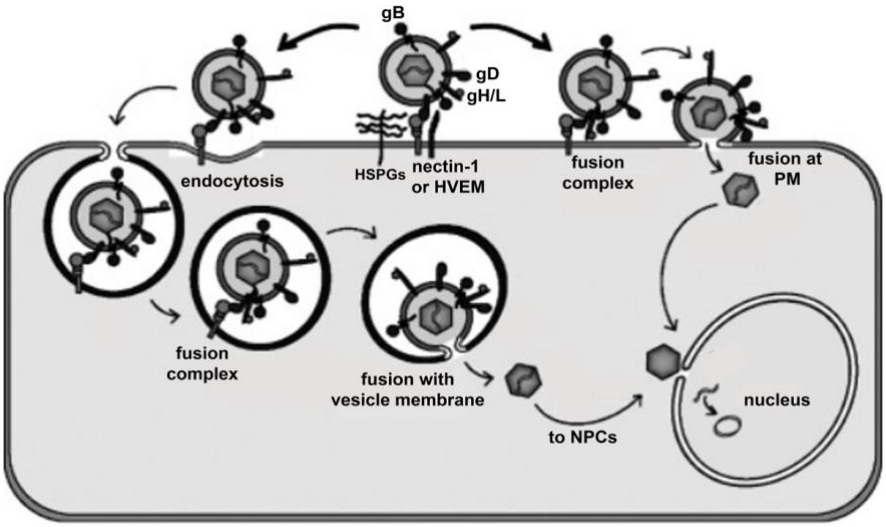

Figure 2. Schematic illustrating a brief overview of HSV-1 cellular entry

After initial attachment to heparan sulfate proteoglycans (HSPGs), binding of viral gD to a cellular receptor (nectin-1 or HVEM) triggers the formation of a fusion complex (gD along with gB and gH/L) upon which the virus will either undergo (1) fusion directly at the cellular plasma membrane (PM) or (2) endocytosis followed by fusion with the vesicle membrane. The viral nucleocapsid and tegument proteins are then released into the host cell cytoplasm. The capsid is delivered to the nuclear pore complex (NPC) for the eventual release of the viral genome into the host cell nucleoplasm (modified from Campadelli-Fiume and Menotti, 2007).

1.2.1 Cellular attachment and binding

The binding of viral gD to a specific cellular receptor is required for successful HSV-1 cellular entry. Prior to binding, however, HSV-1 may contact target cells by utilizing heparan sulfate proteoglycans (HSPGs) for initial attachment. This attachment, mediated by gC or, in the absence of this glycoprotein, gB can promote viral surfing along cellular filopodia which express higher levels of HSPGs (Herold et al., 1994; WuDunn and Spear, 1989; Oh et al., 2010). Since filipodia have been shown not to harbor gD receptors, surfing assists the virus in reaching the cellular body where gD can bind to one of its cellular receptors (Oh et al., 2010). gD binds with high-affinity and subsequently triggers conformational changes that thereby recruit gB and the gH/L homodimer to form a fusion complex with the cell to initiate the internalization of the virus (Eisenberg et al., 2012).

While initial attachment to HSPGs is not required, binding of gD to one of its three cellular receptors: nectin-1, Herpesvirus entry mediator (HVEM), or 3-*O*-sulfated heparan sulfate is absolutely essential for fusion with a cellular membrane to occur (Eisenberg et al., 2012). The

extent of use of each receptor varies depending on the target cell-type. Moreover, the receptors are structurally unrelated and do not act as co-receptors to bind gD during cellular entry. Using receptor knockout (KO) mouse models, we previously found that nectin-1 serves as the major receptor in the epidermis with a limited capability of HVEM as a functional replacement. Moreover, studies with nectin-1/HVEM double KO murine fibroblasts suggest a minor role for 3-*O*-sulfated heparan sulfate as an alternative receptor although with limited efficiency (Petermann et al., 2015a; 2015b). Thus, among these three receptors, nectin-1 is of greatest interest in our current studies.

1.2.1.1 Nectin-1 as a major HSV-1 receptor

Nectins (nectin 1-4) are a family of calcium (Ca^{2+})-independent Immunoglobulin (Ig)-like cell-cell adhesion molecules (CAMs) who homo- and heterophilically interact via their extracellular domains to form adhesive associations between neighboring cells (reviewed in Samanta and Almo, 2015). Aside from cell adhesion, they are implicated in other cellular regulatory processes including cell motility, proliferation, differentiation as well as viral entry (reviewed in Takai et al., 2008). Originally isolated as poliovirus receptor-related (PRR) proteins, nectin-1 and nectin-2 were previously known as PRR-1 and PRR-2, respectively (Eberlé et al., 1995; Morrison and Racaniello, 1992). As they did not indeed act as poliovirus receptors, they were renamed as nectins from the Latin word *necto* meaning “to connect” (Takahashi et al., 1999). Aside from their roles as CAMs, they are also implicated in serving as receptors for HSV. Nectin-1 (also Herpesvirus entry mediator C, HveC) is widely regarded as the main receptor in neurons, keratinocytes, and epithelial cells, the natural targets of HSV-1 (Geraghty et al., 1998; Krummenacher et al., 2004, Simpson et al., 2005; Huber et al., 2001). Poorly expressed in neuronal cells and keratinocytes, nectin-2 (also Herpesvirus entry mediator B, HveB) has also been reported to serve as an HSV-1 receptor but with very limited efficiency, only binding gD in some mutant strains of HSV-1 and works as a better receptor for HSV-2 compared to HSV-1 (Krummenacher et al., 2004; Warner et al., 1998).

As a type I transmembrane protein, nectin-1 has a C-terminus in the cytoplasm containing a PDZ domain and an ectodomain extending into the extracellular space comprising of the N-terminal V-domain along with two C-like domains forming an Ig-like fold (V-C-C) (Irie et al., 2004). The cytoplasmic PDZ domain binds to afadin, an actin-binding protein, thus linking nectin to the cellular actin cytoskeleton. Meanwhile, the nectin-1 V domain mediates cell-cell

adhesion via interaction with the nectin-1 V domains of adjacent cells (Takai and Nakanishi, 2003). As the binding site for gD also occurs in the N-terminal V-domain, gD binding interferes with nectin-1 dimerization which may consequently disrupt the cell-cell adhesion function of nectin-1 and further trigger the conformational changes needed to activate the fusion machinery required for HSV-1 entry (Fig. 3) (Cocchi et al., 2001; Zhang et al., 2011; Di Giovine et al., 2011).

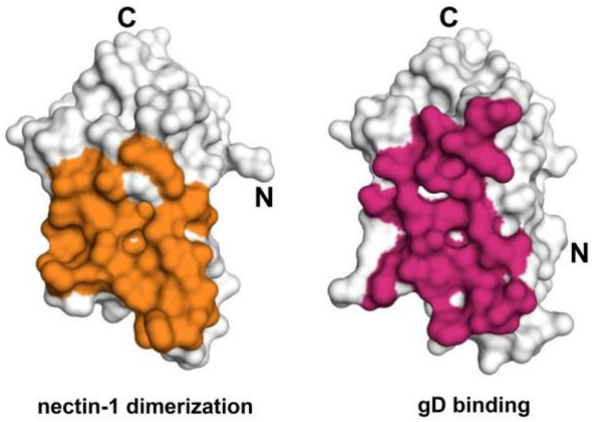

Figure 3. Surface representation of the nectin-1 V domain.
Surface representation highlights the overlapping areas involved between nectin-1 dimerization (orange, left) and gD binding (magenta, right) in the nectin-1 V domain (modified from Di Giovine et al., 2011).

1.2.2 Cellular internalization mechanisms in HSV-1 entry

While binding of gD to a cellular receptor predicates the fusion machinery required for the successful entry of HSV-1 into the cell, fusion does not necessarily have to occur directly at the plasma membrane but may take place following an initial endocytic internalization process in which fusion with a vesicle membrane ensues instead. The preferred mode of HSV-1 entry varies depending on cell type as well as the availability of cellular receptors (Gianni et al., 2004; Milne et al., 2005). In neurons and the African green monkey cell line Vero, for example, fusion occurs at the plasma membrane followed by the immediate release of the de-enveloped capsid into the cytosol while in HeLa cells prior endocytic uptake must take place before fusion (Lycke et al., 1988; Koyama and Uchida, 1987; Nicola et al., 2005). To add to the complexity, some cell types including human keratinocytes and fibroblasts can employ both modes of entry (Rahn et al., 2011). However, since the mechanisms and key players

involved in direct plasma membrane fusion may be similar to those involved in fusion with an endocytic vesicle, assigning the exact contribution of each pathway to successful viral entry is a continued and highly debated subject of interest.

1.2.2.1 Endocytosis and other vesicle uptake mechanisms

Endocytosis, in brief, is the process by which a cell internalizes extracellular substances by being engulfed in cellular plasma membrane-derived vesicles. While many virus families have been found to appropriate endocytic internalization mechanisms for cellular entry, the presentation of endocytosis as a viable mode for HSV-1 entry was initially met with widespread speculation. As Vero cells were the prototype cell line used in studying HSV for many years, early findings insisted that fusion must occur directly at the plasma membrane for successful cellular entry (Morgan et al., 1968; Smith et al., 1974). During the same time, however, evidence for the possibility of endocytic uptake mechanisms was made available using early electron microscopy (EM) micrographs which showed enveloped virus particles within vesicles in HeLa cells and Baby Hamster Kidney fibroblasts (BHK-21) (Epstein et al., 1964; Holmes and Watson; 1963). While vesicle-enclosed virus particles in EM micrographs gave an early glimpse of a possible endocytic mode of uptake for HSV-1, the contribution of such a pathway was very early on dismissed for two main reasons: (1) enveloped HSV-1 particles in vesicles does not necessarily predicate the subsequent and mandatory release of the capsids into the cytosol as no evidence of fusion with the vesicle membrane have been provided and (2) the putative fate that virus particles found in vesicles leads to abortive infection in which they are sent for degradation (Morgan et al., 1968; Campadelli-Fiume et al., 1988). The early postulation that vesicle uptake of HSV-1 leads to abortive infection is not without sound reason. While a subset of endocytic mechanisms is receptor-mediated, not all require the interaction with a cellular receptor to form vesicles at the plasma membrane. The lack of interaction with a cellular receptor, thereof, would present a dilemma for the enveloped HSV-1. In fact, two such mechanisms: (1) phagocytosis and (2) macropinocytosis are mostly implicated in the non-selective uptake of extracellular materials and, compared to its receptor-mediated counterparts, generally form larger vesicles as both involve and are highly-dependent on a large-scale remodelling of the plasma membrane mediated by actin

filaments (May and Machesky, 2001; Commisso et al., 2014; reviewed by Mayor and Pagano, 2007).

With the increase of cell types used in HSV studies, however, more recent findings have provided evidence that HSV-1 can indeed utilize endocytic uptake mechanisms for successful infection. The diversity of endocytic pathways, of which some may be suitable facilitators of HSV-1 entry, makes a complex study. Depending on the cell type, endocytic entry of HSV-1 could be pH-dependent, as with keratinocytes, or pH-independent, like in neurons (Nicola et al., 2005). Adding to the complexity, despite being receptor dependent, clathrin- and caveolin-mediated endocytosis (the main and best characterized endocytic mechanisms in eukaryotic cells) are not involved in HSV-1 entry (Rahn et al., 2011; Devadas et al., 2014; Clement et al., 2006). While macropinocytosis, although believed to be a nonspecific uptake pathway for internalizing large amounts of fluid, has been suggested for HSV-1 entry in studies using keratinocytes, Chinese hamster ovary (CHO) and HeLa cells which found evidence of enveloped particles in large vesicles as well as the co-localization of HSV-1 in (the fluid-phase marker) dextran-positive compartments (Nicola et al., 2005). Moreover, further evidence is provided by the inhibition of phosphoinositide (PI) 3-kinase which blocks the formation of macropinosomes, and concomitantly, the endocytic trafficking of HSV (Sieczkarski and Whittaker, 2002; Nicola and Straus, 2004). Whether macropinocytosis is indeed a viable entry route or whether the evidence presented describes a previously uncharacterized entry pathway that merely incorporates macropinocytosis-like features still requires further elucidation. If macropinocytosis can indeed be implicated in successful HSV-1 entry, the open question that remains is how/when during engulfment does the virus bind to a cellular receptor, a required step that predicates fusion with the vesicle membrane to release a de-enveloped capsid. Once the naked capsid finds its way into the cytosol, it must be transported to the host cell nucleus for the expression of viral genes.

1.2.3 HSV-1 nuclear transport and viral gene expression

Irrespective of the diverse set of entry mechanisms employed, once a de-enveloped capsid is released in the host cell cytoplasm, HSV-1 has successfully entered the cell. From here, the capsid embarks on a journey to the host cell nucleus for the subsequent expression of viral genes which is a highly-coordinated and temporally-ordered cascade classified as immediate-

early (IE), early (E), and late (L) genes (Honess and Roizman, 1974; Clements et al., 1977). Once inside the cytoplasm the de-enveloped capsid, with the help of released viral tegument proteins and the cell's microtubules, is transported to the nucleus where it docks in nuclear pore complexes (NPCs) (Sodeik et al., 1997; Ojala et al., 2000). The viral genome is rapidly released through the central channel of the NPCs and into the nucleoplasm (while the empty capsid is left bound to the NPC) where viral tegument protein VP16, the activating polypeptide, binds to cellular components forming the IE enhancer core complex (Stern and Herr, 1991). This complex, along with cellular RNA polymerase II (RNAP II), mediates the transcription of the IE genes, of which one will encode for infected cell protein 0 (ICP0), the protein used as the readout for successful infection in our studies.

ICP0 is a viral IE-gene product with E3 ubiquitin ligase activity whose many functions include the ability to activate HSV-1 promoters for gene expression, mediate the degradation of cellular proteins (particularly repressors), and evade the host cell's antiviral response (Smith et al., 2011). ICP0 has a distinct localization pattern where, during early infection, it is localized in nuclear foci where it degrades the promyelocytic leukemia (PML) protein as well as the nuclear antigen Sp100 before re-localizing to the cytoplasm at later infection where it blocks interferon regulatory factor 3 (IRF3)-mediated innate immune responses (Everett et al., 1998; Paladino et al., 2010). Because of its distinct localization pattern, ICP0 is used as the readout for successful HSV-1 entry while providing additional temporal information on the state of infection within a given cell in culture as well as in tissue (Schelhaas et al., 2003; Petermann et al., 2009).

1.3 The skin, a natural HSV-1 target

Making up the largest organ of the human body, the skin is a complex organ composed of various tissue structures that can be divided into three, fundamentally distinct layers. This includes (1) the epidermis, a stratified squamous epithelium which forms the outermost layer of the skin which, via the basement membrane, is connected to (2) the dermis, the intermediate layer and skin's connective tissue and (3) the lowermost layer—the subdermal fat also known as the hypodermis (Fig. 4). The layers of the skin work harmoniously, as the dermis, mediated by extrafibrillar matrix and collagen, provides elasticity and stabilizes the

epidermis while the subcutaneous tissue of the hypodermis, which contains fat reserves, provides energy and insulation. Together, the skin provides protection by not only preventing dehydration, but also excluding external environmental assaults like harmful toxins and pathogens such as HSV-1.

Most HSV-1 virus-receptor interaction studies are conducted using cells in culture while invasion at the tissue level has been, for the most part, relatively neglected. Thus, to unravel the molecular and cellular determinants of HSV-1 entry in skin, our lab developed an *ex vivo* HSV-1 infection model using murine and human skin samples (Rahn et al., 2015a; De La Cruz et al., 2022). Using the expression of ICP0 as the readout for successful HSV-1 infection, this *ex vivo* infection assay focuses on the initial infected cells and very early HSV-1 entry events in the skin. While HSV-1 efficiently infected basal keratinocytes in isolated murine epidermis after separation from the dermis, *ex vivo* infection of intact, full-thickness murine skin was not observed (Rahn et al., 2015b). Interestingly, wounding of full-thickness murine skin was still insufficient for infection as mechanical barriers in the skin still prevented HSV-1 entry (Rahn et al., 2017). These initial findings in murine skin hold the first clues in the relevance of epidermal barriers in restricting HSV-1 entry in the skin.

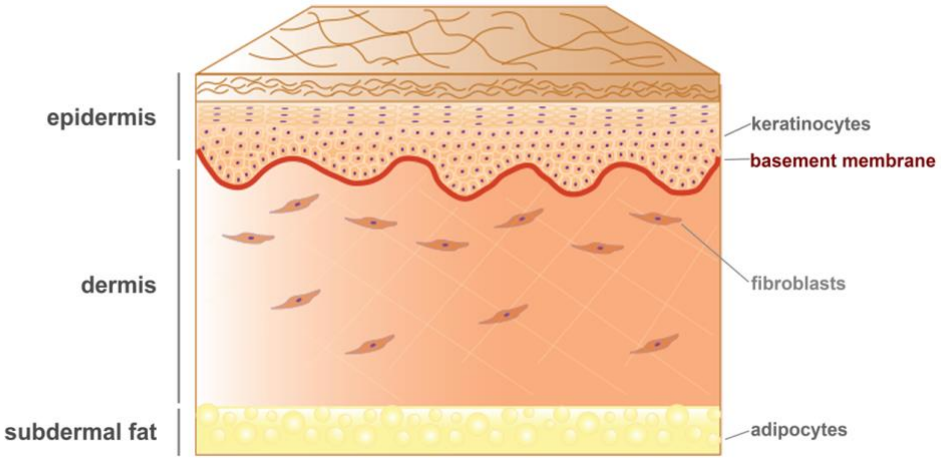

Figure 4. Schematic illustration of human skin.
The skin can be divided into three, functionally and morphologically distinct layers comprising (1) the epidermis, (2) the dermis and (3) subdermal fat (also known as the hypodermis). The principal cell type in the epidermis and dermis are keratinocytes and fibroblasts, respectively, while the subdermal fat is mostly made up of adipocytes (fat cells). The epidermis and dermis are connected via the basement membrane (red).

1.3.1 The stratified squamous epithelium of the human epidermis

Forming the outermost layer of the skin and thus making it the main target of HSV-1 during primary infection, the epidermis, is a stratified squamous epithelium comprised of keratinocytes, melanocytes, Merkel cells, and Langerhans cells of which keratinocytes are the main resident cell type, making up around 90% of epidermis. It can be divided into four layers, or strata, which (from outermost to innermost) consists of (1) the *stratum corneum* (SC, cornified layer), (2) the *stratum granulosum* (granular layer), (3) the *stratum spinosum* (spinous layer), and (4) the *stratum basale* (basal layer) (Fig 5). The basal layer consists of a single layer of actively proliferating keratinocytes that comes in direct contact to the basement membrane. Basal keratinocytes mainly express keratins (K) 5 and K14 as the main structural proteins (Fuchs and Cleveland, 1998). At some point, these cells lose their proliferative capacity and undergo a process of stratification in which they pass through three distinct stages of differentiation sequentially corresponding to the (suprabasal) spinous and granular layers followed by the SC. As a basal cell delaminates, it detaches and moves upwards to give rise to the spinous layer. This transitionary phase involves major changes in the cell's transcriptional, morphological, and functional behavior as it leaves the cell cycle, grows in size, and gains tensile strength established by intercellular connections (reviewed by Fuchs, 2008; Simpson et al., 2011). As the keratinocytes enter the granular layer, the cells begin to flatten, form tight junctions, and enter the final phase of terminal differentiation in which the cells, undergoing a series of biochemical and morphological changes, complete their upward journey as they become the flattened, enucleated dead cells (squames) that make up the cornified layer. The cornified layer is continually replaced by the underlying differentiating cells to effectively maintain the skin barrier. This entire process (from basal cell to corneocyte) occurs within four weeks, showcasing the robust self-renewing capacity of the human epidermis.

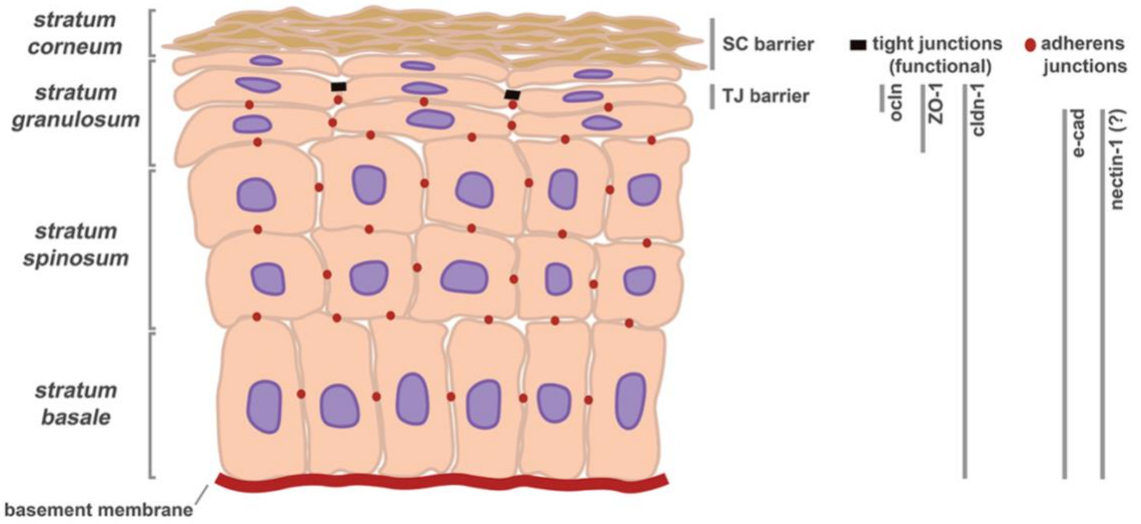

Figure 5. Schematic of the human epidermal layers and associated junctional proteins.
The stratified epithelium of the human epidermis consists of four layers (from top to bottom): (1) *stratum corneum* (SC), (2) *stratum granulosum*, (3) *stratum spinosum*, and (4) *stratum basale*. Basal keratinocytes are anchored to the basement membrane (red line). Physical epidermal barrier function is provided by the SC and tight junctions (TJ). The SC is composed of de-nucleated cells while cell-cell contacts of the underlying nucleated layers are mediated by adherens junctions (red circles), composed of e.g. E-cadherin (e-cad) and nectin-1 and functional tight TJs, composed of e.g. occludin (ocln), zonula occludens 1 (ZO-1) and claudin-1 (cldn-1) which are located in the granular layer. e-cad and nectin-1 can be found in all viable epidermal layers, but a focus of this study is determining if/how well nectin-1 is expressed in the upper granular layers. Claudin-1 protein expression can also be found throughout the viable epidermal layers.

1.3.2 Mechanical barriers of the epidermis

Since the epidermis comes into direct contact with external stimuli on a regular basis, it must possess an effective barrier for organismal maintenance and protection. The epidermal barrier function involves multiple factors which includes a microbial, immunological, and the main focus of this study, a mechanical barrier. Mechanical protection is provided by the composition, integrity, and complex interactions within the epidermal layers which includes multiple lines of defense (from the inside-out and the outside-in) to prevent water loss, exclude external toxins and pathogens, as well as protect the skin from daily wear and tear.

Forming the outer layer of the epidermis, the densely-packed, complex lipid-protein network of the *stratum corneum* (SC) is the first line of mechanical defense from the outside-in (Fig. 5)

(reviewed in Proksch et al., 2008). Specialized substrates of the cornified envelope, an insoluble protein layer, are among the key players in the effective barrier function. Formation of the cornified envelope already starts once an epidermal keratinocyte commits to terminally differentiate in the upper spinous layer with the production of K1 and K10 filaments which are among the first components expressed in the process of cornification. The keratohyalin granules, acquired in the granular layer, contain profilaggrin which gives rise to the interfilamentous protein filaggrin. Filaggrin aggregates keratin filaments into tightly-packed keratin bundles thereby promoting the characteristically collapsed, flat morphology of the corneocytes (Richards et al., 1988; reviewed in Armengot-Carbo et al., 2015). Meanwhile, to reinforce the cornified envelope underneath the plasma membrane, other major structural proteins including involucrin and loricrin are synthesized and covalently cross-linked by transglutaminases (Rice and Green, 1979; Mehrel et al., 1990; Steven and Steinert, 1994; reviewed in Eckert et al., 2005). Furthermore, the lipids (e.g. ceramides, cholesterols, and free fatty acids) stored in lamellar bodies of granular cells are secreted during cornification and interconnect to the cornified envelope to provide the lipid-sealed 'brick and mortar' model of cell-cell contacts (Lavker, 1976; Elias, 1983; reviewed in Matsui and Amagai, 2015).

While the cornified layer provides the initial outside-in barrier function of the skin, the integrity of the underlying epidermal layers mediated by intercellular junctions are just of equal importance. Forming a belt buckle-like adhesive link between cells, tight junction (TJ) components, including the integral membrane proteins claudin-1 and occludin, and the scaffolding protein zonula occludens (ZO-1), in the granular layer provide another line of defense for the epidermal barrier providing a semipermeable, size-/ion-selective barrier (Fig. 5 and 6). By bridging the intercellular space, transmembrane integral TJ proteins are important in regulating the permeability barrier and also form a border between the apical and the basolateral plasma membranes (reviewed in Tsukita et al., 2001). While occludin was the first transmembrane TJ component identified, the finding that its absence still accompanied functional TJs led to the identification of claudin-1 and claudin-2 (Furuse et al., 1993; Furuse et al., 1998). The correct assembly and clustering of TJ must be met but since the transmembrane proteins do not directly interact with each other, cytoplasmic scaffolding molecules must perform this binding function. Thus zonula occludens proteins, such as ZO-1, directly interact with occludin and the claudins via an N-terminal PDZ domain while the C-

terminus forms a direct link to the actin cytoskeleton (Figure 6; reviewed by Niessen, 2007; Schneeberger and Lynch, 2004). The presence of ZO-1 (or ZO-2) is necessary for the polymerization of claudins and maintenance of the barrier function (Umeda et al., 2006). Moreover, linking of ZO-1 to the actin cytoskeleton is important for its localization at TJs. TJ localization is particularly intriguing for our studies since a major focus is to elucidate the exact localization of the HSV-1 cellular receptor nectin-1, one component of the adherens junctions (AJs) which according to literature, should be located immediately underneath TJs.

Similar to TJs, AJ components form complexes that are intimately linked to the actin cytoskeleton and as their name suggests, are responsible for maintaining intercellular adhesion (reviewed in Irie et al., 2004). The AJ is comprised of two adhesive complexes, composed of CAMs and their respective binding partner(s): (1) cadherin-catenin and (2) nectin-afadin. Classical cadherins, such as E-cadherin, form a structurally adhesive unit by binding to β-catenin which forms a bridge with α-catenin, an actin-binding protein that thus provides the link to the cellular cytoskeleton (Fig. 6; reviewed in Aberle et al., 1996). Another actin-binding protein that mediates the link of AJs to the actin cytoskeleton is the nectin-binding partner afadin. While the nectin ectodomain, its V-domain specifically, binds with the nectin V-domain of neighboring cells, the PDZ domain located within the cytoplasmic C-terminus forms a structural adhesion complex with afadin and thereby the actin cytoskeleton (Fig 6; reviewed in Niessen, 2007). While the formation of both adhesion complexes are required for functional AJs, no evidence has been found that nectin and cadherin, themselves directly interact. Rather, it is through the interaction of the cytoplasmic binding partners afadin and α-catenin in which nectin and cadherin are able to organize and co-localize at AJs (Tachibana et al., 2000). Moreover, it has been suggested that while the cadherins mainly play a role in mediating cell-cell adhesion, nectin may be additionally involved in the formation of TJs (Takai and Nakanishi, 2003; Takai et al., 2008). This mutually reinforcing relationship makes it particularly intriguing as to how and under which conditions can HSV-1 overcome TJs to reach its cellular receptor nectin-1 for entry.

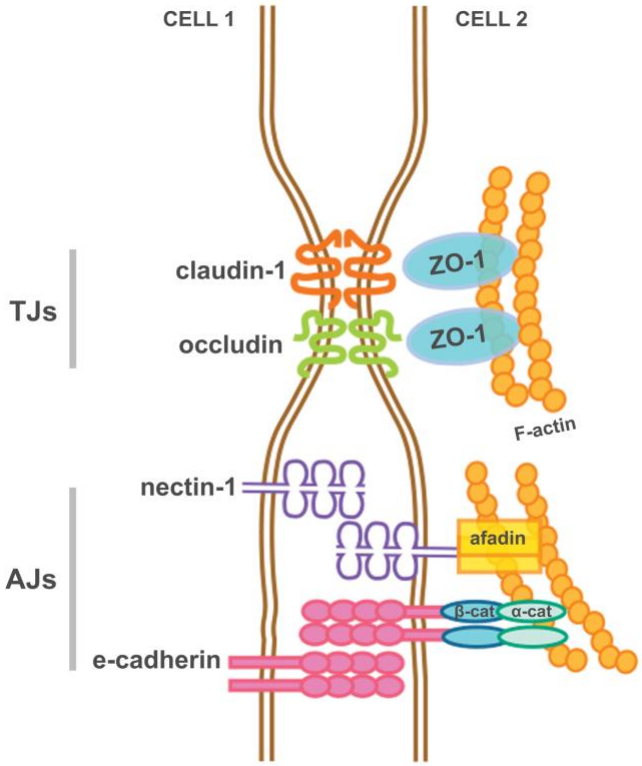

Figure 6. Schematic illustration of tight junctions and adherens junctions.
ZO-1 (or ZO-2, not shown) are localized on the cytosolic side of tight junctions (TJs) and provide a direct link between the integral transmembrane TJs claudin-1 (or claudin-2, not shown) and occludin to the actin cytoskeleton of the cell. Right below the TJs are adherens junctions (AJs) which consists of the nectin-afadin complex and the cadherin-catenin complex. The extracellular domain of nectin-1 dimerizes with nectins of adjacent cells while the cytoplasmic region binds afadin which, in turn, associates with actin bundles. In a similar fashion, cadherins bind with cadherins of neigboring cells. The cytoplasmic region of E-cadherin then binds to β-catenin which forms a bridge to α-catenin which, in turn, associates with actin bundles.

1.3.3 Overcoming the epidermal barrier for HSV-1 invasion

While normal, healthy skin provides robust barriers (as detailed above) against viral invasion, patients with skin lesions can be highly susceptible to primary and recurrent HSV-1 infections which indicates that the virus may opportunistically depend on damaged tissue and/or an impaired skin barrier to reach its receptor and initiate entry. Thus, it is presumed that breaks to the epithelium resulting from mechanical injuries may provide the necessary preconditions for successful HSV-1 invasion. In clinical settings for example, skin lesions such as those resulting from burn wounds and skin abrasions are among known predisposing factors for both primary and recurrent HSV-1 infections (Foley et al., 1970; Shenoy et al., 2015; Becker,

1992; Wilson et al., 2013). Whether a mechanical break in the skin *per se* is sufficient to disturb the epidermal barrier or whether further modifications such as genetic predispositions or an induced immune response are needed to enable HSV-1 to reach its receptor and initiate infection is still open. Indeed, a higher susceptibility to HSV-1 infections is found in individuals afflicted with the pathological skin condition atopic dermatitis (AD) which, aside from being characterized by skin barrier defects, is also coupled with a dysregulated immune system which features an enhanced type 2 inflammation (Langan and Williams, 2019). In fact, patients with AD are at high risk of developing a disseminated HSV infection known as *eczema herpeticum* which usually stems from a primary infection (Singh et al., 2020; Beck et al., 2009). Type 2 inflammation is characterized by the overexpression of cytokines, in particular interleukins (IL)-4 and IL-13, which act on both immune and epithelial cells. For example, AD skin is characterized by reduced late differentiation protein levels such as filaggrin, involucrin, and loricrin compared to healthy individuals therefore contributing to the skin barrier dysfunction (Giustizieri et al., 2001; Hamid et al., 1996; reviewed in Beck et al., 2022). Type 2 inflammation may also affect the function of the TJ barrier. A recent study using IL-4/13-induced filaggrin knockdown skin equivalents reported a decrease in occludin expression (Hönzke et al., 2016). Alternatively, and quite intriguingly so, a study found that while claudin-1 expression in AD skin is reduced, IL-4 and IL-13 stimulation of primary human keratinocytes increased claudin-1 expression and even enhanced TJ barrier function suggesting that the TJ barrier impairment in AD skin may not be a result of enhanced T helper type 2 (Th2) cytokines (De Benedetto et al., 2011). Thus, exactly how Th2-driven cytokine inflammation affects the skin barrier is yet to be fully elucidated.

2. Aims of the Study

In order to persist as a prevalent human pathogen, HSV-1 must find ways to invade its human host through the stratified epithelia of mucosa, skin, or cornea. Our lab is particularly interested in the viral invasion process in the skin. Our focus is on elucidating the cellular and molecular determinants involved in how HSV-1 is able to gain access into this highly-protective tissue and initiate infection of target skin cells. Thus, the publications of this study address:

I. The impact of endocytic entry mechanisms in successful HSV-1 entry in skin cells

Depending on cell-type and/or receptor, HSV-1 can utilize diverse modes of cellular uptake to gain access into its target cells and initiate infection. Our previous studies have shown that in keratinocytes and dermal fibroblasts, two major *in vivo* targets, HSV-1 enters via both direct plasma membrane fusion and endocytosis followed by fusion with a vesicle membrane (Petermann et al., 2015a; Rahn et al., 2011). Since both uptake mechanisms share conserved fusion mechanisms, are highly dynamic, and occur with extreme rapidity, determining the contribution of each pathway in successful entry remains a considerable challenge. Thus, in De La Cruz and Knebel-Mörsdorf (2020) HSV-1 infection is performed at low temperature in an attempt to selectively block endocytosis. The uptake of several markers are employed to address the efficiency of low temperature in impeding endocytic processes. In particular, cholera toxin B is used to address receptor-mediated endocytic processes, while dextran and fluorescently-labelled latex beads consider the possibility of the alternative, non-receptor mediated uptake mechanisms macropinocytosis and phagocytosis, respectively. Moreover, ultrastructural analyses are conducted to visualize virus-containing vesicles and/or free nucleocapsids to thereby characterize the mode(s) of entry in HaCaT keratinocytes. The use of serial sections in transmission electron microscopy (TEM) further elevates the characterization of endocytic entry especially with respect to vesicle prevalence and size. Furthermore, as presence of enveloped particles in vesicles alone does not necessarily ensure eventual capsid release, serial sections aim to provide evidence of fusion with a vesicle membrane ensuing in a de-enveloped capsid in the cellular cytoplasm signifying successful HSV-1 entry.

II. What conditions, mechanical and/or pathological, allow HSV-1 to overcome the epidermal barrier and facilitate HSV-1 invasion

Before HSV-1 can engage in cellular entry of its target skin cells, the virus must first find ways to invade the human skin, which under normal conditions, provides effective barriers against external pathogens. Thus, to unravel the molecular determinants of HSV-1 entry in the skin, the Mörsdorf lab developed an *ex vivo* HSV-1 infection model initially with murine skin (Rahn et al., 2015a). The methods are extended to human skin as described in De La Cruz et al. (2022) in which the *ex vivo* infection assay addresses the very early entry events and initial infected cells during HSV-1 invasion of human skin.

In De La Cruz et al. (2021), *ex vivo* infection studies in human skin are employed to explore whether introduction of mechanical wounds would facilitate viral invasion. Since susceptibility of the human epidermis to *ex vivo* HSV-1 infection serves as a prerequisite for this wounding study, a detailed characterization of infection in the isolated human epidermis is performed by analyzing the role of viral replication, spreading, as well as tissue integrity in the accessibility of HSV-1 to the various epidermal layers. Furthermore, the use of fluorescently-labelled latex beads (500 nm) serves as a readout for epidermal tissue integrity as well as determine whether the mechanically-introduced wounds would, in general, allow particle access in the otherwise highly-protected human skin.

Aside from mechanical wounding, the role of pathological skin conditions for successful viral invasion is explored. *Ex vivo* infection studies found that HSV-1 can overcome defective barriers of lesional atopic dermatitis (AD) skin. Thus, to augment the AD skin results in Möckel et al. (2022) and dissect the parameters that contribute to successful viral invasion, skin samples without pre-existing barrier defects are stimulated with IL-4 and IL-13 to determine whether Th2-driven inflammatory responses introduce skin modifications that are sufficient to enable viral penetration. Moreover, morphological hallmarks of AD and putative barrier alterations upon IL-induction are explored by histological analyses as well as initial immunohistochemistry (IHC) analyses of the SC component filaggrin, a critical barrier component in AD skin.

III. How functional epidermal barriers affect access to the major cellular receptor nectin-1 thereby restricting HSV-1 entry

Overcoming physical epidermal barriers to gain access to its target keratinocytes only presents part of the hurdle during the HSV-1 invasion process. The fundamental next step is to find and engage a cellular receptor for entry, with nectin-1 being the most prevalent receptor in keratinocytes. As a cell-cell adhesion molecule, nectin-1 may be (directly or indirectly) linked to TJ formation. Thus to investigate the localization and accessibility of nectin-1 as well as the correlating HSV-1 infection efficiency during TJ and SC assembly, De La Cruz et al. (to be submitted) utilizes human epidermal equivalents (3D cultures) derived from N/TERT and primary human keratinocytes. Since human epidermal equivalents can also be used to mimic pathological conditions, the 3D cultures are induced with IL-4/IL-13 to potentially introduce molecular and morphological characteristics reminiscent of AD skin. Whether the resulting effects of IL-induction influence nectin-1 localization and HSV-1 susceptibility during 3D culture development are determined using IHC analyses. Furthermore, nectin-1 and TJ localization in human skin (under healthy, pathological, and IL-stimulated conditions) are investigated in detail.

IV. The barrier function of the extracellular matrix in the dermis and its role in particle/viral accessibility to dermal fibroblasts

Once HSV-1 gains access to its cellular receptors in the epidermis and initiates infection, HSV-1 actively replicates in epidermal keratinocytes leading to inflammatory responses in the dermis which can potentially expose dermal fibroblasts to viral invasion. Moreover, during viral reactivation, HSV-1 can be released via nerve endings within the dermis making dermal cells *in vivo* targets of the virus. While primary human and murine fibroblasts in culture are highly susceptible to HSV-1 infection, infected cells are rarely found both in human and murine dermal tissue. Thus to assess whether the organization of the dermis in conjunction with the barrier function of the extracellular matrix contributes to the poor accessibility of HSV-1 to its target cells, Wirtz et al. (2022) applies the use of fluorescently-labelled latex beads (500 nm) as a readout for particle penetration in human and murine dermis. Furthermore, complementary to the particle penetration studies, the extent of viral penetration is assessed by visualizing the HSV-1 major capsid protein VP5 in human dermis.

3. Results

3.1 Preface

The results of this dissertation are described in the following six peer-reviewed publications.

3.2 Publication 1: Endocytic Internalization of Herpes Simplex Virus 1 in Human Keratinocytes at Low Temperature

Authors:	Nydia De La Cruz and Dagmar Knebel-Mörsdorf
Journal:	Journal of Virology
Date of Publication:	28 January 2021
PMID:	33239453
PMCID:	PMC7851553
DOI:	doi:10.1128/JVI.02195-20

*Part of this publication was previously published in my Master's thesis for the University of Cologne, Faculty of Mathematics and Natural Sciences (February 2020). The additional experiments which were performed during my PhD studies are delineated below.

Experiments performed during my PhD studies aimed to further characterize endocytic processes at low temperature using cholera toxin B uptake assays with acid wash (Fig 4b) as well as uptake assays using fluorescein isothiocyanate (FITC)-dextran to exclude the possibility of macropinocytosis at low temperature (Fig 4c). Moreover, infection studies with high passage (passage 7) primary human keratinocytes were performed to visualize whether the poor infection efficiency of these cells can be attributed to the partial F-actin recovery after exposure to low temperature (Fig 3c). Finally, an in-depth TEM study using serial sections (Fig 6) was carefully analyzed to visualize the successful nucleocapsid release from large vesicles at low temperature.

Conception and design of the study was done by DKM together with **NDLC**. Experiments were performed, processed, and analyzed by **NDLC**. Transmission electron microscopy (TEM) samples were prepared by **NDLC** while images were acquired with the support of the CECAD imaging facility. The manuscript was written by DKM with comments, criticisms, revisions, and figures by **NDLC**.

3.3 Publication 2: *Ex Vivo* Infection of Human Skin with Herpes Simplex Virus 1 Reveals Mechanical Wounds as Insufficient Entry Portals via the Skin Surface

Authors:	Nydia C De La Cruz[#], Maureen Möckel[#], Lisa Wirtz[#], Katharina Sunaoglu, Wolfram Malter, Max Zinser, and Dagmar Knebel-Mörsdorf ([#]contributed equally)
Journal:	Journal of Virology
Date of Publication:	13 October 2021
PMID:	34379501
PMCID:	PMC8513464
DOI:	doi:10.1128/JVI.01338-21

Conception and design of the study was done by DKM together with **NDLC**, MM, and LW. **NDLC** performed, processed, and analyzed the experiments involving isolated skin epidermis presented in Fig 2 (with the exception of Fig 2b and 2c) as well the experiments involving latex bead uptake presented in Fig 4h. The manuscript was written by DKM with comments, criticisms, and revisions by **NDLC**, MM, and LW. The figures were assembled by **NDLC**.

3.4 Publication 3: Herpes Simplex Virus 1 Can Bypass Impaired Epidermal Barriers upon *Ex Vivo* Infection of Skin from Atopic Dermatitis Patients

Authors:	Maureen Möckel[#], Nydia De La Cruz[#], Matthias Rübsam, Lisa Wirtz, Iliana Tantcheva-Poor, Wolfram Malter, Max Zinser, Thomas Bieber, and Dagmar Knebel-Mörsdorf ([#]contributed equally)
Journal:	Journal of Virology
Date of Publication:	15 August 2022
PMID:	35969080
PMCID:	PMC9472615
DOI:	doi:10.1128/jvi.00864-22

Conception and design of the study was done by DKM together with MM and **NDLC**. **NDLC** performed, processed, and analyzed experiments involving IL-4/IL-13-induction of human skin presented in Fig 4. The manuscript was written by DKM with comments, criticisms, and revisions by MM, **NDLC**, and LW. The figures were assembled by **NDLC**.

AMERICAN SOCIETY FOR MICROBIOLOGY | Journal of Virology®

VIRUS-CELL INTERACTIONS

Herpes Simplex Virus 1 Can Bypass Impaired Epidermal Barriers upon *Ex Vivo* Infection of Skin from Atopic Dermatitis Patients

Maureen Möckel,[a] Nydia C. De La Cruz,[a] Matthias Rübsam,[c,d] Lisa Wirtz,[a,d] Iliana Tantcheva-Poor,[e] Wolfram Malter,[f] Max Zinser,[g] Thomas Bieber,[h] Dagmar Knebel-Mörsdorf[a,b]

[a]Center for Biochemistry, University Hospital Cologne, University of Cologne, Cologne, Germany
[b]Department of Pediatrics, University Hospital Cologne, University of Cologne, Cologne, Germany
[c]Department Cell Biology of the Skin, University Hospital Cologne, University of Cologne, Cologne, Germany
[d]Cologne Excellence Cluster on Cellular Stress Response in Aging-Associated Diseases, University Hospital Cologne, University of Cologne, Cologne, Germany
[e]Department of Dermatology, University Hospital Cologne, University of Cologne, Cologne, Germany
[f]Department of Gynecology and Obstetrics, University Hospital Cologne, University of Cologne, Cologne, Germany
[g]Department of Plastic, Reconstructive and Aesthetic Surgery, University Hospital Cologne, University of Cologne, Cologne, Germany
[h]Department of Dermatology and Allergy, Christine Kühne-Center for Allergy Research and Education, University Hospital Bonn, Bonn, Germany

Maureen Möckel and Nydia C. De La Cruz contributed equally to this article. The co-first authors are listed in order of increasing seniority.

ABSTRACT To infect its human host, herpes simplex virus 1 (HSV-1) must overcome the protective barriers of skin and mucosa. Here, we addressed whether pathological skin conditions can facilitate viral entry via the skin surface and used *ex vivo* infection studies to explore viral invasion in atopic dermatitis (AD) skin characterized by disturbed barrier functions. Our focus was on the visualization of the onset of infection in single cells to determine the primary entry portals in the epidermis. After *ex vivo* infection of lesional AD skin, we observed infected cells in suprabasal layers indicating successful invasion in the epidermis via the skin surface which was never detected in control skin where only sample edges allowed viral access. The redistribution of filaggrin, loricrin, and tight-junction components in the lesional skin samples suggested multiple defective mechanical barriers. To dissect the parameters that contribute to HSV-1 invasion, we induced an AD-like phenotype by adding the Th2 cytokines interleukin 4 (IL-4) and IL-13 to healthy human skin samples. Strikingly, we detected infected cells in the epidermis, implying that the IL-4/IL-13-driven inflammation is sufficient to induce modifications allowing HSV-1 to penetrate the skin surface. In summary, not only did lesional AD skin facilitate HSV-1 penetration but IL-4/IL-13 responses alone allowed virus invasion. Our results suggest that the defective epidermal barriers of AD skin and the inflammation-induced altered barriers in healthy skin can make receptors accessible for HSV-1.

IMPORTANCE Herpes simplex virus 1 (HSV-1) can target skin to establish primary infection in the epithelium. While the human skin provides effective barriers against viral invasion under healthy conditions, a prominent example of successful invasion is the disseminated HSV-1 infection in the skin of atopic dermatitis (AD) patients. AD is characterized by impaired epidermal barrier functions, chronic inflammation, and dysbiosis of skin microbiota. We addressed the initial invasion process of HSV-1 in atopic dermatitis skin to understand whether the physical barrier functions are sufficiently disturbed to allow the virus to invade skin and reach its receptors on skin cells. Our results demonstrate that HSV-1 can indeed penetrate and initiate infection in atopic dermatitis skin. Since treatment of skin with IL-4 and IL-13 already resulted in successful invasion, we assume that inflammation-induced barrier defects play an important role for the facilitated access of HSV-1 to its target cells.

KEYWORDS HSV-1, atopic dermatitis, human skin, viral entry, epidermal barriers, IL-4/IL-13

Editor Felicia Goodrum, University of Arizona

Address correspondence to Dagmar Knebel-Mörsdorf, dagmar.moersdorf@uni-koeln.de.

The authors declare no conflict of interest.

Received 1 June 2022
Accepted 23 July 2022
Published 15 August 2022

After invasion via mucosal surfaces or skin, herpes simplex virus 1 (HSV-1) establishes primary infection in the epithelium of its human host and becomes latent in neuronal ganglia. Reactivation can lead to recurrent viral shedding near the site of initial infection. HSV-1 generally causes mild infections; however, immune deficiencies and dysregulation are implicated in some severe infections (1). Host and viral factors that are associated with the outcome of HSV infections are mostly not well understood. Preconditions for successful viral invasion in tissue are presumably epithelial breaks due to mechanical injuries. Alternatively, disturbed epithelial integrity and loss of barrier function under pathological conditions such as inflammatory responses or preexisting infections might facilitate viral invasion. Patients with atopic dermatitis (AD) can be seriously affected by disseminated HSV skin infections (termed eczema herpeticum) which, at least in children, usually results from a primary HSV-1 infection (2). Since AD represents a chronic inflammatory skin disease with a complex pathophysiology (3, 4), the risk factors for higher susceptibility to HSV-1 include multiple parameters ranging from impaired epidermal barriers and dysbiosis of skin microbiota to dysregulated immune responses which are most likely mutually reinforcing processes (5–8). In this study, we addressed whether it is a precondition for eczema herpeticum that the lesional skin of AD patients facilitates the initial steps of HSV-1 invasion.

Successful initiation of viral infection in tissue requires the access of viral glycoproteins to its host receptors. Cellular entry of HSV-1 includes attachment to heparan sulfate proteoglycans on the cell surface, followed by the interaction of the viral glycoprotein D (gD) with its receptors, which in turn initiates the fusion of the viral envelope with cellular membranes (9, 10). The primary gD receptors for HSV-1 on human cells are the cell-cell adhesion protein nectin-1 and herpesvirus entry mediator (HVEM), a member of the tumor necrosis factor receptor superfamily (11, 12). Thus far, less is known about how HSV-1 gains access to its receptors in the epithelium to initiate infection.

To dissect the relevance of physical epidermal barriers for HSV-1 invasion, we established an *ex vivo* infection model of murine and human skin (13–15). Once the dermis is separated, murine and human epidermal sheets are highly susceptible to HSV-1 via the basal layer upon *ex vivo* infection; however, the virus cannot penetrate full-thickness skin via the apical surface confirming the effective outside-in barrier function of the skin (14, 15). Even in the absence of the cornified layer, a functional tight-junction (TJ) barrier effectively inhibits infection of lower layers in murine skin (16). Remarkably, mechanical wounds of the human skin surface do not provide *ad hoc* entry portals for HSV-1 upon *ex vivo* infection (15). Here, we explored the role of pathological skin conditions for successful penetration of HSV-1.

AD pathogenesis involves multidirectional interactions of immune dysregulation, microbial dysbiosis and barrier dysfunction (4, 17). Physical barrier dysfunctions are based on alterations of multiple components of the stratum corneum and the TJs which rely on genetic defects and/or inflammation-induced modifications. The best-known dysfunctions comprise the altered lipid and protein structures of the stratum corneum with filaggrin mutations as genetic predisposition for AD (18, 19) and increased risk for eczema herpeticum (20). In addition, TJ proteins are implicated in AD, such as decreased claudin-1 expression, which correlated with disease severity and impaired barriers that may enhance susceptibility to HSV-1 infection (21–24).

In this study, we *ex vivo* infected lesional skin samples to investigate whether AD skin *per se* allows HSV-1 invasion via the skin surface. Since the virus indeed successfully penetrated lesional skin, we visualized key players in barrier function which supported multiple impairments of the physical barriers. To dissect the complex cross talk of barrier function and immune responses that lead to conditions facilitating HSV-1 invasion, we investigated whether the induced Th2 immune response in skin without preexisting barrier defects is sufficient for HSV-1 infection. Intriguingly, after *ex vivo* infection of interleukin-4 (IL-4)/IL-13-treated skin, we observed infected cells supporting that Th2 responses already enabled the virus to overcome the protective skin barrier and gain access to its receptors to initiate infection.

TABLE 1 Characteristics of AD samples

Sample	Age (yrs)	SCORAD	IgE concn (IU/mL)	Eczema[a]	Location of infection[b]	
					16 h p.i.	24 h p.i.
AD1	41	61	6,307	NA	**Apical cells**	NA
AD2	27	66	19.7	NA	**Apical cells**	NA
AD4	35	NA	47.7	chr	**Apical cells**	**All layers**
AD5	55	65	55.6	com	**All layers**	**All layers**
AD6	55	63	8,322	com	Only edges	Only edges
AD7	47	39	799	acu	Only edges	Only edges
AD8	32	55	2,175	sub	**All layers**	Only edges
AD10	56	65	85	acu	Only edges	**All layers**
AD11	38	47	5,850	acu	Only edges	NA
AD12	20	80	13,552	acu	Only edges	Only edges
AD13	58	66	14,236	chr	Only edges	NA

[a]Eczema (chr, chronic; com, commencing; acu, acute; sub, subacute) categorized at time of sample taking.
[b]Boldfacing indicates infection via the skin surface.

RESULTS

***Ex vivo* infection of AD skin.** To explore whether AD predisposes the epidermis to HSV-1 invasion, we *ex vivo* infected lesional skin samples from AD patients and compared them to control skin from healthy donors. Shave biopsy specimens comprising the epidermis and a thin dermal layer were taken from AD patients with severe disease (SCORAD $\geq$ 30) (Table 1) and from healthy donors. Histological analyses determined the state of eczema for each sample which ranged from commencing, subacute, acute to chronic eczema (Fig. 1a and Table 1). All AD samples showed the characteristic epidermal thickening (Fig. 1b), which results from the altered epidermal growth and keratinocyte terminal differentiation (25). To confirm the impaired differentiation programs of the epidermis, we performed K10/K14 stainings (see Fig. 5, below). Lesional skin was characterized by expanded basal keratin 14 (K14) and suprabasal keratin 10 (K10) positive layers leading to enlargement of the epidermis (Fig. 1b).

The heterogeneity of the lesional skin samples allowed us to investigate HSV-1 penetration in AD epidermis under variable conditions (Table 1). After *ex vivo* infection of skin shaves with HSV-1 at ca. 100 PFU/cell, we initially visualized the presence of virus particles by staining the capsid protein VP5. Viruses were visible at the sample edges of control skin shaves, where some viruses accumulated on or in the most upper part of the cornified layer at 6 h postinfection (p.i.) (Fig. 1c). In AD skin samples, we observed virus particles in the cornified layer at this early time, while few particles were found underneath the granular layer at 16 h p.i. suggesting viral penetration (Fig. 1c and d). The granular layer represents the uppermost nucleated epidermal layer under healthy conditions while nucleated cells can be also present in the cornified layer of eczematic skin (see Fig. 5). To explore in more detail whether viruses successfully entered individual cells in AD epidermis via the external skin surface, we visualized the very early expressed viral protein ICP0. Once HSV-1 penetrates cellular membranes and the viral genome is released into the nucleus, ICP0 first localizes in the nucleus and then relocalizes to the cytoplasm during later infection, indicating viral replication (13, 26). After submerging control (n = 3) or AD skin shaves (n = 7) in virus suspension for 6 h, no ICP0-expressing cells were detected even at the sample edges (Fig. 1e). At 16 h p.i., both control (n = 3) and AD skin shaves (n = 11) showed infected keratinocytes at sample edges (Fig. 1f), where loss of tissue integrity was visualized by histological analyses (data not shown). In addition, disruption of the basement membrane at the edges was shown by discontinuous staining of its component collagen VII (Fig. 1f). In line with previous results of various skin samples from healthy donors (15), infected cells were limited to the sample edges in control skin. However, in some AD skin samples (n = 3) we detected single or patches of infected cells in the granular layer with nuclear ICP0, indicating the completion of successful viral entry or cytoplasmic ICP0, which demonstrated the onset of viral replication (Fig. 1g). Furthermore, AD skin

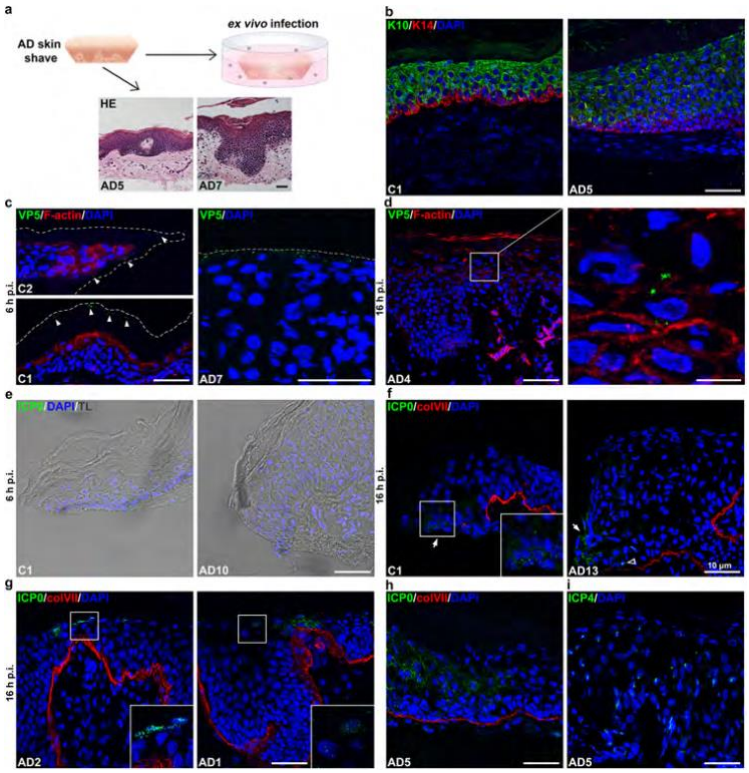

FIG 1 HSV-1 penetration in AD skin shaves. (a) Schematic illustrating *ex vivo* infection of AD skin shaves. HE-stained sections visualize samples with characteristics of commencing (AD5) and acute eczema (AD7). (b to i) After infection with HSV-1 at a multiplicity of infection (MOI) of ca. 100 PFU/cell, cross sections of control (C) and AD skin shaves with DAPI (blue) as nuclear counterstain are shown. Collagen VII (colVII; red) depicts the basement membrane. Scale bars, 50 μm. (b) K10/K14 immunostainings indicate differentiation defects in the eczematic AD skin, including expanded suprabasal layers and nuclei in the stratum corneum. (c) VP5-positive virus particles (green) (arrowheads) at (C2) or below (C1) the control skin surface at 6 h p.i. F-actin (red) depicts the cell morphology. AD skin with virus particles in the stratum corneum containing cell nuclei. Dashed lines indicate sample borders. (d) VP5-positive virus particles (green) underneath the granular layer as shown in the magnification at 16 h p.i. (e) Transmission light (TL) visualizes sample edges with no ICP0-expressing cells at 6 h p.i. (f) At 16 h p.i., nuclear (open arrowhead) and cytoplasmic (arrows) ICP0-expressing cells (green) at the sample edges are shown. (g) ICP0-expressing cells (green) in the granular layer and (h) throughout the epidermis. (i) Nuclear ICP4-expressing cells (green) throughout the epidermis.

samples (n = 2) with areas of infected cells throughout the epidermal layers were found at 16 h p.i. (Fig. 1h), while another sample (n = 1) showed infected areas only at 24 h p.i. (Table 1). These infected areas exhibited a continuous collagen VII staining reflecting an intact basement membrane and showed no infection in the underlying dermal layer. Thus, HSV-1 most likely gained access to the viable epidermis by passing the cornified layer and the TJs (Fig. 1h). To confirm the ICP0 staining pattern throughout the epidermis, we additionally visualized the viral protein ICP4 which marks the nuclear deposition of viral DNA (27). In line with ICP0, the nuclear ICP4 stainings depicted areas with infected cells throughout all epidermal layers (Fig. 1i). Taken together, the *ex vivo* infection studies revealed that AD skin allowed HSV-1 to penetrate via the epidermal surface. The extent of infected cells did not correlate with the state of eczema, SCORAD, or IgE levels (Table 1). Thus, we conclude that a variety of AD conditions can facilitate the initial step of infection.

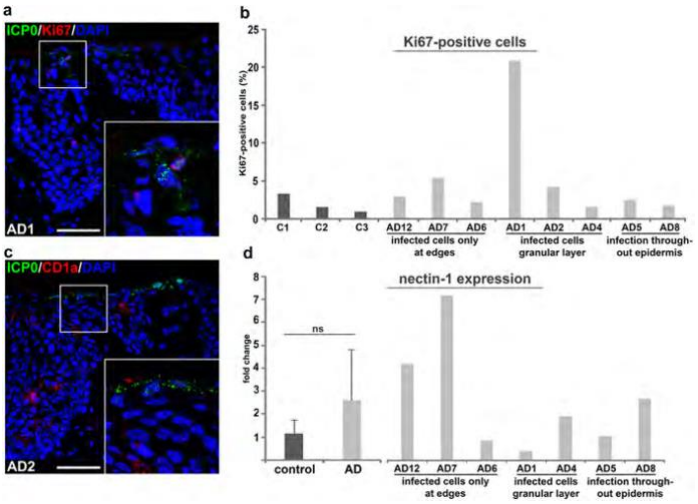

FIG 2 Characterization of HSV-1 penetration in AD skin shaves. (a) Costaining of Ki67 and ICP0 indicates very few proliferating cells with infection. (b) Quantification of Ki67-positive cells is shown for each sample and demonstrates variable numbers in AD (n = 8) compared to control (n = 3) skin shaves. (c) Costaining of CD1a (red) and ICP0 (green) shows no infected Langerhans cells. (d) qRT-PCR demonstrates variable nectin-1 transcript levels in AD (n = 7) compared to control (n = 3) skin shaves. Nectin-1 expression is shown for each infected AD sample.

Since AD is a hyperproliferative skin disease, we performed costainings of the marker Ki67 and ICP0 which demonstrated that proliferative keratinocytes were not preferentially infected (Fig. 2a). In addition, no enhanced infection was found in highly proliferative samples compared to samples with fewer Ki67-positive cells (Fig. 2b).

We next explored whether HSV-1 invades AD skin via epidermal Langerhans cells (LCs). Next to the barrier function of the cornified layer (stratum corneum), TJs, restricted to the granular layer, form a further protective barrier (see Fig. 5, below). The elongated dendrites of LCs can penetrate TJs without disturbing their barrier function which, in turn, might allow pathogen uptake (28, 29). In general, HSV-1 can infect epidermal LCs in human skin (30). Costaining of the LC-specific surface antigen CD1a (31) and ICP0 revealed no infected Langerhans cells in areas of infected keratinocytes (Fig. 2c). Thus, we suggest that extended dendrites of Langerhans cells do not provide a preferred entry portal for HSV-1 invasion but that keratinocytes represent the initial targets upon *ex vivo* infection of the AD skin samples.

To address whether the susceptibility of lesional AD skin to HSV-1 correlated with enhanced receptor presence, we analyzed nectin-1 expression. At least in murine epidermis, HSV-1 entry strongly depends on nectin-1, while HVEM acts as alternative receptor (32). In human epidermis, approximately 40 to 85% of the analyzed epidermal cells express nectin-1 on their surfaces (15). Here, we determined nectin-1 expression by qRT-PCR which demonstrated a high variation among the AD skin samples but no significant difference to control skin (Fig. 2d). Interestingly, the high nectin-1 transcription levels in some AD skin samples did not correlate with enhanced viral invasion (Fig. 2d). These results are a first hint that receptor accessibility rather than receptor presence allows viral entry; however, localization studies of nectin-1 are needed to demonstrate where nectin-1 is present.

Redistributed barrier components in the AD skin shaves. Our *ex vivo* infection studies of AD skin shaves imply that HSV-1 can overcome both barriers, the stratum corneum and the TJs, to reach its receptor nectin-1, which, as a component of adherens

junctions, is located underneath TJs (33). Whether nectin-1 is also expressed on apical surfaces of granular keratinocytes has not yet been determined. Next, we explored the physical barrier modifications in the AD skin samples to address their potential contribution to successful infection. Because of its multifunctional role in barrier formation, we visualized filaggrin in the AD shaves. As expected, filaggrin stainings were less intense in AD ($n = 6$) compared to control ($n = 3$) skin samples, suggesting reduced filaggrin expression and alterations of the cornified envelope (Fig. 3a and c). Furthermore, we stained the differentiation marker loricrin, another barrier component of the squamous layer that is downregulated in AD skin (34). Staining intensities of loricrin were quite heterogenous in AD skin, suggesting a variable extent of impaired differentiation (Fig. 3a). Control skin samples ($n = 3$) showed reduced heterogeneity of loricrin stainings, which was confirmed by additional analyses of breast skin ($n = 3$) from healthy donors (Fig. 3c). Interestingly, reduced filaggrin or loricrin stainings correlated with viral invasion in most AD samples (Fig. 3c).

We then stained TJ components, including the scaffolding protein ZO-1 and the integral membrane proteins occludin and claudin-1. The distinct distribution of ZO-1 in the granular layer, as shown in the control skin ($n = 3$), was replaced by a punctate staining pattern in AD shaves ($n = 7$), while all AD samples ($n = 11$) showed additional ZO-1 stainings underneath the granular layer in the spinous layer supporting an impaired TJ barrier (Fig. 3b). Occludin, which was visible at the apical cells of the granular layer in control skin ($n = 3$), was redistributed in AD shaves ($n = 11$), as visualized by the punctate pattern throughout the suprabasal layers with some heterogeneity in staining intensities (Fig. 3b and c). Finally, we analyzed claudin-1 distribution. As observed for ZO-1 and occludin, claudin-1 stainings were quite distinct in the granular layer of control skin ($n = 3$), while they were reduced in the granular and redistributed to the spinous layer in AD skin ($n = 11$) (Fig. 3b). The significantly lower staining intensities in AD shaves suggest decreased claudin-1 expression (Fig. 3c), which agrees with previous observations (35).

Taken together, all staining patterns confirmed dysregulated barrier components in AD skin. While all AD samples showed reduced claudin-1 stainings, the patterns of ZO-1 and occludin stainings were quite heterogenous among the samples (Fig. 3c), which, in turn, might influence the extent of dysfunctional barriers. Since AD samples with reduced ZO-1 or occludin in addition to low claudin-1 levels were infected from the skin surface (Fig. 3c, black circles), we assume that AD conditions associated with severely impaired TJ barrier promote HSV-1 invasion. This assumption is in line with previous findings in murine skin where functional TJs interfere with HSV-1 entry (16).

***Ex vivo* infection of IL-4/IL-13-treated human skin.** Since Th2 cytokine-driven inflammation and induction of impaired barriers play key roles in AD (36), the Th2 cytokines IL-4 and IL-13 were employed in various human skin models to mimic an AD-like-Th2-driven inflammatory response (37–39). We dissected the parameters that contribute to HSV-1 invasion in AD skin by treating human skin from healthy donors with IL-4/IL-13 to explore whether IL-induced modifications of the epidermal phenotype can *per se* facilitate viral penetration. After treatment of full-thickness skin samples prepared from breast ($n = 3$) and abdominal skin ($n = 2$) with IL-4 and IL-13 for 3 days, we observed marked intercellular edema (discrete spongiosis) (Fig. 4a and b), which represents a hallmark of AD. After infection of IL-4/IL-13-treated skin with HSV-1 at ca. 100 PFU/cell for 24 h, we indeed found single ICP0-expressing cells underneath the cornified layer, though rather rarely in cross sections (Fig. 4c), while the sample edges were well infected. In addition, a patch of infected cells in suprabasal layers away from the edges was occasionally detected (Fig. 4c). In mock-treated skin ($n = 5$), ICP0-expressing cells were exclusively detected at sample edges (Fig. 4c). To better visualize the rare events of infected cells in IL-4/IL-13-stimulated skin, we infected full-thickness breast ($n = 2$) and abdominal skin ($n = 2$) and then separated the dermis from the epidermis to prepare epidermal whole mounts (Fig. 4a). Intriguingly, the view on the basal side of all epidermal samples revealed multiple spots of infected cells ranging from mostly single cells to small cell clusters (Fig. 4d). Quantification illustrates 3 to 12 infected spots per whole-mount

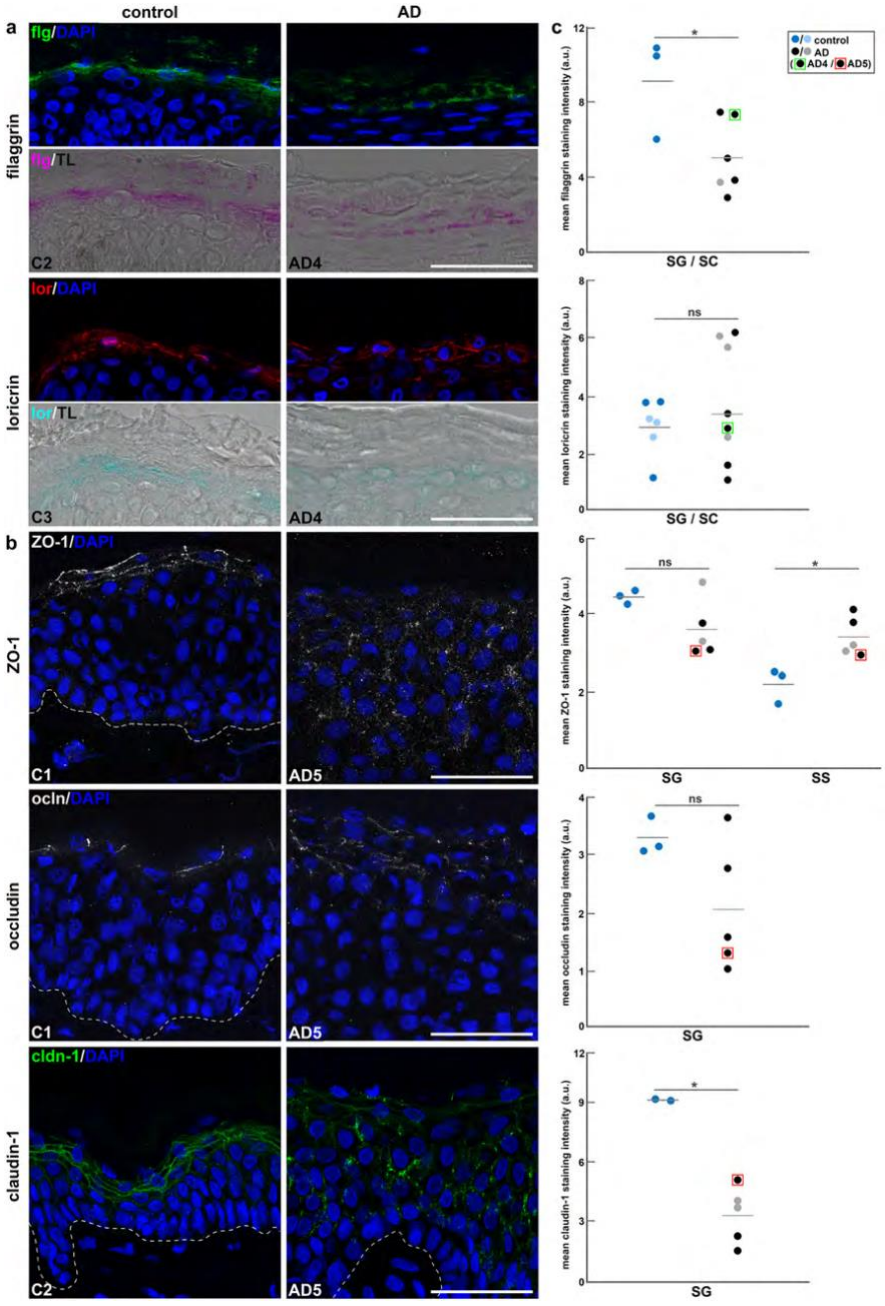

FIG 3 Redistribution of barrier components in AD skin. (a) Immunostainings of skin shaves show redistributed filaggrin (flg) and loricrin (lor) in AD compared to control (C) skin with DAPI (blue) as nuclear counterstain. Transmission light (TL) visualizes the

(Continued on next page)

preparation after IL-4/IL-13-treatment, while 1 to 2 spots were detected in few mock-treated samples, though only very close to the edges (Fig. 4e). Intriguingly, some of the hair follicles in IL-4/IL-13-treated skin showed infected cells close to the interfollicular epidermis, which we never observed at hair follicles from mock-treated skin (Fig. 4d and f). These results suggest that modifications in IL-4/IL-13-stimulated skin may lead to viral access via the hair shaft. In murine skin, we found that cells in the bulge and hair germ of hair follicles are in principle susceptible to HSV-1, but only after *ex vivo* infection of epidermal sheets with preserved hair follicles (14).

Our initial attempt to visualize potential barrier alterations included filaggrin since it is known as a critical barrier component in AD skin. After IL-4/IL-13-treatment, we observed no obvious redistribution or decreased intensities of filaggrin stainings (Fig. 4g). The results, taken together, show that *ex vivo* infection with HSV-1 revealed successful viral penetration in IL-4/IL-13-stimulated skin, supporting that the virus can gain access via the external skin surface due to the Th2 cytokine-induced modifications.

DISCUSSION

Only a subset (~3%) of AD patients develops eczema herpeticum, suggesting that in addition to gaining access to its receptors in AD skin, HSV-1 must also find conditions of various dysregulated immune responses that allow a widespread infection. Thus far, very little is known about the predisposing factors that are associated with the severe outcome of HSV-1 infection (8, 40). The assumption that impaired barrier function correlates with facilitated viral penetration was recently supported by a three-dimensional skin barrier dysfunction model that enables HSV-1 infection (41). Moreover, clinical trials showed that treatment with the monoclonal antibody dupilumab, which inhibits IL-4/IL-13 signaling, was associated with a decreased risk of eczema herpeticum. Thus, improved AD severity is thought to be related to a decrease of eczema herpeticum; however, the underlying mechanism still remains elusive (42). We investigated whether the disturbed barrier function of AD skin and/or the induction of Th2 inflammatory responses *per se* is sufficient to allow HSV-1 to initiate infection in the epidermis.

Our *ex vivo* infection studies in AD skin samples revealed infected cells in suprabasal layers away from the edges. Since we never observed infection of the epidermis by HSV-1 passing through the dermal layer in healthy (15) or AD skin shaves, we conclude that the virus invades the lesional AD skin surface. The precondition for successful invasion is that the impaired barrier function allows the virus to overcome both the stratum corneum and the TJ barriers. Visualization of filaggrin and loricrin, as well as ZO-1, occludin, and claudin-1, demonstrated that all barrier components were redistributed in the AD compared to the control skin samples although to various extents in each sample. The number of AD samples and the complexity of pathological modifications made it difficult to identify a distinct pattern of redistributed barrier components that could be directly attributed to facilitated invasion of HSV-1. Impaired barrier function in AD is mostly determined by measuring transepidermal water loss implying the impairment of the TJ barrier (4). In our experiments, HSV-1 served as a sensor to support that the barrier functions, including the stratum corneum and the TJs, are disrupted to an extent that allows viral penetration in AD lesions (Fig. 5). Under *in vivo* conditions, this initial step of infection might be facilitated by the enhanced *Staphylococcus aureus* colonization of AD skin (43) since these

FIG 3 Legend (Continued)
morphology of the stratum corneum (SC) and the stratum granulosum (SG). (b) Immunostainings of AD skin shaves show redistribution of ZO-1, occludin (ocln), and claudin-1 (cldn-1) in the suprabasal layers compared to control shaves. Dashed lines represent the basement membrane. Scale bars, 50 μm. (c) Quantification of fluorescence shows intensities in control skin shaves (dark blue) (n = 3) and breast skin (light blue) (n = 3) versus AD skin shaves with detectable (black) (n = 3 to 5) or undetectable apical infection (gray) (n = 1 to 3). In AD skin shaves, filaggrin staining intensities are significantly lower in the SG in the stratum granulosum and the corneum (SG/SC). The redistribution of ZO-1 to the stratum spinosum led to significantly higher intensities the stratum spinosum (SS) led to significantly compared to control shaves. The discontinuous claudin-1 stainings in AD skin shaves showed significantly lower intensities in the stratum granulosum (SG) compared to control shaves. P value (*) $\leq$ 0.05.

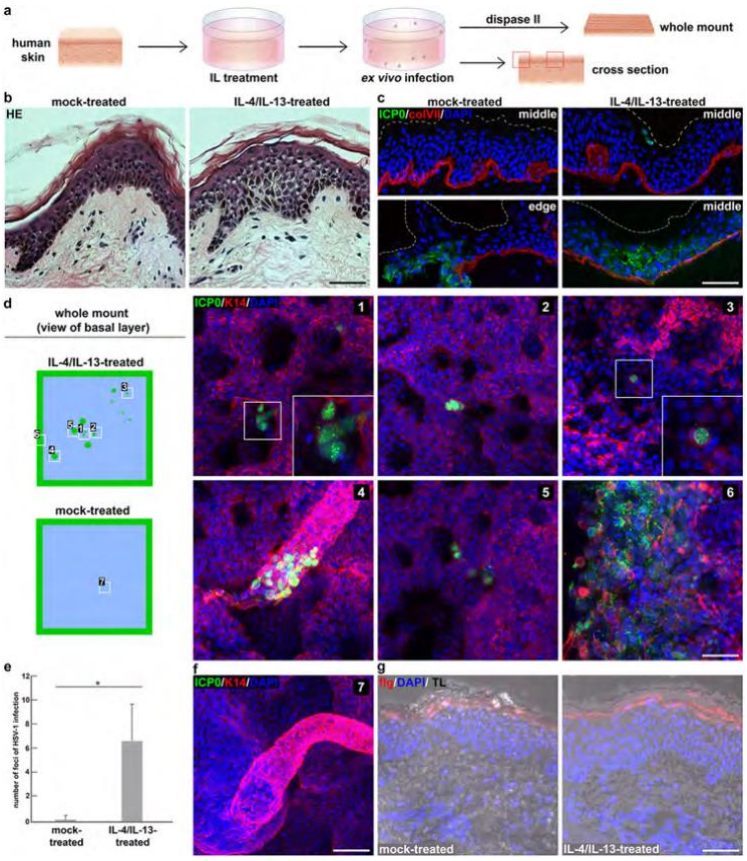

FIG 4 HSV-1 entry in IL-4/IL-13-treated human skin. (a) Schematic illustrating IL-4/IL-13-treatment of full-thickness human skin (n = 5) followed by *ex vivo* infection and analyses of infected cells. Epidermal whole mounts were prepared after infection by dispase II treatment to show the distribution of the infected cells in the basal layer. Localization of the immunostainings at the edge or middle of the cross sections is indicated with dotted boxes (red). (b) HE staining visualizes discrete spongiosis after IL-4/IL-13-treatment of abdominal skin sample for 3 days. (c) After infection of skin with HSV-1 at ca. 100 PFU/cell for 24 h, cross sections show ICP0-expressing cells (green) only at edges after mock-treatment. Single infected (green) suprabasal cells and infected cell layers are visible after IL-4/IL-13-treatment. DAPI (blue) serves as a nuclear counterstain, and collagen VII (coVII; red) depicts the basement membrane. Dashed lines represent the apical sample border. (d) Scheme of epidermal whole mount prepared 24 h p.i. showing the distribution of infected cells. Immunostainings of epidermal whole mounts from IL-4/IL-13-treated skin visualize ICP0-expressing single cells (green) (2, 3) and cell clusters at the hair follicles (4), in the interfollicular epidermis (1, 5), and at the sample edge (6). K14 stainings depict basal keratinocytes. (e) Quantification of infected areas in mock-treated (seven replicates from three individuals) and IL-4/IL-13-treated human skin (ten replicates from four individuals). *, $P \leq 0.05$. (f) Uninfected hair follicle of mock-treated skin 24 h p.i. (g) Cross sections show comparable filaggrin (red) distribution in mock- and IL-4/IL-13-treated skin. Transmission light (TL) visualizes the skin morphology. Scale bars, 50 μm.

microbes can target TJs, leading to disturbed junctional integrity (44). The development of a disseminated HSV-1 infection in a subset of AD patients additionally relies on the extent of immune dysregulations.

As soon as 3 h p.i., HSV-1 infects basal keratinocytes if the virus can directly access receptors in the basal layer of epidermal sheets separated from the dermis (15). ICP0-expressing cells in AD skin were not detected before 16 to 24 h p.i., suggesting that the receptors were not easily accessible throughout the epidermis. Expression of the

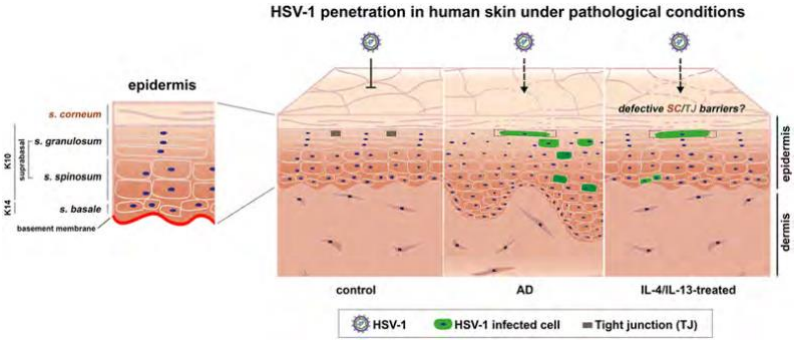

FIG 5 Schematic representation of how HSV-1 penetrates human skin under pathological conditions. Schematic illustrating the structure of human epidermal layers with respective markers. The stratum corneum (SC) and the tight junctions (TJs) form protective barriers to inhibit virus invasion via the skin surfaces of healthy individuals. Atopic dermatitis (AD) skin characterized by epidermal thickening, disturbed SC barriers (dotted lines), and impaired TJs (dotted boxes) offers the virus access to keratinocytes throughout the epidermis to initiate infection. After IL-4/IL-13-treatment of human skin, infected cells are detected which might result from an impaired stratum corneum (SC) and dysfunctional TJs.

receptor nectin-1 was comparable in AD and control skin samples; however, we cannot exclude that impaired differentiation in AD skin leads to a redistribution of nectin-1 that may facilitate access for the virus.

The finding that AD skin samples could be infected with HSV-1 irrespective of the eczema state suggests that successful invasion depends on the structural outcome of dysregulated immune responses rather than on transient inflammatory microenvironments. Future experimentation will address whether facilitated viral invasion relies on barrier defects of genetic origin by analyzing infection of nonlesional AD skin. Here, we stimulated healthy skin with IL-4/IL-13 prior to infection to explore the impact of the Th2 cytokine responses on HSV-1 invasion. Various mouse models helped to establish the role of IL-4/IL-13 in AD pathogenesis and revealed their contribution to allergic inflammation and attenuated barrier function often based on the downregulation of antimicrobial peptides and filaggrin (45). Supplementation of human skin equivalents with IL-4/IL-13 supports that the Th2 inflammation supports hyperproliferation, impaired lipid composition, and reduced skin protein expression, influencing keratinocyte integrity and barrier function (38, 46).

In IL-4/IL-13-stimulated human skin, we observed penetration of HSV-1 via the skin surface, although to a limited and variable extent (Fig. 5). Clusters of single infected cells with either nuclear or cytoplasmic ICP0 expression at 24 h p.i. indicated that some cells are still in the early phase of infection, while others already initiated viral replication. We assume that the IL-4/IL-13 stimulation induced initial alterations in the skin samples that sufficiently alter the integrity of cell-cell junctions that allow the virus to reach its receptors and initiate infection (Fig. 5). Although some viruses evolved strategies to alter cell-cell junctions (47), HSV-1 is thought to opportunistically rely on conditions that lead to junctional disruption that facilitates the accessibility of receptors. How receptor accessibility might be achieved after supplementation with IL-4/IL-13 could rely on various conditions. Recent studies of IL-4/IL-13-treated stratified human keratinocytes showed increased HSV-1 expression which may correlate with the induction of reduced filaggrin expression. This observation led to the speculation that filaggrin deficiency modifies the local pH and thereby enhances viral entry (48). Whether and how IL-4/IL-13 treatment of skin induces impaired physical barriers that allow viral invasion or whether further induced modifications influence receptor distribution and successful invasion is open for future investigation.

MATERIALS AND METHODS

Preparation of human skin. Skin shaves of lesional skin from various areas were taken with a scalpel from patients (n = 11) with diagnosed AD (Table 1). The estimated state of eczema is based on

hematoxylin and eosin (HE) stainings (Table 1). Immediately after surgery, skin samples were transported in Dulbecco modified Eagle medium (DMEM)/high-glucose/GlutaMAX (Life Technologies) with 10% fetal calf serum (FCS), penicillin (100 IU/mL), and streptomycin (100 μg/mL) and prepared for infection. Control skin shaves were taken from the upper leg of healthy donors (n = 3) comparably to AD patients. In addition, shave biopsy specimens (n = 3 individuals) were prepared from skin derived from patients undergoing breast surgery as described previously (15, 49). All skin shaves had a comparable size (ca. 3 × 3 mm). For IL treatment, full-thickness skin samples, which were taken from patients undergoing breast (n = 3 individuals) or plastic surgery (n = 2 individuals), were cut in pieces (ca. 4 × 4 mm) after removal of subcutaneous fat (49). The size of breast and abdominal skin samples allowed infection experiments with two to three replicates per explant. After infection, epidermal whole mounts from total skin were prepared by using dispase II (4 U/mL; Roche) treatment overnight at 4°C to separate the epidermis from the dermis (49).

Ethics statement. Human skin specimens were obtained after informed consent from all patients. The study was approved by the Ethics Commission of the Medical Faculty, University of Cologne (approval 17-481).

Interleukin treatment. Immediately after surgery, total human skin samples were treated with IL-4 (25 ng/mL) and IL-13 (25 ng/mL) diluted in DMEM/high-glucose/GlutaMAX (Life Technologies) with 10% FCS, penicillin (100 IU/mL), streptomycin (100 μg/mL), and 0.05% bovine serum albumin (BSA). After 3 days, mock- and IL-4/IL-13-treated samples were infected with HSV-1 at ca. 100 PFU/cell for 24 h in the absence of IL-4/IL-13.

Virus. Infection studies were performed with HSV-1 wild-type (Glasgow) strain 17+ from purified virus preparations obtained from the supernatant of infected BHK cells, as described previously (49). The calculation of the virus dose was based on the estimated cell number (ca. 2.5 × 10^5) of the superficial areas of skin shaves and full-thickness skin. HSV-1 was given to the tissue samples at 37°C defining time point zero. Skin shaves and total skin were infected at ca. 100 PFU/cell by submerging them in virus-containing medium for various times (49).

Histochemistry, immunocytochemistry, and antibodies. For HE staining, shaves and full-thickness skin samples were fixed with 3.4% formaldehyde overnight at 4°C or for 2 h at room temperature. Fixed samples were prepared as paraffin sections (8 μm), as described previously (49). The morphology of all samples was assessed by HE stainings.

For cryosections, skin samples were embedded in OCT compound (Sakura), frozen at −80°C, and cut into 8 μm thick cross sections (49). Cryosections were fixed with 2% formaldehyde for 10 min at room temperature, and epidermal whole-mount preparations were fixed with 3.4% formaldehyde overnight at 4°C (49). For stainings of claudin-1, occludin, and ZO-1, cryosections were fixed with ice-cold ethanol for 30 min and then with acetone (–20°C) for 3 min. Sections of total skin and shaves were incubated with primary antibodies overnight at 4°C, followed by incubation with the species-specific Alexa Fluor-conjugated secondary antibodies and DAPI (4′,6′-diamidino-2-phenylindole) for 45 min at room temperature. Epidermal whole mounts were incubated with primary antibodies overnight at room temperature and with the secondary antibodies and DAPI overnight at 4°C. The following primary antibodies were used: mouse anti-ICP0 (MAb 11060; 1:50) (50), mouse anti-ICP4 (MAb 58S; 1:1,000), mouse anti-VP5 (MAb DM165; 1:1,000) (51), mouse anti-collagen VII (1:500; Santa Cruz Biotechnology), rabbit anti-loricrin (1:1,000; BioLegend), mouse anti-CD1a (1:50) (31), mouse anti-claudin-1 (1:500; A9; Santa Cruz), mouse anti-filaggrin (1:500) (AKH1; Santa Cruz), mouse anti-occludin (1:400; OC-3F10; Thermo Fisher Scientific), rabbit anti-ZO-1 (1:400; Thermo Fisher Scientific), rabbit anti-K10 (1:1,000; BioLegend), guinea pig anti-K14 (1:150; GP-CK14; Progen), and rabbit anti-Ki67 (1:400; Thermo Fisher Scientific). F-actin was labeled with phalloidin-Atto 565 (1:2,000; Sigma) for 45 min at room temperature.

Microscopy of several continuous sections per sample was performed using an epifluorescence microscope (Zeiss Axiophot) equipped with a Nikon Digital Sight camera system (DS-2MV)/NIS Elements software (for HE stainings) and a Leica DM IRBE microscope linked to a Leica TCS-SP/5 confocal unit. Images were assembled using Photoshop (Elements 2018; Adobe) and Illustrator (version CS5; Adobe). Confocal projections and merged images are shown. Images were analyzed using Fiji (version 2.0.0-rc-65/1.51s) (52) by measuring the mean fluorescence intensity of three different areas per sample.

RNA preparation and qRT-PCR. RNA was isolated from 150 μm thick cryosections of skin shaves embedded 6 h p.i. by using an RNeasy Plus minikit (Qiagen). cDNA was synthesized using SuperScript II reverse transcriptase (Life Technologies). qPCRs were performed using the SYBR GreenER qPCR SuperMix Universal (Life Technologies) on the DNAengine-Opticon 2 System (Bio-Rad). Nectin-1-specific primers (forward, 5′-CTGCAAAGCTGATGCTAACC-3′; reverse, 5′-GATGGGTCCCTTGAAGAAGA-3′) were used; for normalization, RPLP0 (60S acidic ribosomal protein P0) primers (forward, 5′-ACTCTGCATTCTCGCTTCCT-3′; reverse, 5′-GGACTCGTTTGTACCCGTTG-3′) were used. The efficiency for each primer pair was determined, and the relative expression levels were calculated using the threshold cycle ($\Delta\Delta C_T$) method.

Statistics. For statistical analyses, Student t tests were performed to calculate P values using the unpaired two-tailed method. Differences were considered to be statistically significant with P values of ≤0.05 (*).

ACKNOWLEDGMENTS

We thank Roger Everett for ICP0 and ICP4 antibodies, Claude Krummenacher for nectin-1 antibodies (CK41), Frazer Rixon for VP5 antibodies, and Mario Fabri for CD1a antibodies. We also thank Hanna Niehues, Ellen van den Bogaard, Johanna Brandner, and Natalija Novak for helpful discussions and Laura Maintz, Tim Stroisch, and Simone Willms for help with the AD skin samples.

This research was supported by the Deutsche Forschungsgemeinschaft (SFB829 Z4 project, KN536/16-3), the Cologne Fortune Program/Faculty of Medicine, University of Cologne, and the Maria-Pesch foundation.

REFERENCES

1. Singh M, Goodyear HM, Breuer J. 2020. Herpes simplex virus infections. *In* Hoeger P, Kinsler V, Yan A, Harper J, Oranje A, Bodemer C, Larralde M, Luk D, Mendiratta V, Purvis D (ed), Harper's textbook of pediatric dermatology, 4th ed. Wiley, New York, NY.
2. Goodyear HM. 2011. Eczema herpeticum. *In* Irvine AD, Hoeger PH, Yan AC (ed), Harper's textbook of pediatric dermatology, 3rd ed. Wiley, New York, NY.
3. Langan SM, Irvine AD, Weidinger S. 2020. Atopic dermatitis. Lancet 396:345–360. https://doi.org/10.1016/S0140-6736(20)31286-1.
4. Patrick GJ, Archer NK, Miller LS. 2021. Which way do we go? Complex interactions in atopic dermatitis pathogenesis. J Invest Dermatol 141:274–284. https://doi.org/10.1016/j.jid.2020.07.006.
5. Bussmann C, Peng WM, Bieber T, Novak N. 2008. Molecular pathogenesis and clinical implications of eczema herpeticum. Expert Rev Mol Med 10:e21. https://doi.org/10.1017/S1462399408000756.
6. Beck LA, Boguniewicz M, Hata T, Schneider LC, Hanifin J, Gallo R, Paller AS, Lieff S, Reese J, Zaccaro D, Milgrom H, Barnes KC, Leung DY. 2009. Phenotype of atopic dermatitis subjects with a history of eczema herpeticum. J Allergy Clin Immunol 124:260–269. https://doi.org/10.1016/j.jaci.2009.05.020.
7. Weidinger S, Novak N. 2016. Atopic dermatitis. Lancet 387:1109–1122. https://doi.org/10.1016/S0140-6736(15)00149-X.
8. Damour A, Garcia M, Seneschal J, Lévêque N, Bodet C. 2020. Eczema herpeticum: clinical and pathophysiological aspects. Clin Rev Allergy Immunol 59:1–18. https://doi.org/10.1007/s12016-019-08768-3.
9. Heldwein EE, Krummenacher C. 2008. Entry of herpesviruses into mammalian cells. Cell Mol Life Sci 65:1653–1668. https://doi.org/10.1007/s00018-008-7570-z.
10. Connolly SA, Jardetzky TS, Longnecker R. 2021. The structural basis of herpesvirus entry. Nat Rev Microbiol 19:110–121. https://doi.org/10.1038/s41579-020-00448-w.
11. Montgomery RI, Warner MS, Lum BJ, Spear PG. 1996. Herpes simplex virus-1 entry into cells mediated by a novel member of the TNF/NGF receptor family. Cell 87:427–436. https://doi.org/10.1016/s0092-8674(00)81363-x.
12. Geraghty RJ, Krummenacher C, Cohen GH, Eisenberg RJ, Spear PG. 1998. Entry of alphaherpesviruses mediated by poliovirus receptor-related protein 1 and poliovirus receptor. Science 280:1618–1620. https://doi.org/10.1126/science.280.5369.1618.
13. Petermann P, Haase I, Knebel-Mörsdorf D. 2009. Impact of Rac1 and Cdc42 signaling during early herpes simplex virus type 1 infection of keratinocytes. J Virol 83:9759–9772. https://doi.org/10.1128/JVI.00835-09.
14. Rahn E, Petermann P, Thier K, Bloch W, Morgner J, Wickström SA, Knebel-Mörsdorf D. 2015. Invasion of herpes simplex virus type 1 into murine epidermis: an *ex vivo* infection study. J Invest Dermatol 135:3009–3016. https://doi.org/10.1038/jid.2015.290.
15. De La Cruz NC, Möckel M, Wirtz L, Sunaoglu K, Malter W, Zinser M, Knebel-Mörsdorf D. 2021. *Ex vivo* infection of human skin with herpes simplex virus 1 reveals mechanical wounds as insufficient entry portals via the skin surface. J Virol 95:e0133821. https://doi.org/10.1128/JVI.01338-21.
16. Rahn E, Thier K, Petermann P, Rübsam M, Staeheli P, Iden S, Niessen CM, Knebel-Mörsdorf D. 2017. Epithelial barriers in murine skin during herpes simplex virus 1 infection: the role of tight junction formation. J Invest Dermatol 137:884–893. https://doi.org/10.1016/j.jid.2016.11.027.
17. Luger T, Amagai M, Dreno B, Dagnelie MA, Liao W, Kabashima K, Schikowski T, Proksch E, Elias PM, Simon M, Simpson E, Grinich E, Schmuth M. 2021. Atopic dermatitis: role of the skin barrier, environment, microbiome, and therapeutic agents. J Dermatol Sci 102:142–157. https://doi.org/10.1016/j.jdermsci.2021.04.007.
18. Palmer CN, Irvine AD, Terron-Kwiatkowski A, Zhao Y, Liao H, Lee SP, Goudie DR, Sandilands A, Campbell LE, Smith FJ, O'Regan GM, Watson RM, Cecil JE, Bale SJ, Compton JG, DiGiovanna JJ, Fleckman P, Lewis-Jones S, Arseculeratne G, Sergeant A, Munro CS, El Houate B, McElreavey K, Halkjaer LB, Bisgaard H, Mukhopadhyay S, McLean WH. 2006. Common loss-of-function variants of the epidermal barrier protein filaggrin are a major predisposing factor for atopic dermatitis. Nat Genet 38:441–446. https://doi.org/10.1038/ng1767.
19. McAleer MA, Irvine AD. 2013. The multifunctional role of filaggrin in allergic skin disease. J Allergy Clin Immunol 131:280–291. https://doi.org/10.1016/j.jaci.2012.12.668.
20. Gao PS, Rafaels NM, Hand T, Murray T, Boguniewicz M, Hata T, Schneider L, Hanifin JM, Gallo RL, Gao L, Beaty TH, Beck LA, Barnes KC, Leung DY. 2009. Filaggrin mutations that confer risk of atopic dermatitis confer greater risk for eczema herpeticum. J Allergy Clin Immunol 124:507–513. https://doi.org/10.1016/j.jaci.2009.07.034.
21. De Benedetto A, Rafaels NM, McGirt LY, Ivanov AI, Georas SN, Cheadle C, Berger AE, Zhang K, Vidyasagar S, Yoshida T, Boguniewicz M, Hata T, Schneider LC, Hanifin JM, Gallo RL, Novak N, Weidinger S, Beaty TH, Leung DY, Barnes KC, Beck LA. 2011. Tight junction defects in patients with atopic dermatitis. J Allergy Clin Immunol 127:773–786.e1-7. https://doi.org/10.1016/j.jaci.2010.10.018.
22. De Benedetto A, Slifka MK, Rafaels NM, Kuo IH, Georas SN, Boguniewicz M, Hata T, Schneider LC, Hanifin JM, Gallo RL, Johnson DC, Barnes KC, Leung DY, Beck LA. 2011. Reductions in claudin-1 may enhance susceptibility to herpes simplex virus 1 infections in atopic dermatitis. J Allergy Clin Immunol 128:242–246.e5. https://doi.org/10.1016/j.jaci.2011.02.014.
23. Gruber R, Börnchen C, Rose K, Daubmann A, Volksdorf T, Wladykowski E, Vidal-Y-Sy S, Peters EM, Danso M, Bouwstra JA, Hennies HC, Moll I, Schmuth M, Brandner JM. 2015. Diverse regulation of claudin-1 and claudin-4 in atopic dermatitis. Am J Pathol 185:2777–2789. https://doi.org/10.1016/j.ajpath.2015.06.021.
24. Bergmann S, von Buenau B, Vidal-Y-Sy S, Haftek M, Wladykowski E, Houdek P, Lezius S, Duplan H, Bäsler K, Dähnhardt-Pfeiffer S, Gorzelanny C, Schneider SW, Rodriguez E, Stölzl D, Weidinger S, Brandner JM. 2020. Claudin-1 decrease impacts epidermal barrier function in atopic dermatitis lesions dose dependently. Sci Rep 10:2024. https://doi.org/10.1038/s41598-020-58718-9.
25. Guttman-Yassky E, Suárez-Fariñas M, Chiricozzi A, Nograles KE, Shemer A, Fuentes-Duculan J, Cardinale I, Lin P, Bergman R, Bowcock AM, Krueger JG. 2009. Broad defects in epidermal cornification in atopic dermatitis identified through genomic analysis. J Allergy Clin Immunol 124:1235–1244.e58. https://doi.org/10.1016/j.jaci.2009.09.031.
26. Lopez P, Van Sant C, Roizman B. 2001. Requirements for the nuclear-cytoplasmic translocation of infected-cell protein 0 of herpes simplex virus 1. J Virol 75:3832–3840. https://doi.org/10.1128/JVI.75.8.3832-3840.2001.
27. Everett RD, Sourvinos G, Orr A. 2003. Recruitment of herpes simplex virus type 1 transcriptional regulatory protein ICP4 into foci juxtaposed to ND10 in live, infected cells. J Virol 77:3680–3689. https://doi.org/10.1128/jvi.77.6.3680-3689.2003.
28. Kubo A, Nagao K, Yokouchi M, Sasaki H, Amagai M. 2009. External antigen uptake by Langerhans cells with reorganization of epidermal tight junction barriers. J Exp Med 206:2937–2946. https://doi.org/10.1084/jem.20091527.
29. Yoshida K, Kubo A, Fujita H, Yokouchi M, Ishii K, Kawasaki H, Nomura T, Shimizu H, Kouyama K, Ebihara T, Nagao K, Amagai M. 2014. Distinct behavior of human Langerhans cells and inflammatory dendritic epidermal cells at tight junctions in patients with atopic dermatitis. J Allergy Clin Immunol 134:856–864. https://doi.org/10.1016/j.jaci.2014.08.001.
30. Kim M, Truong NR, James V, Bosnjak L, Sandgren KJ, Harman AN, Nasr N, Bertram KM, Olbourne N, Sawleshwarkar S, McKinnon K, Cohen RC, Cunningham AL. 2015. Relay of herpes simplex virus between Langerhans cells and dermal dendritic cells in human skin. PLoS Pathog 11:e1004812. https://doi.org/10.1371/journal.ppat.1004812.
31. Fithian E, Kung P, Goldstein G, Rubenfeld M, Fenoglio C, Edelson R. 1981. CD1a: reactivity of Langerhans cells with hybridoma antibody. Proc Natl Acad Sci U S A 78:2541–2544. https://doi.org/10.1073/pnas.78.4.2541.
32. Petermann P, Thier K, Rahn E, Rixon FJ, Bloch W, Özcelik S, Krummenacher C, Barron MJ, Dixon MJ, Scheu S, Pfeffer K, Knebel-Mörsdorf D. 2015. Entry mechanisms of herpes simplex virus 1 into murine epidermis: involvement of nectin-1 and herpesvirus entry mediator as cellular receptors. J Virol 89:262–274. https://doi.org/10.1128/JVI.02917-14.
33. Irie K, Shimizu K, Sakisaka T, Ikeda W, Takai Y. 2004. Roles and modes of action of nectins in cell-cell adhesion. Semin Cell Dev Biol 15:643–656. https://doi.org/10.1016/j.semcdb.2004.09.002.

34. Kim BE, Leung DY, Boguniewicz M, Howell MD. 2008. Loricrin and involucrin expression is down-regulated by Th2 cytokines through STAT-6. Clin Immunol 126:332–337. https://doi.org/10.1016/j.clim.2007.11.006.
35. Tokumasu R, Yamaga K, Yamazaki Y, Murota H, Suzuki K, Tamura A, Bando K, Furuta Y, Katayama I, Tsukita S. 2016. Dose-dependent role of claudin-1 *in vivo* in orchestrating features of atopic dermatitis. Proc Natl Acad Sci U S A 113:E4061–E4068. https://doi.org/10.1073/pnas.1525474113.
36. Beck LA, Cork MJ, Amagai M, De Benedetto A, Kabashima K, Hamilton JD, Rossi AB. 2022. Type 2 inflammation contributes to skin barrier dysfunction in atopic dermatitis. JID Innov. https://doi.org/10.1016/j.xjidi.2022.100131.
37. Kamsteeg M, Bergers M, de Boer R, Zeeuwen PL, Hato SV, Schalkwijk J, Tjabringa GS. 2011. Type 2 helper T-cell cytokines induce morphologic and molecular characteristics of atopic dermatitis in human skin equivalent. Am J Pathol 178:2091–2099. https://doi.org/10.1016/j.ajpath.2011.01.037.
38. Danso MO, van Drongelen V, Mulder A, van Esch J, Scott H, van Smeden J, El Ghalbzouri A, Bouwstra JA. 2014. TNF-α and Th2 cytokines induce atopic dermatitis-like features on epidermal differentiation proteins and stratum corneum lipids in human skin equivalents. J Invest Dermatol 134:1941–1950. https://doi.org/10.1038/jid.2014.83.
39. Smits JPH, Niehues H, Rikken G, van Vlijmen-Willems IMJJ, van de Zande G, Zeeuwen PLJM, Schalkwijk J, van den Bogaard EH. 2017. Immortalized N/TERT keratinocytes as an alternative cell source in 3D human epidermal models. Sci Rep 7:11838. https://doi.org/10.1038/s41598-017-12041-y.
40. Leung DY. 2013. Why is eczema herpeticum unexpectedly rare? Antiviral Res 98:153–157. https://doi.org/10.1016/j.antiviral.2013.02.010.
41. Sato E, Hiromatsu K, Murata K, Imafuku S. 2018. Loss of ATP2A2 Allows herpes simplex virus 1 infection of a human epidermis model by disrupting innate immunity and barrier function. J Invest Dermatol 138:2540–2549. https://doi.org/10.1016/j.jid.2018.05.019.
42. Fleming P, Drucker AM. 2018. Risk of infection in patients with atopic dermatitis treated with dupilumab: a meta-analysis of randomized controlled trials. J Am Acad Dermatol 78:62–69.e1. https://doi.org/10.1016/j.jaad.2017.09.052.
43. Leung DY. 2003. Infection in atopic dermatitis. Curr Opin Pediatr 15:399–404. https://doi.org/10.1097/00008480-200308000-00008.
44. Ohnemus U, Kohrmeyer K, Houdek P, Rohde H, Wladykowski E, Vidal S, Horstkotte MA, Aepfelbacher M, Kirschner N, Behne MJ, Moll I, Brandner JM. 2008. Regulation of epidermal tight-junctions (TJ) during infection with exfoliative toxin-negative *Staphylococcus* strains. J Invest Dermatol 128:906–916. https://doi.org/10.1038/sj.jid.5701070.
45. Brandt EB, Sivaprasad U. 2011. Th2 cytokines and atopic dermatitis. J Clin Cell Immunol 2:110.
46. Hönzke S, Wallmeyer L, Ostrowski A, Radbruch M, Mundhenk L, Schäfer-Korting M, Hedtrich S. 2016. Influence of Th2 cytokines on the cornified envelope, tight junction proteins, and β-defensins in filaggrin-deficient skin equivalents. J Invest Dermatol 136:631–639. https://doi.org/10.1016/j.jid.2015.11.007.
47. Torres-Flores JM, Arias CF. 2015. Tight junctions go viral! Viruses 7:5145–5154. https://doi.org/10.3390/v7092865.
48. Kim BE, Bin L, Ye YM, Ramamoorthy P, Leung DYM. 2013. IL-25 enhances HSV-1 replication by inhibiting filaggrin expression, and acts synergistically with Th2 cytokines to enhance HSV-1 replication. J Invest Dermatol 133:2678–2685. https://doi.org/10.1038/jid.2013.223.
49. De La Cruz NC, Möckel M, Wirtz L, Knebel-Mörsdorf D. 2022. Ex vivo human skin infection with herpes simplex virus 1. Bio Protoc 12:e4411. https://doi.org/10.21769/BioProtoc.4411.
50. Everett RD, Cross A, Orr A. 1993. A truncated form of herpes simplex virus type 1 immediate-early protein Vmw110 is expressed in a cell type-dependent manner. Virology 197:751–756. https://doi.org/10.1006/viro.1993.1651.
51. McClelland DA, Aitken JD, Bhella D, McNab D, Mitchell J, Kelly SM, Price NC, Rixon FJ. 2002. pH reduction as a trigger for dissociation of herpes simplex virus type 1 scaffolds. J Virol 76:7407–7417. https://doi.org/10.1128/jvi.76.15.7407-7417.2002.
52. Schindelin J, Arganda-Carreras I, Frise E, Kaynig V, Longair M, Pietzsch T, Preibisch S, Rueden C, Saalfeld S, Schmid B, Tinevez JY, White DJ, Hartenstein V, Eliceiri K, Tomancak P, Cardona A. 2012. Fiji: an open-source platform for biological-image analysis. Nat Methods 9:676–682. https://doi.org/10.1038/nmeth.2019.

3.5 Publication 4: Ex Vivo Infection of Human Skin Models with Herpes Simplex Virus 1: Accessibility of the Receptor Nectin-1 during Formation or Impairment of Epidermal Barriers Is Restricted by Tight Junctions

Authors:	Nydia C De La Cruz, Maureen Möckel, Hanna Niehues, Matthias Rübsam, Wolfram Malter, Max Zinser, Claude Krummenacher, and Dagmar Knebel-Mörsdorf
Journal:	Journal of Virology
Date of Publication:	8 June 2023
PMID:	37289055
PMCID:	PMC10308952
DOI:	doi:10.1128/jvi.00262-23

Conception and design of the study was done by DKM together with **NDLC** and MM. **NDLC** performed, processed, and analyzed the experiments involving N/TERT cells, specifically nectin-1 localization in infected stratified cultures (Fig 1d), latex bead uptake during 3D culture development (Fig 2h), and latex bead uptake and nectin-1 localization in IL-4/IL-13-induced 3D cultures (Fig 3d and 3f). **NDLC** performed, processed, and analyzed all experiments involving 3D cultures generated from primary human keratinocytes summarized in Fig 4 and Fig 5. **NDLC** also performed, processed, and analyzed cellular and tight junction localization studies of all skin samples (control, IL-induced, and AD) depicted in Fig 6 and Fig 7. The manuscript was written by DKM with comments, criticisms, and figures by **NDLC.**

AMERICAN SOCIETY FOR MICROBIOLOGY | Journal of Virology®

VIRUS-CELL INTERACTIONS

Ex Vivo Infection of Human Skin Models with Herpes Simplex Virus 1: Accessibility of the Receptor Nectin-1 during Formation or Impairment of Epidermal Barriers Is Restricted by Tight Junctions

Nydia C. De La Cruz,[a] Maureen Möckel,[a] Hanna Niehues,[c] Matthias Rübsam,[d,e] Wolfram Malter,[f] Max Zinser,[g] Claude Krummenacher,[h] Dagmar Knebel-Mörsdorf[a,b]

[a]Center for Biochemistry, University Hospital Cologne, University of Cologne, Cologne, Germany
[b]Department of Pediatrics, University Hospital Cologne, University of Cologne, Cologne, Germany
[c]Department of Dermatology, Radboud University Medical Center, Radboud Institute for Molecular Life Sciences, Nijmegen, The Netherlands
[d]Department Cell Biology of the Skin, University Hospital Cologne, University of Cologne, Cologne, Germany
[e]Cologne Excellence Cluster on Cellular Stress Response in Aging-associated Diseases, University Hospital Cologne, University of Cologne, Cologne, Germany
[f]Department of Gynecology and Obstetrics, University Hospital Cologne, University of Cologne, Cologne, Germany
[g]Department of Plastic, Reconstructive and Aesthetic Surgery, University Hospital Cologne, University of Cologne, Cologne, Germany
[h]Department of Biological and Biomedical Sciences, Rowan University, Glassboro, New Jersey, USA

ABSTRACT Herpes simplex virus 1 (HSV-1) must overcome epidermal barriers to reach its receptors on keratinocytes and initiate infection in human skin. The cell-adhesion molecule nectin-1, which is expressed in human epidermis, acts as an efficient receptor for HSV-1 but is not within reach of the virus upon exposure of human skin under nonpathological conditions. Atopic dermatitis skin, however, can provide an entry portal for HSV-1 emphasizing the role of impaired barrier functions. Here, we explored how epidermal barriers impact HSV-1 invasion in human epidermis and influence the accessibility of nectin-1 for the virus. Using human epidermal equivalents, we observed a correlation of the number of infected cells with tight-junction formation, suggesting that mature tight junctions prior to formation of the stratum corneum prevent viral access to nectin-1. Consequently, impaired epidermal barriers driven by Th2-inflammatory cytokines interleukin 4 (IL-4) and IL-13 as well as the genetic predisposition of nonlesional atopic dermatitis keratinocytes correlated with enhanced infection supporting the impact of functional tight junctions for preventing infection in human epidermis. Comparable to E-cadherin, nectin-1 was distributed throughout the epidermal layers and localized just underneath the tight-junctions. While nectin-1 was evenly distributed on primary human keratinocytes in culture, the receptor was enriched at lateral surfaces of basal and suprabasal cells during differentiation. Nectin-1 showed no major redistribution in the thickened atopic dermatitis and IL-4/IL-13-treated human epidermis in which HSV-1 can invade. However, nectin-1 localization toward tight junction components changed, suggesting that defective tight-junction barriers make nectin-1 accessible for HSV-1 which enables facilitated viral penetration.

IMPORTANCE Herpes simplex virus 1 (HSV-1) is a widely distributed human pathogen which productively infects epithelia. The open question is which barriers of the highly protected epithelia must the virus overcome to reach its receptor nectin-1. Here, we used human epidermal equivalents to understand how physical barrier formation and nectin-1 distribution contribute to successful viral invasion. Inflammation-induced barrier defects led to facilitated viral penetration strengthening the role of functional tight-junctions in hindering viral access to nectin-1 that is localized just underneath tight junctions and distributed throughout all layers. We also found nectin-1 ubiquitously localized in the

Editor Felicia Goodrum, University of Arizona

Address correspondence to Dagmar Knebel-Mörsdorf, dagmar.moersdorf@uni-koeln.de.

The authors declare no conflict of interest.

Received 17 February 2023
Accepted 18 May 2023
Published 8 June 2023

epidermis of atopic dermatitis and IL-4/IL-13-treated human skin implying that impaired tight-junctions in combination with a defective cornified layer allow the accessibility of nectin-1 to HSV-1. Our results support that successful invasion of HSV-1 in human skin relies on defective epidermal barriers, which not only include a dysfunctional cornified layer but also depend on impaired tight junctions.

KEYWORDS HSV-1, nectin-1, epidermal equivalents, N/TERT-1 cells, primary human keratinocytes, nonlesional atopic dermatitis skin, human skin, virus entry, epidermal barriers, IL-4/IL-13, human keratinocytes, nonlesional atopic dermatis keratinocytes, tight junctions

Virus entry in cells is mostly well studied with respect to virus-receptor interactions; the challenge, however, is to understand how these findings relate to entry events *in vivo*, and how viruses gain access to their receptors on target cells in tissue. Herpes simplex virus 1 (HSV-1) penetrates the human host organism via mucosal surfaces or skin and establishes productive infection largely in the epithelium, which is followed by latent infection in sensory ganglia for the life of the host. Cellular entry of HSV-1 depends on the interaction between components of the host cellular membranes and viral glycoproteins (1, 2). The cell-adhesion molecule nectin-1 serves as the primary receptor for HSV-1 to infect human epithelial cells and neurons, while herpesvirus entry mediator (HVEM) and modified 3-O-sulfated-heparan sulfate represent further receptors (3–5). HSV-1 binds to nectin-1 via its envelope glycoprotein D (gD), which is essential for fusion with a cellular membrane to occur (6). Infection studies in nectin-1- or HVEM-deficient epidermis identified nectin-1 as the major receptor in murine epidermis, while HVEM has a more limited role (7).

Nectin-1 belongs to the calcium-independent immunoglobulin superfamily of adhesion molecules comprising four members, all of which can transinteract with each other through their extracellular domains and form various cell-cell adhesion complexes (8). Nectins initially form cis-homo dimers, which then undergo lateral cluster formation on the cell surface followed by transinteraction with nectin clusters on the opposing cell surface (9). The cytoplasmic tail of nectins bind afadin, an F-actin-binding protein. Together with cadherin-catenin complexes, the nectin-afadin complexes constitute adherens junctions (AJ), which are characterized by different adhesive properties of cadherins and nectins (10). The formation of nectin-afadin complexes precedes the assembly of cadherin-catenin complexes at AJs, and the presence of AJs, in turn, is a prerequisite for the formation of tight junctions (TJ). While AJs provide the mechanical connection of adjacent cells, TJs present in the most apical viable epidermal layer act as barriers, which control the paracellular transport of molecules. The minimal TJ complex comprises the integral membrane proteins occludin and claudin-1 and the scaffolding protein ZO-1 which links TJs to the actin cytoskeleton. While occludin and ZO-1 localize in the apical granular layer of the epidermis, claudin-1 is also present outside TJs and distributed throughout the suprabasal epidermal layers (11).

Upon exposure of human skin to HSV-1, the virus must overcome multiple barriers to reach its receptor nectin-1 in the epidermis. The initial epidermal barrier is based on antimicrobial peptides and a physical protection provided by the uppermost stratum corneum with its lipid-sealed cell-cell contacts. Together with the stratum corneum, TJs form the physical barriers of the epidermis. *Ex vivo* infection studies of human skin and oral mucosa confirm that HSV-1 cannot penetrate skin or mucosa via the external surface; only when the dermis is separated, the virus can gain access to the epidermis or oral epithelium via the basal layer and infect both undifferentiated and differentiated keratinocytes (12, 13). Conditions that allow the virus to overcome the epidermal barriers of human skin could be mechanical injuries resulting in epithelial breaks or pathological skin conditions leading to impaired barrier functions. Unexpectedly, the wounded human skin surface does not allow penetration of HSV-1 upon *ex vivo* infection (13). However, we observed successful invasion in lesional atopic dermatitis skin,

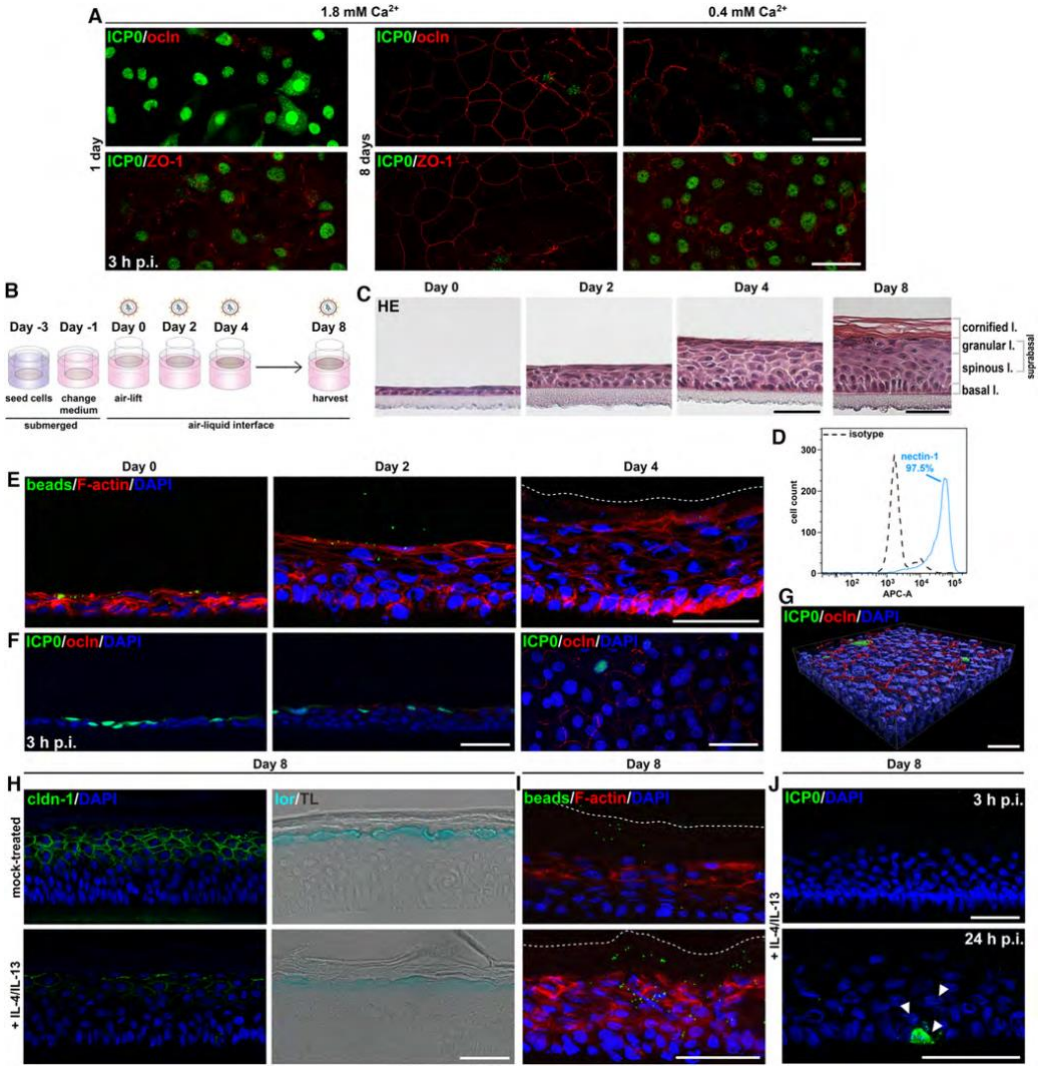

FIG 1 HSV-1 penetration in human epidermal equivalents based on N/TERT-1 cells. (A) N/TERT-1 cells under differentiating (1.8 mM Ca^{2+}) and nondifferentiating (0.4 mM Ca^{2+}) conditions were infected with HSV-1 at a multiplicity of infection (MOI) of 20 PFU/cell. ICP0-expressing cells (green) correlated with the absence or discontinuous occludin (ocln; red) and diffuse ZO-1 (red) stainings after 1 day of differentiation and 8 days under low calcium (0.4 mM Ca^{2+}). In contrast, cultures differentiated for 8 days with distinct occludin (red) or ZO-1 stainings (red) at suprabasal cells only show single infected cells ($n > 3$ independent experimental settings). (B) Schematic illustrating the generation of 3D cultures on collagen-coated transwell filters and time points of infection. Two days after seeding (day -1), the medium of the submerged cultures was exchanged with 3D differentiation medium. (C) H&E stains depict the development of the 3D cultures with a thin layer of still nucleated corneocytes at day 4 and a fully cornified layer at day 8. (D) Flow cytometry shows nectin-1-positive cells from basal and suprabasal layers of the 3D culture at day 8 ($n = 2$). (E) After incubation with 500-nm beads for 3 h, cross sections indicate uptake of beads (green) in apical cell layers at day 0 and day 2 and only single beads at day 4 ($n = 3$). The dashed line indicates the border of the thin cornified layer. F-actin (red) depicts cell morphology. (F) After infection with HSV-1 at 20 PFU/cell for 3 h, cross sections visualize ICP0-expressing cells (green) in the absence of occludin (ocln; red) prior to airlift (day 0), and few infected cells at day 2 with some punctate occludin staining. Staining of whole mount prepared from a 3D culture at day 4 shows the distribution of cells with punctate occludin (red) staining and single ICP0-expressing cells (green) with a view on the apical surface of the culture ($n = 3$). (G) 3D surface-rendered image of the whole mount shown in panel F visualizes the few ICP0-expressing cells (green) in correlation with punctate occludin (red) at intercellular junctions of the granular layer ($n = 3$). (h) Immunostainings at day 8 show strong decrease of claudin-1 (cldn-1; green) and decreased loricrin (lor; blue) in the granular layer after 7 days of IL-4/IL-13

(Continued on next page)

which is characterized by inflammation-induced modifications and dysfunctional physical barriers (14). Patients with atopic dermatitis can be seriously affected by HSV skin infections termed eczema herpeticum (15, 16). We also demonstrated that induced Th2 immune responses, which mimic an atopic dermatitis-like phenotype, can lead to successful viral penetration as shown by infected cells in interleukin-4 (IL-4)/IL-13-treated human skin (14). Thus, we conclude that HSV-1 opportunistically relies on skin conditions that facilitate the accessibility of nectin-1. The open questions are whether and how the impairment of intercellular junctions influences the presence and localization of nectin-1 so that the receptor can be reached by HSV-1.

Here, we explored how formation of the TJ barrier contributes to viral accessibility of nectin-1 in the human epidermis by using human epidermal equivalents derived from N/TERT-1 cells or primary human keratinocytes. As human epidermal equivalents permit terminal differentiation of keratinocytes which then resemble features of fully stratified epidermis (17), this model allows the analysis of HSV-1 infection and nectin-1 distribution during differentiation and functional barrier formation. Differentiation includes extensive reorganization of intercellular junctions, thus the accessibility of nectin-1 to HSV-1 might differ during junction formation. Our focus was on how the viral receptor nectin-1 is distributed on keratinocytes during the differentiation process and under pathological skin conditions. Furthermore, we investigated how inflammation-induced impairment of epidermal barriers can influence the accessibility of nectin-1 for HSV-1 in human skin and whether the facilitated viral invasion in atopic dermatitis skin relies on the redistribution of the receptor.

RESULTS

Susceptibility of N/TERT-1 cells to HSV-1 during epidermal barrier formation. To explore how barrier formation impacts HSV-1 invasion during differentiation, we utilized human epidermal equivalents derived from the keratinocyte cell line N/TERT-1. Human N/TERT-1 keratinocytes were shown to retain differentiation and barrier characteristics of primary keratinocytes in organotypic skin models and can be used to generate an epidermal equivalent with atopic dermatitis features (18, 19). We confirmed the efficient infection of N/TERT-1 cells by HSV-1 in culture as shown recently (20) and demonstrated expression of the receptor nectin-1 on nearly all cells by flow cytometry (data not shown).

After infection of stratified cultures of various murine knockout keratinocytes, we found that successful HSV-1 entry depends on the extent of impaired TJ integrity (21). Here, we investigated how TJ formation during differentiation of human N/TERT-1 cells influences viral susceptibility by initially employing the *in vitro* differentiation model induced by elevating extracellular calcium levels (22). Under differentiating conditions (1.8 mM Ca^{2+}) for 1 day, we observed discontinuous stainings of the TJ components occludin and ZO-1 at the plasma membrane, which were comparable to nondifferentiating conditions (Fig. 1A). In contrast, continuous staining of occludin and ZO-1 was visible after 8 days under differentiating conditions indicating the formation of mature TJs in the apical layer (Fig. 1A). Infected cells were determined by visualizing the immediate early expressed viral protein ICP0 which first localizes in the nucleus and then relocalizes to the cytoplasm during later infection, indicating viral replication (23, 24). Upon infection, ICP0-expressing cells were detected at 3 h postinfection (hpi) under short-term (1 day) differentiation conditions, while only single apical cells with no continuous ZO-1 or occludin stainings were infected after 8 days of differentiation (Fig.

FIG 1 Legend (Continued)
treatment compared to mock-treated cultures (n = 3). Transmission light (TL) visualizes the epidermal layers. (I) After incubation with beads for 24 h, cross sections indicate some beads (green) in the cornified layer of mock-treated cultures and enhanced uptake of beads (green) in the cornified and granular layers after IL-4/IL-13 treatment (n = 2). The dashed line indicates the border of the cornified layer. (J) After infection of IL-4/IL-13-treated cultures with HSV-1 at 20 PFU/cell (n = 3), no ICP0-expressing cells (green) were observed at 3 hpi and only one small cluster of infected cells (arrowheads) was detected at 24 hpi. DAPI (blue) serves as a nuclear counterstain. Scale bars, 50 μm.

1A). These results support that TJ formation in N/TERT-1 cells can strongly interfere with HSV-1 susceptibility.

Next, we generated human epidermal equivalents with N/TERT-1 cells to explore HSV-1 susceptibility during formation of multiple epidermal barriers in detail (Fig. 1B). Histological sections demonstrated a 1- to 2-layer culture at day 0 with further suprabasal cells after raising the cultures to the air-liquid interface (day 2), indicating early differentiation (Fig. 1C). At day 4, several layers of differentiating cells emerged with a very thin layer of cornification, and at day 8, the cultures were fully differentiated with multiple layers of the stratum corneum (Fig. 1C). To analyze nectin-1 expression on cells from fully stratified epidermal equivalents, we performed flow cytometric analyses, which indicated 97.5% of nectin-1-positive cells representing basal and suprabasal cells (Fig. 1D). The high number of nectin-1-expressing undifferentiated and differentiated N/TERT-1 cells does not mimic the heterogeneous nectin-1 level in human epidermis (13).

The extent of functional barrier formation during the differentiation processes of epidermal equivalents was investigated by penetration assays with latex beads. Penetration of beads was easily detected prior to airlift (day 0) and was still observed at day 2 (Fig. 1E). At day 4, however, only single beads passed the thin layer of cornification, indicating some barrier function of the early cornified layer (Fig. 1E).

Upon infection by HSV-1 prior to airlift (day 0), ICP0 was expressed in many cells at 3 hpi (Fig. 1F). Infection at day 2 resulted in less ICP0-expressing cells compared to day 0 (Fig. 1F), but nearly all apical cells were infected at 9 hpi (data not shown). The delayed efficiency of infection at day 2 correlated with occludin stainings at the membranes of some apical cells, suggesting an early stage of TJ formation, which was not yet apparent at day 0 (Fig. 1F). Infection at day 4 led to single infected cells, which correlated with a strong enrichment of occludin at lateral membranes in the most apical granular layer, as shown by whole-mount stainings (Fig. 1F and G). The 3D image visualizes single apical infected cells in areas with discontinuous occludin staining (Fig. 1G). Our results indicated that TJ formation prior to barrier formation of the stratum corneum strongly interfered with viral invasion. As the initial cornification at day 4 hindered penetration of latex beads, we assume that the thin cornified layer additionally influences the extent of virus invasion.

Th2-inflammation-induced modifications of N/TERT-1 cultures do not enhance HSV-1 susceptibility. To further explore the role of TJs and the stratum corneum barrier, we chose conditions that lead to impaired barrier functions. The Th2 cytokines IL-4 and IL-13 were employed in various human skin models to mimic an atopic dermatitis-like Th2-driven inflammation, which results in hyperproliferation, impaired lipid composition of the cornified layer, and reduced skin protein expression; these alterations, in turn, impair keratinocyte barrier functions (25–27). As IL-4/IL-13 treatment of epidermal equivalents based on N/TERT-1 cells can induce histopathological and molecular hallmarks of atopic dermatitis (19), we investigated whether the cytokine-induced barrier alterations enhance HSV-1 invasion. After IL-4/IL-13 addition to the cultures at day 1, we analyzed barrier components after 7 days of treatment (day 8) and observed reduced staining of the terminal differentiation marker loricrin and a strong decrease of the TJ component claudin-1 (Fig. 1H) as described (28) indicating impaired TJs and a dysfunctional epidermal barrier. Effects on differentiation processes were further supported by an aberrant enrichment of F-actin below the granular layer of the cytokine-stimulated cultures (Fig. 1I). Interestingly, penetration assays demonstrated some areas where latex beads invaded the cornified as well as the granular layer after IL-4/IL-13 treatment, which was unlike mock-treated cultures (Fig. 1I). In contrast, infected cells were detected neither in cytokine- (Fig. 1J) nor mock-treated cultures (data not shown) at 3 hpi; only at 24 hpi, one cluster of single ICP0-expressing cells was found after cytokine treatment (Fig. 1J), which was not observed in mock-treated cultures (data not shown). These results suggest that IL-4/IL-13 stimulation alters differentiation processes influencing TJ formation and induces some changes of functional barriers in the cornified layer, however, these changes were insufficient to substantially allow HSV-1 invasion.

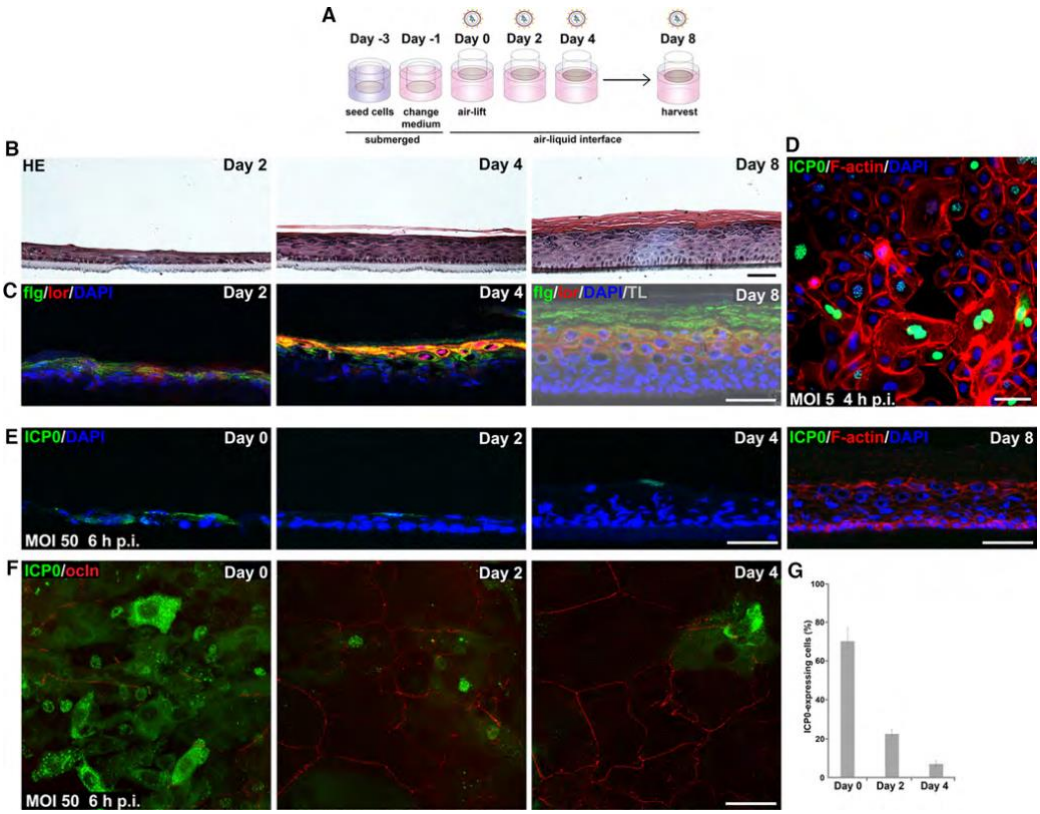

FIG 2 HSV-1 entry in epidermal equivalents based on primary human keratinocytes. (A) Schematic illustrating the generation of 3D cultures on collagen-coated transwell filters and time points of infection. (B) HE-stained sections show the morphology of the developing 3D cultures. (C) Filaggrin (flg; green) and loricrin (lor; red) are detected in the most apical layer at day 2 and 4 and are distributed throughout the cornified and granular layers, respectively, at day 8 (n = 2). Transmission light (TL) visualizes the fully cornified layer. (D) As a control, immunostainings demonstrate ICP0-expressing cells (green) after infection of primary human keratinocytes with HSV-1 at 5 PFU/cell for 4 h with F-actin as a cellular counterstain ($n > 3$). (E) After infection with HSV-1 at 50 PFU/cell for 6 h, most cells expressed ICP0 at day 0, small clusters of infected cells were present at day 2, some cells at day 4, and no infected cells at day 8 ($n \geq 3$). F-actin served as a cellular counterstain. (F) Stainings of whole-mount preparations with view on the apical surface of the cultures visualize the decreasing number of ICP0-expressing cells (green) at day 2 and 4 in correlation with increasing occludin (ocln; red) network in the suprabasal layers. (G) Quantification shows the decreased number of ICP0-expressing cells at day 2 and 4 (n = 3). DAPI (blue) serves as a nuclear counterstain. Scale bars, 50 μm.

Susceptibility of primary human keratinocytes to HSV-1 in epidermal equivalents. To dissect barrier formation and successful viral invasion in more detail, we extended our infection studies to epidermal equivalents based on primary human keratinocytes (Fig. 2A) which more closely resemble epidermal homeostasis *in vivo*. The focus was on infection prior to the formation of a fully stratified human epidermis to explore the impact of developing TJs preceding the establishment of a cornified layer. Histological sections demonstrated faster stratification and more heterogeneity compared to N/TERT-1 cells (Fig. 2C). Already at day 2 after airlift, stainings of filaggrin and loricrin, representing barrier components of the squamous layer revealed both markers (Fig. 2D). The histological section at day 4 depicted the initiating cornification, which was supported by the enhanced presence of filaggrin and loricrin in the apical layer (Fig. 2C and D). At day 8, filaggrin and loricrin stainings indicated an intact cornified barrier formation with filaggrin in the stratum corneum and loricrin in the terminally differentiated keratinocytes (Fig. 2D).

Primary human keratinocytes in culture are well infected by HSV-1 (29). When we infected densely grown primary human keratinocytes prior to induced differentiation, we observed approximately 40% of infected cells at 4 hpi (data not shown), visualized in Fig. 2B, which indicated a delayed onset of infection compared to less densely seeded cells and a major delay compared to N/TERT-1 cells. Upon infection of epidermal equivalents prior to airlift (day 0), large areas with most apical but also basal cells infected were observed, while only small clusters of apical cells expressing ICP0 were present at day 2, single cells at day 4, and no infected cells at day 8 (Fig. 2E–G). The strongly decreased number of infected cells at day 2 correlated with areas showing an occludin network of large suprabasal cells (Fig. 2F and G). Thus, we conclude that areas with TJs at day 2 already hamper successful viral invasion while areas with less TJ formation still allow infection. More continuous occludin stainings were observed at day 4 indicating mature TJs, which correlated with infection of only some cells (Fig. 2F). Initiating cornification may additionally contribute to hindered viral accessibility as in N/TERT-1 3D cultures.

By treating epidermal equivalents with IL-4/IL-13 (Fig. 3A), we further analyzed the effects of early TJ formation on viral susceptibility and addressed whether inflammation-induced changes sufficiently alter TJs prior to the establishment of the cornified layer to enhance HSV-1 invasion. After treatment with IL-4/IL-13 at day 1 followed by infection 24 h later, we observed increased intensities of ICP0 stainings compared to untreated cultures supporting enhanced efficiency of infection (Fig. 3B and C). After the short-term cytokine incubation of 24 h, changes of the occludin network, which was still heterogeneous at this time point (day 2), were difficult to judge. Still, we speculate that in the absence of the stratum corneum, cytokine-induced changes affecting TJ formation correlate with enhanced infection.

To further investigate the impact of defective barriers for HSV-1 invasion, we used primary human keratinocytes of nonlesional atopic dermititis skin for the generation of epidermal equivalents to explore whether genetically induced weakening of epidermal barriers can influence viral invasion. Nonlesional atopic dermatitis skin is characterized by differentiation defects and abnormalities of the stratum corneum (30, 31), although we still know little about genetic barrier defects. Our experiments with epidermal equivalents derived from nonlesional keratinocytes indicated a disordered morphology with a strong delay of TJ and cornified layer formation compared to cultures based on keratinocytes of healthy individuals, supporting an intrinsic predisposition of nonlesional keratinocytes to defective barrier formation. At day 2, we observed most cells infected except small areas with an initial occludin network, which expanded at day 4 when clusters of infected cells were still present (Fig. 3D and E) while only single infected cells were detected at day 8 (Fig. 3F). At this time, the suprabasal layers showed some morphological abnormalities with only initial cornification (Fig. 3F), which was absent at day 4 (data not shown). These results indicated a correlation of delayed and impaired barrier formation, and increased viral invasion, which strengthens our assumption that early TJ formation already interferes with viral infection.

Distribution of nectin-1 in human epidermal equivalents. To reveal how TJs impact the accessibility of nectin-1 to HSV-1, we investigated the localization and distribution of the receptor regarding barrier-forming TJs. When we initially visualized the receptor on primary human keratinocytes in culture, we found nectin-1 all over the cell surface even in densely grown cultures (Fig. 4A–C). This finding correlated with efficient infection of undifferentiated keratinocytes (Fig. 2B). We next investigated how nectin-1 is distributed throughout the layers of epidermal equivalents derived from primary human keratinocytes during differentiation and barrier formation. Prior to airlift (day 0) when most cells were infected (Fig. 2E and F), nectin-1 was present at basal and apical cells with some apical cells showing areas with enriched nectin-1 at lateral membranes; at this early time of differentiation, ZO-1 was rarely visible (Fig. 4E). Intriguingly, at day 1, we observed areas with ZO-1 in addition to nectin-1 enriched at lateral membranes with nectin-1 localizing underneath ZO-1 (Fig. 4F) which supports initial formation of TJs.

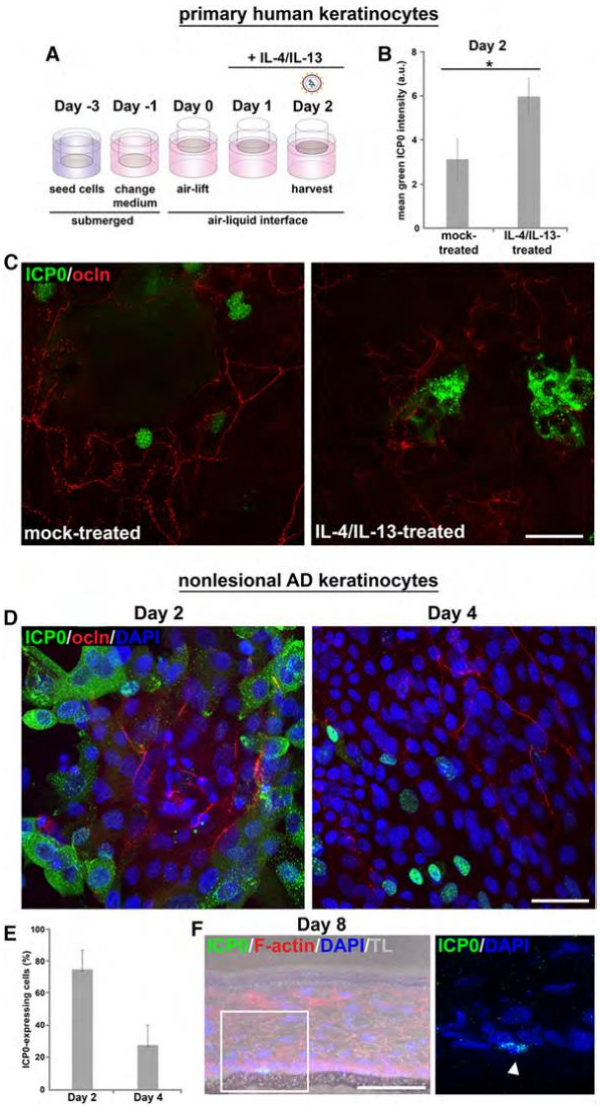

FIG 3 HSV-1 penetration in epidermal equivalents based on primary human keratinocytes treated with IL-4/IL-13 or based on nonlesional atopic dermatitis (AD) keratinocytes. (A) Schematic illustrating the generation of 3D cultures with IL-4/IL-13 treatment at day 1 followed by infection 24 h later. (B) Quantification of fluorescence shows increased ICP0 intensities in IL-4/IL-13-treated cultures at day 2 compared to mock-treated cultures ($n = 3$). *, $P \leq 0.05$. (C) Max projections of whole mounts prepared at day 2, which were infected with HSV-1 at 50 PFU/cell for 6 h, depict increased staining intensities of ICP0 (green) in IL-4/IL-13- compared to mock-treated cultures ($n = 3$). (D) Whole mounts prepared of 3D cultures based on nonlesional AD keratinocytes were infected with HSV-1 at 50 PFU/cell for 6 h. At day 2, most cells expressed ICP0 (green) except areas with initial occludin (red) network. At day 4, areas with continuous occludin staining enlarged and a reduced number of ICP0-expressing cells was observed ($n = 3$). (E) Quantification shows the decreased number of ICP0-expressing cells at day 4 ($n = 3$). (F) At day 8, single infected cells (green; arrowhead) were visualized ($n = 3$). Transmission light (TL) visualizes the thin cornified layer. F-actin (red) served as a cellular and DAPI (blue) as a nuclear counterstain. Scale bars, 50 μm.

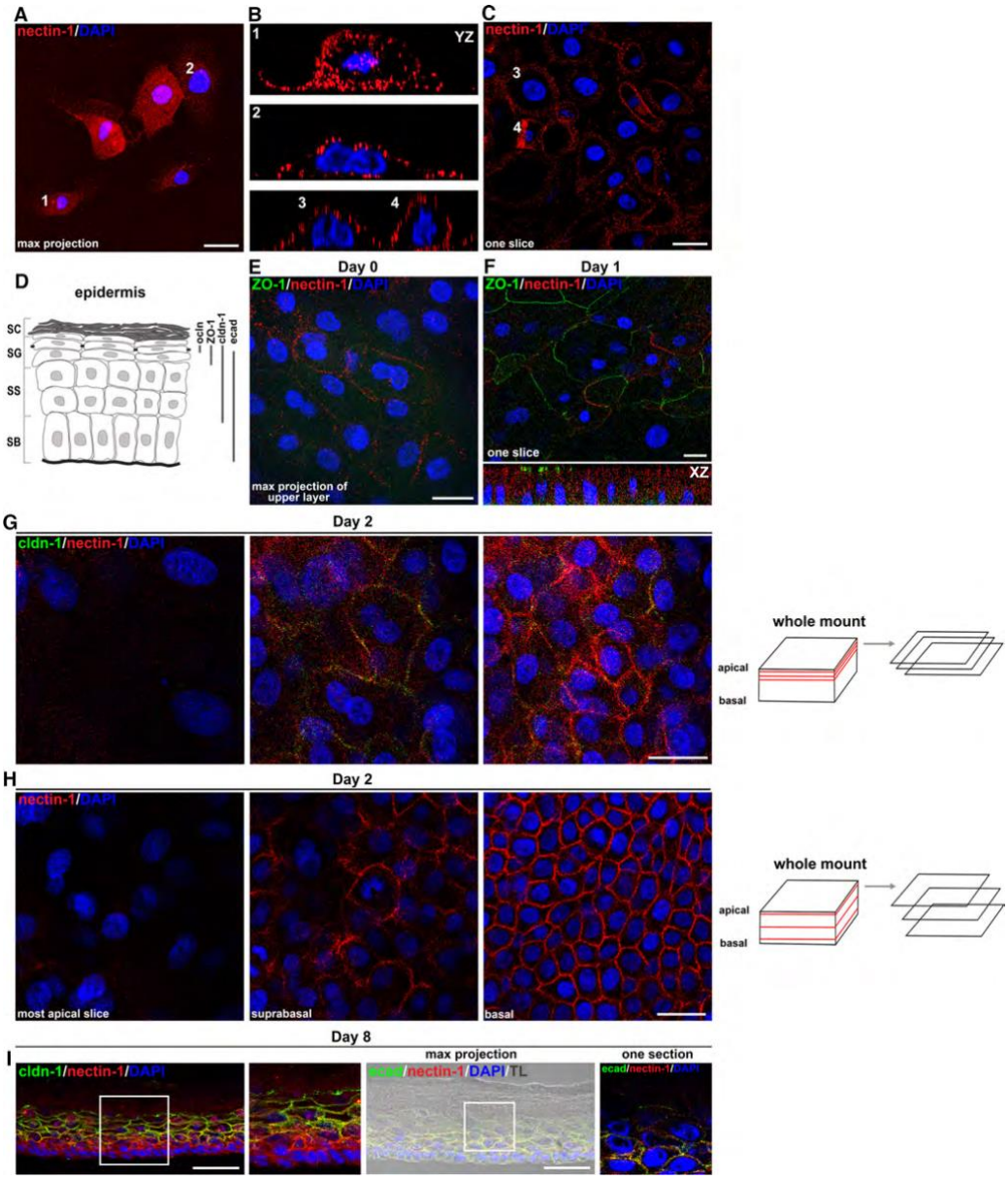

FIG 4 Nectin-1 distribution in primary human keratinocytes and epidermal equivalents. (A) Primary human keratinocytes seeded at low density show nectin-1 (red) localization. (B) YZ images demonstrate equally distributed nectin-1 on basolateral and apical surfaces of cells 1 to 4. (C) Confocal slice of densely seeded keratinocytes visualizes nectin-1 (red) at lateral membranes (D) Schematic illustrating the distribution of the TJ components occludin (ocln), ZO-1, and claudin-1 (cldn-1), and the AJ component E-cadherin (ecad) in the stratum corneum (SC), stratum granulosum (SG), stratum spinosum (SS), and stratum basale (SB). (E) Whole mount of epidermal equivalents prior to airlift (day 0) visualize areas with nectin-1 (red) enriched at lateral membranes in the absence of ZO-1. (F) Apical slice of whole-mount preparation at day 1 show lateral nectin-1 (red) and ZO-1 (green) at the most apical cells. Nectin-1 underneath ZO-1 is shown in the XZ axis. (G) Three apical slices by the apical surface of whole-mount preparations at day 2 demonstrate the absence of

(Continued on next page)

We next stained claudin-1, which is distributed throughout the suprabasal layers in fully stratified epidermis (Fig. 4D) to further characterize the localization of TJ components with regard to nectin-1. After taking various slices of the apical layer at day 2, the most apical nucleated cell layer showed neither nectin-1 nor claudin-1, while the cell layers just underneath indicated colocalization of nectin-1 and claudin-1 (Fig. 4G). Enriched nectin-1 at lateral membranes increased from apical to basal layers with strong lateral nectin-1 at all basal cells (Fig. 4G and H). Taken together with the initial occludin network observed at day 2 (Fig. 2F), which correlated with strongly decreased numbers of infected cells (Fig. 2G), we conclude that initial TJ formation can hinder the accessibility of nectin-1, which is present in the various epidermal layers. When we analyzed nectin-1 distribution in fully stratified epidermis (day 8) where no infected cells were found (Fig. 2B), nectin-1 and claudin-1 were present throughout the granular layer (Fig. 4I). Only claudin-1, however, was detected at the most apical nucleated cells (Fig. 4I). Costaining of nectin-1 and E-cadherin confirmed that both adherens junction (AJ) components colocalized in all epidermal layers (Fig. 4I); some areas showed nectin-1 localizing underneath E-cadherin in the most apical granular layer (Fig. 4I, magnification). These results demonstrate that nectin-1 is present at AJs in the granular layer but functional TJs prevent the accessibility of nectin-1 to HSV-1 in human epidermal equivalents. Taken together, nectin-1 is present on all keratinocytes during the differentiation processes while TJs are progressively formed until the cultures are fully stratified which, in turn, correlates with decreasing accessibility of nectin-1 to the virus.

To investigate whether the defective barriers in epidermal equivalents of nonlesional keratinocytes influence the localization of nectin-1 toward TJs, we visualized the receptor during barrier formation. At day 2, nectin-1 was present next to ZO-1 in the apical layer and only some areas with ZO-1 above nectin-1 were observed at day 4 (Fig. 5A) which correlated with fewer infected cells compared to day 2 (Fig. 3E). These results support that the delayed TJ formation results in better exposure of nectin-1 to the virus compared to 3D cultures of keratinocytes from healthy individuals. Even at day 8, when single infected cells were detected (Fig. 3F), the cultures of nonlesional keratinocytes did not resemble fully stratified epidermis (Fig. 5B) but only showed early cornification, as depicted by the filaggrin and loricrin stainings (Fig. 5C). Claudin-1 and nectin-1 were observed throughout the suprabasal layers while nectin-1 was also strongly present in the basal layer (Fig. 5D). Thus, we conclude that the defective cornified layer in addition to the underdeveloped TJs allows HSV-1 to access single cells.

Nectin-1 distribution in atopic dermatitis skin and in IL-4/IL-13-treated human skin. Recent infection studies revealed successful HSV-1 invasion in skin under pathological conditions such as atopic dermatitis skin, which is characterized by various disturbed barrier functions; we demonstrated the redistribution of the TJ markers claudin-1, ZO-1, and occludin in lesional skin samples supporting impaired TJ barriers (14). Here, we addressed whether redistribution of the TJ markers influences the presence and distribution of nectin-1, leading to viral entry in lesional atopic dermatitis skin. In control skin, nectin-1 was present in all epidermal layers, while distinct ZO-1 in the most apical nucleated layer was strictly above nectin-1, as expected (Fig. 6A). In contrast, the discontinuous ZO-1 in the granular layer of the thickened atopic dermatitis epidermis no longer localized above nectin-1 and was redistributed to the spinous layer (Fig. 6A). Nectin-1 was still observed on the expanded suprabasal layers, however, the stainings were more diffused (Fig. 6A), which unexpectedly correlates with increased nectin-1 transcript levels compared to controls (14). Costainings with claudin-1 further demonstrated nectin-1 throughout the granular layer with a punctate and reduced pattern of claudin-1 (Fig. 6B)

FIG 4 Legend (Continued)
nectin-1 (red) and claudin-1 (cldn; green) at the most apical nucleated cells, colocalization of nectin-1 and claudin-1 in the following slices and increased lateral nectin-1 in the third slice. (H) Three slices throughout the whole-mount preparation show the heterogeneous distribution of lateral nectin-1 (red) at suprabasal cells and the strong continuous nectin-1 staining in the basal layer. (I) Cross sections of epidermal equivalents at day 8 show strong nectin-1 (red) in the basal layer and colocalization with claudin-1 (green) in the spinous and granular layer except the most apical granular layer where only claudin-1 is present as shown in the magnification. Colocalization of E-cadherin (ecad; green) and nectin-1 (red) is shown in all epidermal layers. Transmission light (TL) visualizes the morphology of the nucleated and cornified layers. DAPI (blue) serves as a nuclear counterstain. Scale bars, 25 μm (A–H), 50 μm (I).

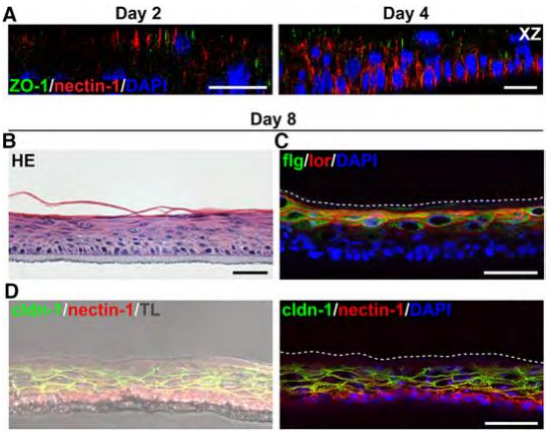

FIG 5 Distribution of nectin-1 in epidermal equivalents based on nonlesional AD keratinocytes. (A) Nectin-1 next to ZO-1 in the apical layer is depicted in the XZ axis. An area with ZO-1 above nectin-1 is shown at day 4. (B) HE-stained section shows the morphology with a thin cornified layer. (C) Filaggrin (flg; green) and loricrin (lor; red) are detected in the most apical nucleated layer. (D) Colocalization of claudin-1 (cldn-1; green) and nectin-1 was present in the suprabasal layers and increased nectin-1 stainings were observed in the basal layer. Transmission light (TL) visualizes the morphology and the dashed line indicates the border of the thin cornified layer. DAPI (blue) serves as a nuclear counterstain. Scale bars, 25 μm (A), 50 μm (B–D).

indicative of the strongly redistributed TJ marker in atopic dermatitis epidermis (14). As lesional skin is characterized by epidermal thickening resulting from the altered epidermal growth and keratinocyte terminal differentiation (32), we analyzed potentially redistributed AJs under impaired differentiation conditions and stained E-cadherin. This major AJ component was evenly distributed in the thickened atopic dermatitis epidermis and colocalized with nectin-1 throughout all layers, which was comparable to control skin suggesting that formation of AJs still takes place in the thickened epidermis (Fig. 6C). Our results indicate that impaired differentiation and defective TJs do not influence the presence of nectin-1 throughout the epidermal layers but most likely provide better accessibility of nectin-1 to HSV-1.

To further dissect the parameters that contribute to the viral access of nectin-1 under pathological conditions, we investigated the distribution of TJ and AJ components with regard to the presence of nectin-1 in healthy human skin samples stimulated with IL-4/IL-13. Recent studies demonstrated some penetration of HSV-1 via the skin surface after cytokine induction, although we observed no obvious impairment of the cornified layer (14). Here, we explored potential alterations of TJ components. Occludin, visible in the apical granular layer, showed a punctate staining pattern in IL-4/IL-13-treated skin compared to the distinct pattern in mock-treated skin (Fig. 7A). Although still present in the granular layer, ZO-1 was redistributed to the spinous layer of cytokine-stimulated epidermis (Fig. 7B) and whole-mount preparations visualized the change from a distinct to a punctate staining pattern of ZO-1 in the most apical granular layer (Fig. 7C). The distinct distribution of claudin-1 in mock-treated skin also changed to a punctate staining (Fig. 7E) and showed enhanced redistribution to the spinous and basal layers (Fig. 7D and E). These altered staining patterns support the idea that the IL-4/IL-13 treatment can induce impaired TJs. Costainings indicated relocalization of claudin-1 regarding nectin-1 in the most apical granular layer upon IL-4/IL-13 treatment (Fig. 7F), while we detected nectin-1 underneath ZO-1 both in mock- and cytokine-treated skin (Fig. 7G). As in atopic dermatitis epidermis, we found no obvious redistribution of E-cadherin throughout the IL-4/IL-13-treated skin (Fig. 7H). In summary, the cytokine-induced alterations of TJs and the presence of nectin-1 in the granular layer further supports that HSV-1 can gain access to its receptor just underneath impaired TJs.

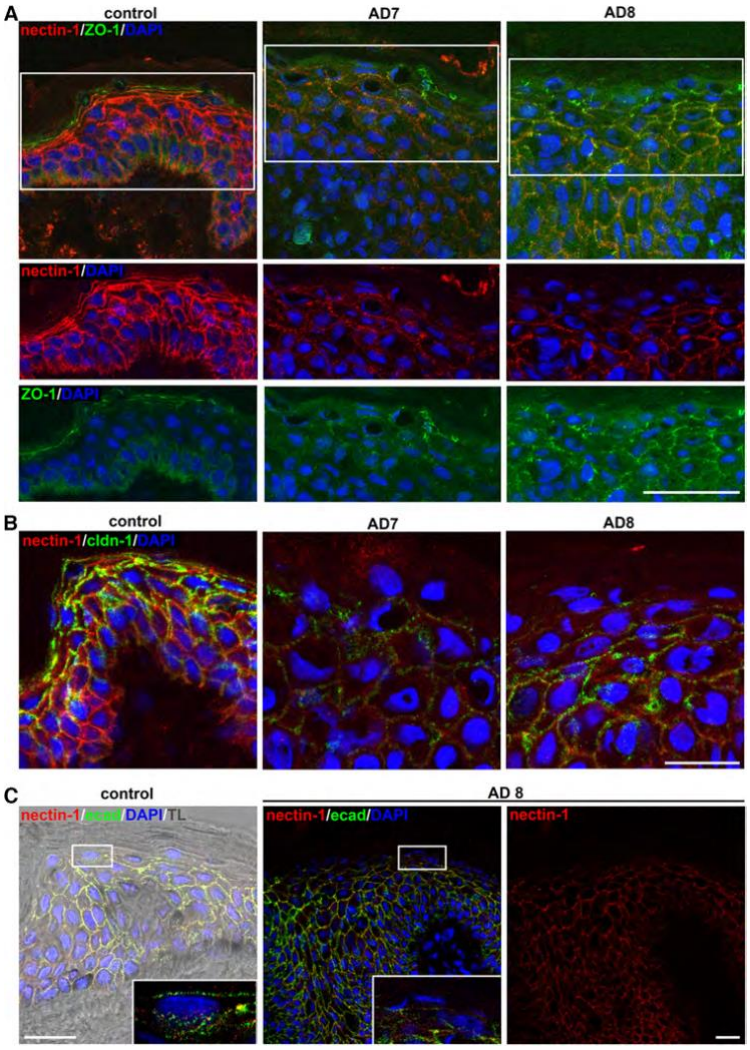

FIG 6 Localization of nectin-1 in atopic dermatitis skin. (A) Cross section of human control skin show nectin-1 (red) throughout the epidermal layers underneath the distinct staining of ZO-1 (green). Cross sections of thickened atopic dermatitis skin (samples AD7 and AD8) demonstrate the redistribution of ZO-1 in the granular and spinous layers compared to control skin. Nectin-1 stainings were diffused in AD7 and AD8 skin samples. (B) Control skin shows distinct claudin-1 in the granular layer while claudin-1 was reduced in AD7 and AD8 with a more punctate staining pattern. Costainings visualize nectin-1 throughout the suprabasal layers both in control and AD7/AD8 skin samples. (C) Colocalization of nectin-1 (red) and E-cadherin (ecad; green) is visible throughout the epidermis in control skin. Colocalization in the apical granular layer is magnified. Transmission light (TL) visualizes the morphology of the epidermis. The staining pattern of E-cadherin and nectin-1 is comparable in control and AD8 skin. DAPI (blue) serves as a nuclear counterstain. Scale bars, 25 μm (B, C), 50 μm (A).

DISCUSSION

As nectin-1 represents the primary receptor for HSV-1 entry, the intriguing question is how this component of AJs can be reached by HSV-1 upon exposure of human skin. Analyses of human skin revealed nectin-1 on 40% to 85% of epidermal cells, including

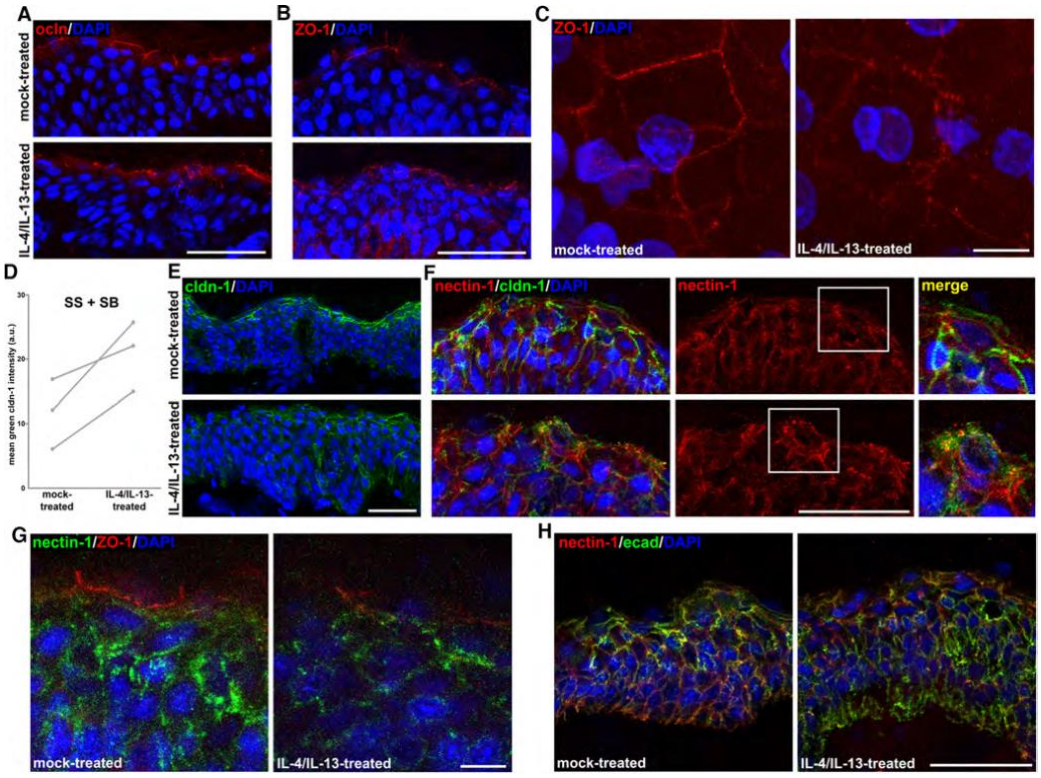

FIG 7 Localization of nectin-1 in IL-4/IL-13-treated human skin. (A) Cross sections depict distinct occludin (ocln; red) in the granular layer of mock-treated skin compared to punctate occludin staining after IL-4/IL-13 treatment ($n \geq 3$). (B) ZO-1 (red) was present in the granular layer and redistributed to the spinous layer in IL-4/IL-13-treated skin ($n \geq 3$). (C) Whole mount prepared from human skin after exfoliative toxin-A treatment visualizes the distinct ZO-1 staining (red) in the granular layer of mock-treated skin compared to the punctate ZO-1 staining after IL-4/IL-13 treatment. (D) Quantification of fluorescence shows increased claudin-1 in the stratum spinosum (SS) and the stratum basale (SB) after IL-4/IL-13 treatment ($n = 3$). (E) Cross sections show distinct claudin-1 (cldn-1; green) in mock-treated skin compared to punctate claudin-1 staining after IL-4/IL-13 treatment ($n \geq 3$). (F) Cross sections demonstrate the redistribution of claudin-1 (cldn-1; green) with regard to nectin-1 (red) in the most apical nucleated cells after IL-4/IL-13 treatment (magnification) and the presence of nectin-1 (red) throughout the epidermal layers of IL-4/IL-13- and mock-treated skin ($n = 3$). (G) Cross sections of the granular layer show nectin-1 (green) underneath ZO-1 (red) in mock- and IL-4/IL-13-treated skin ($n = 2$). (H) Cross sections visualize colocalization of E-cadherin (ecad; green) and nectin-1 (red), which was comparable in mock- and IL-4/IL-13-treated skin. DAPI (blue) serves as a nuclear counterstain. Scale bars, 50 μm (A, B, E), 10 μm (D, C).

undifferentiated and differentiated keratinocytes (13). While the variable nectin-1 expression correlated neither with age nor with skin area, it is still open whether the distribution throughout the epidermal layers can vary (13). Here, we demonstrated the distribution of nectin-1 in human epidermis and how the formation and impairment of TJ formation in human epidermis correlated with successful HSV-1 invasion which revealed the conditions under which nectin-1 was accessible to the virus. We found that TJ formation in stratified cultures of N/TERT-1 cells interfered with HSV-1 entry and infection of human epidermal equivalents confirmed that the extent of TJ formation during differentiation correlated with the number of infected cells in the suprabasal layers. While mature TJs limited viral invasion, early cornification during the differentiation process provided a further barrier, as uptake of beads as well as viral penetration was restricted. To follow up with studies in an epidermal model closer to *in vivo* skin homeostasis, we adopted epidermal equivalents based on primary human keratinocytes which showed some heterogeneity in their morphology more closely reflecting the situation in skin. During differentiation, cell areas with

TJ formation prevented viral penetration strengthening the role of TJs as effective barriers. Further TJ formation and early cornification processes strongly interfered with viral invasion; however, the contribution of the stratum corneum barrier remained vague. Barrier formation of the cornified layer and TJs have an interdependent relationship as cornification results from denucleation of keratinocytes of the granular layer and replacement of the plasma membranes by cornified lipid envelopes still harboring junction components (33). This makes it difficult to assess the contribution of each barrier in restricting HSV-1 invasion. *Ex vivo* infection of murine skin revealed that removal of the stratum corneum was insufficient to allow HSV-1 invasion, emphasizing the role of functional TJs (21).

To further explore the role of functional TJs and the cornified layer, we asked how impairment of epidermal barriers contribute to facilitated viral penetration. We confirmed that induction of Th2 responses by treatment of N/TERT-1 3D cultures results in impaired epidermal barriers (17, 25–27), as latex beads penetrated in the granular layer. However, viral penetration was still restricted, suggesting that additional demands of impaired barriers are needed for successful invasion. The challenge of HSV-1 is to gain access to its receptor nectin-1, implying that the virus must not only penetrate the cornified layer but must also overcome the TJs to reach nectin-1. We then investigated inflammation-induced effects on the early state of TJ formation in 3D cultures based on primary keratinocytes. Our results support that the cytokine responses after short induction by IL-4/IL-13 can already interfere with TJ development which, in turn, correlates with enhanced infection efficiency, suggesting that the Th2 cytokines can target the TJs rather early. Furthermore, enhanced infection was found in epidermal equivalents based on nonlesional atopic dermatitis keratinocytes, which demonstrated an intrinsic predisposition to defective barrier formation and strengthened the role of TJ formation. This finding further supports the idea that defective epidermal barriers of atopic dermatitis skin facilitate HSV-1 infection (14).

Next to barrier formation, the nectin-1 distribution in the epidermal layers plays a major role in understanding the viral access of the receptor. Nectin-1 was strongly present in the basal layer, as expected, and during differentiation, enriched lateral nectin-1 gradually decreased toward the most apical nucleated cells and was visible just underneath TJs. As HSV-1 can penetrate lesional skin of atopic dermatitis patients (14), we explored how these pathological skin conditions influence the presence and/or distribution of the receptor. Nectin-1 was present throughout all epidermal layers of atopic dermatitis skin; however, its distribution toward the TJ markers ZO-1 and claudin-1 strongly changed suggesting that impaired TJs make nectin-1 more accessible to the virus. Impaired TJs next to the well-known dysfunctions of the stratum corneum are implicated in atopic dermatitis (28, 34–36). Furthermore, defective TJs have been shown to modulate the barrier formation of the stratum corneum (37). Thus, we cannot dissect the impact of the individual barriers provided by either the stratum corneum or the TJs but suggest that the abnormal cornified layer of atopic dermatitis skin facilitates viral penetration and that only the impaired TJs allow viral access to its receptor nectin-1.

We also observed viral invasion via the skin surface after IL-4/IL-13 stimulation of human skin from healthy individuals, which was less efficient than in atopic dermatitis skin (14). Comparable to atopic dermatitis skin, claudin-1 was redistributed upon cytokine treatment and occludin and ZO-1 patterns were also changed. Although nectin-1 remained localized underneath ZO-1 as in mock-treated skin, the redistributed TJ components most likely indicate impaired TJ barriers which facilitate receptor accessibility. In contrast to atopic dermatitis skin, we observed no obvious defects of the cornified layer upon cytokine treatment of human skin (14). As reduced claudin-1 might alter the stratum corneum barrier (38, 39), we speculate that minor effects on the barrier function could contribute to limited viral invasion, while dysfunctional TJs led to nectin-1 accessibility.

Next to the physical barriers, Langerhans cells, as major players of the immune barrier, comprise an important element of the skin barrier. As epidermal Langerhans cells can elongate their dendrites to penetrate TJs (40), penetration of these mononuclear phagocytes might offer an alternative pathway to overcome the TJ barrier in epithelia with minor or no cornification. While infection of oral human mucosa or lesional atopic

dermatitis skin revealed no preferred infection of Langerhans cells (14, 21), initial infection of various skin mononuclear phagocytes was described in human foreskin epidermis characterized by minor cornification (41). Thus, the role of skin barriers for HSV-1 invasion is, most likely, tightly connected to the type of epithelia and the distribution of nectin-1.

Taken together, we conclude that access of HSV-1 to its receptor nectin-1 in human skin depends on dysfunctional TJs under pathological conditions such as in atopic dermatitis and in cytokine-treated skin which comprise multiple impaired physical barriers.

MATERIALS AND METHODS

Cells and human epidermal equivalents. The human keratinocyte cell line N/TERT-1 (18, 19) was maintained in K-SFM medium (Gibco) containing 0.4 mM $CaCl_2$, 25 μg/mL bovine pituitary extract (BPE), 0.2 ng/μL epidermal growth factor (EGF), 100 IU/mL penicillin, and 100 μg/mL streptomycin and was only grown up to 30% confluence to avoid spontaneous differentiation.

Primary keratinocytes isolated from human juvenile foreskin or adult breast skin were cultured on dishes coated with rat-tail collagen I (30 μg/mL) (Corning), maintained in CnT-PRIME epithelial proliferation medium (CELLnTEC), and grown until 70% confluence. Isolates of atopic dermatitis nonlesional keratinocytes (n = 2 individuals) were obtained from Ellen van den Bogaard (Radboud University Medical Center, Nijmegen).

For stratified cultures of N/TERT-1 cells, 1.5×10^5 cells were seeded in K-SFM medium on coverslips coated with rat-tail collagen I (40 μg/mL) (Corning). Stratification was induced 24 h postseeding by switching to differentiation medium by supplementing 1.8 mM Ca^{2+} to DMEM/Ham's F12 (1:3) (Life Technologies) containing 10% fetal calf serum (FCS; calcium free), penicillin (100 IU/mL), streptomycin (100 μg/mL), epidermal growth factor (EGF) (10 ng/mL), adenine (1.8×10^{-4} M), hydrocortisone (0.5 μg/mL), cholera toxin (10^{-10} M), insulin (5 μg/mL) and ascorbic acid (0.05 mg/mL). Cultures were refreshed with medium every other day and infected at day 1 or 8 post-calcium induction.

Human epidermal equivalents were generated with N/TERT-1 cells or with primary human keratinocytes isolated from skin of healthy individuals or from nonlesional skin of atopic dermatitis patients as described (19, 42). Briefly, 1.5×10^5 cells were seeded on transwell filters (pore size 0.4 μm) (Life Technologies) coated with rat-tail collagen I (100 μg/mL) (Corning) and grown to confluence in K-SFM medium (Gibco) for N/TERT-1 cells or in CnT-PRIME medium (CELLnTEC) for primary human keratinocytes. After 48 h, culture medium was replaced by 3D differentiation medium (80% CnT-3D barrier) (CELLnTEC)/20% DMEM (Sigma), and submerged culture inserts were grown for ca. 16 h and then lifted to the air-liquid interface for 8 days. Cultures were refreshed with differentiation medium every other day and infected at various times at day 0 or after airlift.

Preparation of human skin. For IL treatment, full-thickness skin samples which were taken from patients undergoing breast (n = 4 individuals) or plastic surgery (n = 3 individuals) were cut in pieces (ca. 4 × 4 mm) after removal of subcutaneous fat (43). After IL-treatment, epidermal whole mounts were prepared by mechanical removal of as much dermis as possible using surgical scissors. The remaining skin was floated onto a 200-μL droplet of exfoliative toxin A (2 mg/mL) (MyBioSource, MBS1223672) diluted in phosphate-buffered saline (PBS) containing 1 mM $CaCl_2$ and incubated at 37°C for 35 min in a humidified chamber. After incubation, the cornified and connected granular layers were separated from the underlying epidermal and remaining dermal layers using forceps.

Ethics statement. Human skin specimens were obtained after informed consent from all patients. The study was approved by the Ethics Commission of the Medical Faculty, University of Cologne (approval no. 17-481).

Interleukin treatment. To induce an atopic dermatitis-like phenotype, human skin samples and human epidermal equivalents were treated with IL-4 and IL-13. Immediately after surgery, skin samples were treated with IL-4 (25 ng/mL) and IL-13 (25 ng/mL) diluted in DMEM/high-glucose/GlutaMAX (Life Technologies) with 10% fetal calf serum (FCS), penicillin (100 IU/mL), streptomycin (100 μg/mL), and 0.05% bovine serum albumin (BSA) for 3 days. Epidermal equivalents derived from N/TERT-1 or primary human keratinocytes were treated with IL-4 (30 and 50 ng/mL, respectively) and IL-13 (30 and 50 ng/mL, respectively) dissolved in differentiation medium with 0.05% BSA (19, 25). IL-4/13 was added to the human epidermal equivalents at day 1 after airlifting. After 7 days of incubation, mock- and IL-4/13-treated N/TERT-1 epidermal equivalents were infected with HSV-1 at ca. 20 PFU/cell for 3 h. After 1 or 3 days of incubation, mock- and IL-4/13-treated epidermal equivalents from primary keratinocytes were infected with HSV-1 at ca. 50 PFU/cell for 2 h before removal of viral suspension, then further incubated for 4 h with a dry top. The medium containing IL-4/13 was refreshed every second day prior to infection.

Virus. Infection studies were performed with HSV-1 wild-type (Glasgow) strain 17+ from purified virus preparations obtained from the supernatant of infected BHK cells, as described (43). The calculation of the virus dose was based on the estimated cell number of the apical surface in the human epidermal equivalents at confluence (ca. 2.0×10^5). HSV-1 was administered to human epidermal equivalents at 37°C defining time point 0.

Penetration assay. Sulfate-modified polystyrene, fluorescently labeled latex beads (500 nm) (Sigma) served as a marker for penetration of particles in tissue. Human epidermal equivalents were incubated

with beads (2×10^9 beads/sample) for 3 h or 24 h at 37°C. Samples were thoroughly washed three times and immediately embedded for preparation of cryosections.

Histochemistry, immunocytochemistry, and antibodies. For hematoxylin and eosin (H&E) stains, human epidermal equivalents were fixed with 3.4% formaldehyde for 10 min at room temperature (RT) (day 0), 30 min at room temperature (day 2), or overnight at 4°C (day 4 to 8), and fixed samples were prepared as paraffin sections (8 μm). The morphology of the developing epidermal equivalents was assessed by H&E stains.

Stratified cultures and cells seeded on coverslips were fixed with 2% formaldehyde for 10 min at room temperature and permeabilized with 0.5% NP-40 (Sigma) in PBS for 10 min for staining of F-actin or left unpermeabilized for staining of nectin-1, occludin, and ZO-1.

For cryosections, epidermal equivalents and skin samples were embedded in OCT compound (Sakura), frozen at −80°C, and cut into 8-μm-thick cross sections (43). Cryosections were fixed with 2% formaldehyde for 10 min at RT, and epidermal whole-mount preparations of epidermal equivalents were fixed with 3.4% formaldehyde for 10 min at room temperature (day 0), 30 min at room temperature (day 2), or overnight at 4°C (day 4 to 8) (43). For stainings of nectin-1, claudin-1, occludin, and ZO-1, cryosections were fixed with ice-cold ethanol for 30 min and then with acetone (–20°C) for 3 min. Sections of skin and epidermal equivalents were incubated with primary antibodies overnight at 4°C followed by incubation with the species-specific Alexa Fluor-conjugated secondary antibodies and 4′,6-diamidino-2-phenylindole (DAPI) for 45 min at RT. Whole mounts of epidermal equivalents were incubated with primary antibodies overnight at RT and with the secondary antibodies and DAPI overnight at 4°C. The following primary antibodies were used: mouse anti-ICP0 (MAb 11060; 1:60) (44), rabbit anti-loricrin (1:1000; BioLegend), mouse anti-claudin-1 (1:500; A9; Santa Cruz), mouse anti-filaggrin (1:500; AKH1; Santa Cruz), mouse anti-occludin (1:400; OC-3F10; Thermo Fisher Scientific), mouse anti-E-cadherin (1:400; BD-610181; BD Biosciences), rabbit anti-ZO-1 (1:400; Thermo Fisher Scientific), and mouse anti-nectin-1 antibody (1:250 for whole mounts, 1:500 for cryosections; CK41) (45). F-actin was labeled with phalloidin-Atto 565 (1:2000) (Sigma) for 45 min at room temperature.

Microscopy was performed using an epifluorescence microscope (Zeiss Axiophot) equipped with a Nikon Digital Sight camera system (DS-2MV)/NIS Elements software (for H&E stains) and a Leica DM IRBE microscope linked to a Leica TCS-SP/5 confocal unit. Images were assembled using Photoshop (Elements 2018; Adobe) and Illustrator (version CS5; Adobe). Confocal projections and merged images are shown. Images were analyzed using Fiji (version 2.0.0-rc-65/1.51s) (46) by measuring the mean fluorescence intensity of three different areas per sample. XZ/YZ orthogonal and 3D projections of whole mounts were generated using Fiji (version 2.0.0-rc-65/1.51s) and Imaris X64 9.5.1 (Oxford Instruments Group), respectively.

Statistics. For the statistical analyses Student's *t* tests were performed to calculate *P* values using the unpaired two-tailed method. Differences were considered statistically significant with *P* values ≤ 0.05 (*).

Flow cytometric analysis. Epidermal equivalents (day 8) based on N/TERT-1 cells were incubated with TrypLE Select (Life Technologies) and processed as described (7). Dissociation of the epidermal equivalents resulted in the dissociation of basal and suprabasal cells; apical granular cells were not dissociated and still connected to the cornified layer as shown by H&E stains (data not shown). Cell suspensions were incubated in PBS-5% FCS on ice for 30 min with mouse anti-nectin-1 (CK41; 1:100) (45) and visualized with anti-mouse IgG-Cy5 (1:100) (Jackson Immunoresearch Laboratories Inc.). Mouse IgG1 (Life Technologies, 1:20) was used as isotype control.

ACKNOWLEDGMENTS

We thank Roger Everett for ICP0 antibodies and Ellen van den Bogaard for discussion.

This research was supported by the Deutsche Forschungsgemeinschaft (KN536/16-3), the Cologne Fortune Program/Faculty of Medicine, University of Cologne, and the Maria-Pesch foundation.

REFERENCES

1. Heldwein EE, Krummenacher C. 2008. Entry of herpesviruses into mammalian cells. Cell Mol Life Sci 65:1653–1668. https://doi.org/10.1007/s00018-008-7570-z.
2. Connolly SA, Jardetzky TS, Longnecker R. 2021. The structural basis of herpesvirus entry. Nat Rev Microbiol 19:110–121. https://doi.org/10.1038/s41579-020-00448-w.
3. Montgomery RI, Warner MS, Lum BJ, Spear PG. 1996. Herpes simplex virus-1 entry into cells mediated by a novel member of the TNF/NGF receptor family. Cell 87:427–436. https://doi.org/10.1016/s0092-8674(00)81363-x.
4. Geraghty RJ, Krummenacher C, Cohen GH, Eisenberg RJ, Spear PG. 1998. Entry of alphaherpesviruses mediated by poliovirus receptor-related protein 1 and poliovirus receptor. Science 280:1618–1620. https://doi.org/10.1126/science.280.5369.1618.
5. Shukla D, Liu J, Blaiklock P, Shworak NW, Bai X, Esko JD, Cohen GH, Eisenberg RJ, Rosenberg RD, Spear PG. 1999. A novel role for 3-O-sulfated heparan sulfate in herpes simplex virus 1 entry. Cell 99:13–22. https://doi.org/10.1016/s0092-8674(00)80058-6.
6. Eisenberg RJ, Atanasiu D, Cairns TM, Gallagher JR, Krummenacher C, Cohen GH. 2012. Herpes virus fusion and entry: a story with many characters. Viruses 4:800–832. https://doi.org/10.3390/v4050800.
7. Petermann P, Thier K, Rahn E, Rixon FJ, Bloch W, Özcelik S, Krummenacher C, Barron MJ, Dixon MJ, Scheu S, Pfeffer K, Knebel-Mörsdorf D. 2015. Entry mechanisms of herpes simplex virus 1 into murine epidermis: involvement of nectin-1 and herpesvirus entry mediator as cellular receptors. J Virol 89:262–274. https://doi.org/10.1128/JVI.02917-14.
8. Takai Y, Ikeda W, Ogita H, Rikitake Y. 2008. The immunoglobulin-like cell adhesion molecule nectin and its associated protein afadin. Annu Rev Cell Dev Biol 24:309–342. https://doi.org/10.1146/annurev.cellbio.24.110707.175339.
9. Rikitake Y, Mandai K, Takai Y. 2012. The role of nectins in different types of cell-cell adhesion. J Cell Sci 125:3713–3722. https://doi.org/10.1242/jcs.099572.
10. Mizutani K, Takai Y. 2016. Nectin spot: a novel type of nectin-mediated cell adhesion apparatus. Biochem J 473:2691–2715. https://doi.org/10.1042/BCJ20160235.
11. Tsukita S, Furuse M. 2002. Claudin-based barrier in simple and stratified cellular sheets. Curr Opin Cell Biol 14:531–536. https://doi.org/10.1016/s0955-0674(02)00362-9.
12. Thier K, Petermann P, Rahn E, Rothamel D, Bloch W, Knebel-Mörsdorf D. 2017. Mechanical barriers restrict invasion of herpes simplex virus 1 into human oral mucosa. J Virol 91:e01295-17. https://doi.org/10.1128/JVI.01295-17.

13. De La Cruz NC, Möckel M, Wirtz L, Sunaoglu K, Malter W, Zinser M, Knebel-Mörsdorf D. 2021. Ex vivo infection of human skin with herpes simplex virus 1 reveals mechanical wounds as insufficient entry portals via the skin surface. J Virol 95:e0133821. https://doi.org/10.1128/JVI.01338-21.
14. Möckel M, De La Cruz NC, Rübsam M, Wirtz L, Tantcheva-Poor I, Malter W, Zinser M, Bieber T, Knebel-Mörsdorf D. 2022. Herpes simplex virus 1 can bypass impaired epidermal barriers upon ex vivo infection of skin from atopic dermatitis patients. J Virol 96:e0086422. https://doi.org/10.1128/jvi.00864-22.
15. Goodyear HM. 2011. Eczema herpeticum. *In* Irvine AD, Hoeger PH, Yan AC (ed), Harper's textbook of pediatric dermatology, 3rd ed Wiley, New York, NY.
16. Damour A, Garcia M, Seneschal J, Lévêque N, Bodet C. 2020. Eczema herpeticum: clinical and pathophysiological aspects. Clin Rev Allergy Immunol 59:1–18. https://doi.org/10.1007/s12016-019-08768-3.
17. Niehues H, Bouwstra JA, El Ghalbzouri A, Brandner JM, Zeeuwen PLJM, van den Bogaard EH. 2018. 3D skin models for 3R research: the potential of 3D reconstructed skin models to study skin barrier function. Exp Dermatol 27:501–511. https://doi.org/10.1111/exd.13531.
18. Dickson MA, Hahn WC, Ino Y, Ronfard V, Wu JY, Weinberg RA, Louis DN, Li FP, Rheinwald JG. 2000. Human keratinocytes that express hTERT and also bypass a p16(INK4a)-enforced mechanism that limits life span become immortal yet retain normal growth and differentiation characteristics. Mol Cell Biol 20:1436–1447. https://doi.org/10.1128/MCB.20.4.1436-1447.2000.
19. Smits JPH, Niehues H, Rikken G, van Vlijmen-Willems IMJJ, van de Zande G, Zeeuwen PLJM, Schalkwijk J, van den Bogaard EH. 2017. Immortalized N/TERT keratinocytes as an alternative cell source in 3D human epidermal models. Sci Rep 7:11838. https://doi.org/10.1038/s41598-017-12041-y.
20. Sayers CL, Elliott G. 2016. Herpes simplex virus 1 enters human keratinocytes by a nectin-1-dependent, rapid plasma membrane fusion pathway that functions at low temperature. J Virol 90:10379–10389. https://doi.org/10.1128/JVI.01582-16.
21. Rahn E, Thier K, Petermann P, Rübsam M, Staeheli P, Iden S, Niessen CM, Knebel-Mörsdorf D. 2017. Epithelial barriers in murine skin during herpes simplex virus 1 infection: the role of tight junction formation. J Invest Dermatol 137:884–893. https://doi.org/10.1016/j.jid.2016.11.027.
22. O'Keefe EJ, Briggaman RA, Herman B. 1987. Calcium-induced assembly of adherens junctions in keratinocytes. J Cell Biol 105:807–817. https://doi.org/10.1083/jcb.105.2.807.
23. Lopez P, Van Sant C, Roizman B. 2001. Requirements for the nuclear-cytoplasmic translocation of infected-cell protein 0 of herpes simplex virus 1. J Virol 75:3832–3840. https://doi.org/10.1128/JVI.75.8.3832-3840.2001.
24. Petermann P, Haase I, Knebel-Mörsdorf D. 2009. Impact of Rac1 and Cdc42 signaling during early herpes simplex virus type 1 infection of keratinocytes. J Virol 83:9759–9772. https://doi.org/10.1128/JVI.00835-09.
25. Kamsteeg M, Bergers M, de Boer R, Zeeuwen PL, Hato SV, Schalkwijk J, Tjabringa GS. 2011. Type 2 helper T-cell cytokines induce morphologic and molecular characteristics of atopic dermatitis in human skin equivalent. Am J Pathol 178:2091–2099. https://doi.org/10.1016/j.ajpath.2011.01.037.
26. Danso MO, van Drongelen V, Mulder A, van Esch J, Scott H, van Smeden J, El Ghalbzouri A, Bouwstra JA. 2014. TNF-α and Th2 cytokines induce atopic dermatitis-like features on epidermal differentiation proteins and stratum corneum lipids in human skin equivalents. J Invest Dermatol 134:1941–1950. https://doi.org/10.1038/jid.2014.83.
27. Hönzke S, Wallmeyer L, Ostrowski A, Radbruch M, Mundhenk L, Schäfer-Korting M, Hedtrich S. 2016. Influence of Th2 cytokines on the cornified envelope, tight junction proteins, and ß-defensins in filaggrin-deficient skin equivalents. J Invest Dermatol 136:631–639. https://doi.org/10.1016/j.jid.2015.11.007.
28. Bergmann S, von Buenau B, Vidal-Y-Sy S, Haftek M, Wladykowski E, Houdek P, Lezius S, Duplan H, Bäsler K, Dähnhardt-Pfeiffer S, Gorzelanny C, Schneider SW, Rodriguez E, Stölzl D, Weidinger S, Brandner JM. 2020. Claudin-1 decrease impacts epidermal barrier function in atopic dermatitis lesions dose-dependently. Sci Rep 10:2024. https://doi.org/10.1038/s41598-020-58718-9.
29. De La Cruz N, Knebel-Mörsdorf D. 2021. Endocytic internalization of herpes simplex virus 1 in human keratinocytes at low temperature. J Virol 95:e02195-20. https://doi.org/10.1128/JVI.02195-20.
30. Jensen JM, Fölster-Holst R, Baranowsky A, Schunck M, Winoto-Morbach S, Neumann C, Schütze S, Proksch E. 2004. Impaired sphingomyelinase activity and epidermal differentiation in atopic dermatitis. J Invest Dermatol 122:1423–1431. https://doi.org/10.1111/j.0022-202X.2004.22621.x.
31. Suárez-Fariñas M, Tintle SJ, Shemer A, Chiricozzi A, Nograles K, Cardinale I, Duan S, Bowcock AM, Krueger JG, Guttman-Yassky E. 2011. Nonlesional atopic dermatitis skin is characterized by broad terminal differentiation defects and variable immune abnormalities. J Allergy Clin Immunol 127:954–964.e1-4. https://doi.org/10.1016/j.jaci.2010.12.1124.
32. Guttman-Yassky E, Suárez-Fariñas M, Chiricozzi A, Nograles KE, Shemer A, Fuentes-Duculan J, Cardinale I, Lin P, Bergman R, Bowcock AM, Krueger JG. 2009. Broad defects in epidermal cornification in atopic dermatitis identified through genomic analysis. J Allergy Clin Immunol 124:1235–1244.e58. https://doi.org/10.1016/j.jaci.2009.09.031.
33. Yokouchi M, Kubo A. 2018. Maintenance of tight junction barrier integrity in cell turnover and skin diseases. Exp Dermatol 27:876–883. https://doi.org/10.1111/exd.13742.
34. De Benedetto A, Rafaels NM, McGirt LY, Ivanov AI, Georas SN, Cheadle C, Berger AE, Zhang K, Vidyasagar S, Yoshida T, Boguniewicz M, Hata T, Schneider LC, Hanifin JM, Gallo RL, Novak N, Weidinger S, Beaty TH, Leung DY, Barnes KC, Beck LA. 2011. Tight junction defects in patients with atopic dermatitis. J Allergy Clin Immunol 127:773–786.e17. https://doi.org/10.1016/j.jaci.2010.10.018.
35. De Benedetto A, Slifka MK, Rafaels NM, Kuo IH, Georas SN, Boguniewicz M, Hata T, Schneider LC, Hanifin JM, Gallo RL, Johnson DC, Barnes KC, Leung DY, Beck LA. 2011. Reductions in claudin-1 may enhance susceptibility to herpes simplex virus 1 infections in atopic dermatitis. J Allergy Clin Immunol 128:242–246.e5. https://doi.org/10.1016/j.jaci.2011.02.014.
36. Gruber R, Börnchen C, Rose K, Daubmann A, Volksdorf T, Wladykowski E, Vidal-Y-Sy S, Peters EM, Danso M, Bouwstra JA, Hennies HC, Moll I, Schmuth M, Brandner JM. 2015. Diverse regulation of claudin-1 and claudin-4 in atopic dermatitis. Am J Pathol 185:2777–2789. https://doi.org/10.1016/j.ajpath.2015.06.021.
37. Yuki T, Komiya A, Kusaka A, Kuze T, Sugiyama Y, Inoue S. 2013. Impaired tight junctions obstruct stratum corneum formation by altering polar lipid and profilaggrin processing. J Dermatol Sci 69:148–158. https://doi.org/10.1016/j.jdermsci.2012.11.595.
38. Haftek M, Callejon S, Sandjeu Y, Padois K, Falson F, Pirot F, Portes P, Demarne F, Jannin V. 2011. Compartmentalization of the human stratum corneum by persistent tight junction-like structures. Exp Dermatol 20:617–621. https://doi.org/10.1111/j.1600-0625.2011.01315.x.
39. Igawa S, Kishibe M, Murakami M, Honma M, Takahashi H, Iizuka H, Ishida-Yamamoto A. 2011. Tight junctions in the stratum corneum explain spatial differences in corneodesmosome degradation. Exp Dermatol 20:53–57. https://doi.org/10.1111/j.1600-0625.2010.01170.x.
40. Kubo A, Nagao K, Yokouchi M, Sasaki H, Amagai M. 2009. External antigen uptake by Langerhans cells with reorganization of epidermal tight junction barriers. J Exp Med 206:2937–2946. https://doi.org/10.1084/jem.20091527.
41. Bertram KM, Truong NR, Smith JB, Kim M, Sandgren KJ, Feng KL, Herbert JJ, Rana H, Danastas K, Miranda-Saksena M, Rhodes JW, Patrick E, Cohen RC, Lim J, Merten SL, Harman AN, Cunningham AL. 2021. Herpes Simplex Virus type 1 infects Langerhans cells and the novel epidermal dendritic cell, Epi-cDC2s, via different entry pathways. PLoS Pathog 17:e1009536. https://doi.org/10.1371/journal.ppat.1009536.
42. Niehues H, Schalkwijk J, van Vlijmen-Willems IMJJ, Rodijk-Olthuis D, van Rossum MM, Wladykowski E, Brandner JM, van den Bogaard EHJ, Zeeuwen PLJM. 2017. Epidermal equivalents of filaggrin null keratinocytes do not show impaired skin barrier function. J Allergy Clin Immunol 139:1979–1981.e13. https://doi.org/10.1016/j.jaci.2016.09.016.
43. De La Cruz NC, Möckel M, Wirtz L, Knebel-Mörsdorf D. 2022. Ex vivo human skin infection with herpes simplex virus 1. Bio Protoc 12:e4411. https://doi.org/10.21769/BioProtoc.4411.
44. Everett RD, Cross A, Orr A. 1993. A truncated form of herpes simplex virus type 1 immediate-early protein Vmw110 is expressed in a cell type dependent manner. Virology 197:751–756. https://doi.org/10.1006/viro.1993.1651.
45. Krummenacher C, Baribaud I, Ponce de Leon M, Whitbeck JC, Lou H, Cohen GH, Eisenberg RJ. 2000. Localization of a binding site for herpes simplex virus glycoprotein D on herpesvirus entry mediator C by using antireceptor monoclonal antibodies. J Virol 74:10863–10872. https://doi.org/10.1128/jvi.74.23.10863-10872.2000.
46. Schindelin J, Arganda-Carreras I, Frise E, Kaynig V, Longair M, Pietzsch T, Preibisch S, Rueden C, Saalfeld S, Schmid B, Tinevez JY, White DJ, Hartenstein V, Eliceiri K, Tomancak P, Cardona A. 2012. Fiji: an open-source platform for biological-image analysis. Nat Methods 9:676–682. https://doi.org/10.1038/nmeth.2019.

3.6 Publication 5: Susceptibility of Human and Murine Dermal Fibroblasts to Herpes Simplex Virus 1 in the Absence and Presence of Extracellular Matrix

Authors:	Lisa Wirtz, Nydia C De La Cruz, Maureen Möckel, and Dagmar Knebel-Mörsdorf
Journal:	Journal of Virology
Date of Publication:	15 December 2021
PMID:	34908440
PMCID:	PMC8865408
DOI:	doi:10.1128/JVI.02068-21

Conception and design of the study was done by DKM together with LW. **NDLC** performed, processed, and analyzed the experiments involving the particle penetration assays using latex bead uptake in human dermis, human skin shaves, HFFF2 cells, and murine dermis summarized in Fig 3. **NDLC** also performed, processed, and analyzed experiments involving viral localization studies shown in Fig 4. The manuscript was written by DKM with comments, criticisms, and revisions by **NDLC** and LW. The figures were assembled by **NDLC**.

3.7 Publication 6: *Ex vivo* Human Skin Infection with Herpes Simplex Virus 1

Authors:	Nydia C De La Cruz, Maureen Möckel, Lisa Wirtz, and Dagmar Knebel-Mörsdorf
Journal:	Bio-protocol
Date of Publication:	5 May 2022
PMID:	35800458
PMCID:	PMC9090582
DOI:	doi:10.21769/BioProtoc.4411

The major aim of our lab is to investigate the very early HSV-1 entry events and initial invasion process in human skin, thus the development of an *ex vivo* infection assay using human skin explants serves as an experimental tool to address the various questions involved. The following protocol details the major methods, techniques, and possible pitfalls involved in our *ex vivo* infection studies using human skin.

The manuscript was written by **NDLC**, MM, and DKM. Figures were assembled by MM and **NDLC**.

4. Discussion

4.1 Cellular internalization of HSV-1: the impact of endocytosis in successful viral entry

As a prevalent human pathogen, HSV-1 has found ways to exploit multiple mechanisms to accomplish cellular entry in a given target cell. One focus of this study was to investigate entry in human keratinocytes, a major *in vivo* HSV-1 target, where the virus has previously been shown to appropriate dual uptake mechanisms—fusion directly at the plasma membrane and endocytic modes of entry (Rahn et al., 2011). Irrespective of whether fusion occurs directly at the plasma membrane or in a vesicle membrane, the highly dynamic entry pathways share conserved fusion machineries which makes analyzing the impact of either entry pathway to successful HSV-1 infection difficult. Since endocytosis is an energy-requiring process, we employed infection of keratinocytes at low temperature (7°C) in De La Cruz and Knebel-Mörsdorf (2020) to selectively block endocytic mechanisms while allowing direct fusion at the plasma membrane to proceed (Larrick et al., 1985; reviewed by Lippincott-Schwartz et al., 2000). This was confirmed by the inhibited uptake of the markers cholera toxin B, dextran, and fluorescently-labelled latex beads showing that receptor-mediated endocytic mechanisms, macropinocytosis, and phagocytosis do not proceed at 7°C.

Intriguingly, ICP0-expressing cells were found, although delayed compared to internalization at 37°C, after viral exposure at low temperature. This finding brought forth the initial hypothesis that direct plasma membrane fusion is the primary mode of entry at 7°C, a temperature where endocytic uptake mechanisms should not proceed. Indeed, ultrastructural analyses (TEM) revealed evidence of HSV-1 particles undergoing direct fusion and free nucleocapsids just underneath the plasma membrane in line with a previous study which attributed low temperature HSV-1 entry in N/TERT and HaCaT keratinocytes solely on direct plasma membrane fusion (Sayers and Elliot, 2016). However, our TEM studies also strikingly revealed enveloped virus particles contained within vesicles at 7°C. Interestingly, the vesicles found at 7°C were unusually large and often contained several HSV-1 particles. These findings were reminiscent of results from a previous study using nectin-1 knockout (KO) primary murine keratinocytes which found large vesicles containing multiple virus particles; however since ICP0-expressing cells were rarely found in these cells, the virus particles found

within vesicles were most likely sent for lysosomal degradation (Petermann et al., 2015b). The abortive fate of virus within vesicles in nectin-1 KO primary murine keratinocytes, which also showed barely detectable levels of alternative receptor HVEM, is feasible as gD binding to a cellular receptor is a pre-requisite for HSV-1 cellular entry. Contrary to findings in murine keratinocytes, however, the TEM analyses of human keratinocytes at low temperature in De La Cruz and Knebel-Mörsdorf (2020) showed HSV-1 particles undergoing fusion with a vesicle membrane providing evidence that endocytic internalization at 7°C did not lead to abortive infection but instead led to successful cellular entry.

In an effort to characterize the endocytic vesicles found in human keratinocytes at 7°C, serial sections were employed in our TEM studies. Serial sections demonstrated the efficiency of HSV-1 entry at low temperature since in any given area, multiple virus particles are undergoing cellular internalization whether the particles are directly fusing at the plasma membrane or fusing with a vesicle membrane. Moreover, the serial sections visualized the extent and gravity of these large, virus-containing vesicles. Because of their large size, vesicle uptake at low temperature could point to macropinocytosis as a putative candidate for HSV-1 cellular entry. While macropinocytosis is usually associated with the nonspecific uptake of large amounts of extracellular fluid, this mechanism was briefly suggested in a previous study using CHO and HeLa cells which not only found virus particles within large vesicles in ultrastructural analyses, but also found the co-localization of HSV-1 with the fluid-phase uptake marker dextran (Nicola et al., 2005). Since we found only very limited uptake of dextran at 7°C, it is likely that the vesicle entry mechanism at low temperature is not distinctly macropinocytosis but is rather a previously uncharacterized, unconventional endocytic pathway that employs macropinocytic-like features.

4.2 HSV-1 invasion in human skin

While viral entry of HSV-1 are thoroughly investigated in cultured cells, viral invasion in tissue is only beginning to be unravelled. Since HSV-1 must first find ways to bypass epithelial barriers before reaching its cellular receptors for entry, elucidating mechanisms involved in viral invasion at the tissue level is another main focus in our studies. Here, we addressed the initial invasion process in human skin in an effort to identify cellular and molecular determinants that facilitate or impede the virus in overcoming epidermal barriers and initiate infection.

4.2.1 The susceptibility of human skin to *ex vivo* HSV-1 infection

Representing one of HSV-1's major *in vivo* targets, the human skin provides multiple barriers against viral invasion. Physical barriers of the skin are provided by the SC as well as the integrity of the underlying epidermal layers mediated by cellular junctions, in particular TJs. However, since a variety of viruses exploit transmembrane proteins of cellular junctions as receptors for cellular entry (in the way that HSV-1 hijacks the AJ component nectin-1), understanding the molecular mechanisms involved during HSV-1 invasion of the skin is an important aspect in skin pathology (Mateo et al., 2015). To explore under which circumstances HSV-1 is able to approach its cellular receptors and initiate infection in tissue, we employed *ex vivo* infection studies of human skin samples in De La Cruz et al. (2021).

Initial experiments focused on determining the susceptibility of the human epidermal layers to *ex vivo* HSV-1 infection. Previous studies using murine skin found that once the epidermis is separated from the underlying basement membrane and dermis, efficient infection was observed in basal as well as in the differentiated suprabasal keratinocytes (Rahn et al., 2015b). We confirmed that the isolated human epidermis is also susceptible to *ex vivo* infection, commencing as single, infected basal keratinocytes and then spreads to the suprabasal layers over time (Fig. 7). Compared to murine epidermis, HSV-1 infection of the human epidermal layers does not rapidly occur, taking 3 hours before the first indication of infected basal cells and at least 6 to 9 hours for infected suprabasal cells to appear. Moreover, it can take as long

as 24 hours until granular cells can be infected which is accompanied by cytopathic effects (CPE) which may have helped facilitate viral access.

Concomitantly, the invasion route and delay in infection of human skin poses a question as to how the virus spreads from one basal cell to another as well as cells of the overlying suprabasal layers. HSV-1 can possibly undergo (1) cell-free spread in which free-floating virus from the input inoculum or from produced viral progeny achieves access to other layers after loss of epithelial integrity or (2) cell-to-cell spread in which the virus passes directly through the cellular junctions in order to infect neighboring cells (Johnson and Huber, 2002; Mateo et al., 2015). In an effort to understand whether the delayed onset of infection was due to spread of viral progeny or by the loss of tissue integrity over time, we blocked viral replication to prevent the contribution of viral production during infection. Interestingly, all epidermal layers including cells of the upper granular layer were still infected in the absence of viral replication. Moreover, inhibiting viral replication did not rescue effects of tissue integrity loss which suggests that early infection already leads to tissue damage including disrupted cellular junctions that may thereby expose upper layers of the epidermis for infection. Virus-induced tissue damage was further supported by the application of latex beads, which at 500 nm is around twice in size as HSV-1. While epidermal sheets incubated in bead-containing medium alone only led to limited penetration in suprabasal layers, co-incubation of virus and beads in the same suspension led to the enhanced penetration of beads up to the granular cells. This suggests that infection of the underlying epidermal layers induces tissue damage and disruptions to cellular junctions that precedes access of the virus to all layers of the epidermis.

The high susceptibility of the human epidermis to *ex vivo* HSV-1 infection is only achieved after the separation of the dermis. Since dermal fibroblasts also represent an *in vivo* HSV-1 target during primary infection and reactivation, the isolated dermis after separation from the epidermis was also subjected to *ex vivo* infection in De La Cruz et al. (2021). However, this only led to rare infected cells restricted to the papillary dermis whereas previous studies using juvenile murine dermis found a higher occurrence of infected cells (Fig. 7; Wirtz et al., 2020). The higher susceptibility of murine dermis to HSV-1 may be due to a higher nectin-1 expression in murine dermal cells compared to the surface expression values found in human (Wirtz et al., 2020). To further explore the species-specific differences in the susceptibility of

dermal tissue to HSV-1 infection, the penetration of latex beads in human and murine dermis was explored in Wirtz et al. (2022). In both human and murine dermis, latex beads were restricted to the upper papillary dermis, although slightly more efficient uptake in murine compared to human dermis was found. Restricted latex bead penetration may be attributed to the differences in organization between the papillary and reticular dermis. While the papillary dermis is home to a dense fibroblast population and thin collagen fibrils, the reticular dermis contains a densely packed extracellular matrix (ECM) with large collagen fibrils (Sorrell and Caplan, 2004; Driskell et al., 2013). Visualization of virus particles in infected human dermis by staining the viral capsid component VP5 supports that the virus is only granted limited access to the upper part of the papillary dermis.

Interestingly, murine and human dermal fibroblasts are highly susceptible to HSV-1 infection once they are taken into culture (Petermann et al., 2015a). Multiple parameters may contribute to the low infection efficiency of dermal fibroblasts in tissue. Studies have found that the basement membrane serves as a barrier against HSV-1 (Weeks et al., 2000). However, since the basement membrane zone region is cleaved during dispase treatment, components of the basement membrane are likely not effective agents against HSV-1 penetration in the isolated human dermis (Stenn et al., 1989). What more likely contributes is the ECM. While Wirtz et al. (2022) observed only a slight delay in infection of the otherwise highly susceptible primary human fibroblasts after collagen embedding, previous studies using murine fibroblasts found a strong delay thus supporting a role for the ECM (Wirtz et al., 2020). Taken together, organizational and structural differences in ECM organization may reflect the less efficient HSV-1 invasion and bead penetration in human compared to murine dermis.

4.2.2 Mechanical wounds are insufficient entry portals for HSV-1 invasion

While the human epidermis and dermis are susceptible to *ex vivo* HSV-1 infection after separation from one another, infection of full-thickness skin, as expected, provides effective barriers against apical HSV-1 invasion. In De La Cruz et al. (2021), *ex vivo* infection of total skin samples demonstrated infected cells only at the sample edges (Fig. 7). This is in line with previous *ex vivo* infection studies using murine skin in which HSV-1 penetration via the apical surface was not found (Rahn et al., 2017). Moreover, since infection of sample edges in

human skin only occurred after long incubation times with the virus (at least 16 h post-infection), it can be presumed that loss of the basement membrane at the sample edges precedes HSV-1 access to receptors on epidermal keratinocytes. Since integrity loss at the sample edge also occurs after incubation in medium alone, the effects are most likely not virus-induced (data not shown). It could be presumed that HSV-1 invasion at the sample edges undergo an invasion route similar to that of the isolated epidermis, in which basal keratinocytes are infected first (which are completely exposed after basement membrane integrity loss) before spreading to neighboring cells and overlying epidermal layers (Fig. 7). Together, infection studies of total skin samples strengthens the role of physical epidermal barriers in restricting HSV-1 access from the apical surface.

While intact, full-thickness skin is resistant to HSV-1 invasion, it is generally assumed that skin lesions can provide entry portals for HSV-1. *In vivo*, primary HSV-1 infections have been found in damaged skin resulting from burn wounds or mechanical abrasion (Foley et al., 1970; Shenoy et al., 2015). Previous studies using murine skin found that the wounding strategy of slitting newborn back or adult tail skin with a scalpel demonstrated no infected cells (Rahn et al., 2017). Moreover, wax stripping of newborn back skin to remove the cornified layer only led to rare, single infected cells underneath the granular layer (Rahn et al., 2017). In this study, we utilized the use of microneedles as a more reproducible wounding method to introduce mechanical lesions that give access to the various epidermal layers as well as the underlying dermis. A recent study that aimed to provide an *ex vivo* infection model for the study of antiviral drugs suggested that microneedle-pretreatment of human abdominal skin led to productive HSV-1 infection (Tajpara et al., 2019). However, our findings showed that microneedle wounding of full-thickness skin was insufficient in providing entry for HSV-1 in which only one out of 13 patient samples led to viral invasion. Thus, mechanically introduced lesions in total skin biopsies are not sufficient for *ex vivo* HSV-1 infection from the apical surface. In contrast, microneedle treatment of skin shaves, in which wounds penetrated all the way through the dermal layer led to efficient infection. This led to the hypothesis that wounded shaves allow virus access from the open dermal layer. Thus, it can be proposed that the invasion route in wounded skin shaves is reminiscent of *ex vivo* infection of isolated human epidermis in which HSV-1 invasion commences in the exposed basal keratinocytes to later gain access to upper epidermal layers. One possible explanation may be that CPE on cells

of the basal layer destroy cellular junctions to expose cellular receptors and does so in a ripple effect to cells of the overlying epidermal layers. Whether the successful infection of the basal keratinocytes acts as a prerequisite for viral invasion of the upper epidermal layers in full thickness skin is still open.

Since our *ex vivo* wounding and infection model of human biopsies lacks the aspect of mechanical skin tension (from body movement, stretching, friction, etc.) that is present during *in vivo* conditions, we sought to understand whether wound closure could contribute to the inhibited viral access in full-thickness skin. A classical representation of wound closure is depicted by the purse-string model in which the cells on the separated wounded edge are laterally linked and closed as if they were pulled together by a string composed of actomyosin ring contractions (Kiehart, 1999; reviewed in Harn et al., 2019). Thus to determine whether wound closure prevented access to the cells of the epidermis, we utilized fluorescently-labelled latex beads (500 nm) to assess whether the administered lesions allowed particles to penetrate the wounded areas at all. Strikingly, we found that incubation of wounded full-thickness skin samples with fluorescently-labelled latex beads harbored large clusters of internalized beads in some lesions while a few beads are found in more closed lesions (Fig. 7). This asserts that, in general, HSV-1 particles should at least have access to areas in close vicinity of its target keratinocytes in some wounds. Moreover, since both wounds (open and closed) did not harbor infected cells, we assume that wound closure is not the reason for restricted viral infection. Rather, it may be the lack of sufficient access to receptors on both open and closed wounds that restricts successful viral invasion.

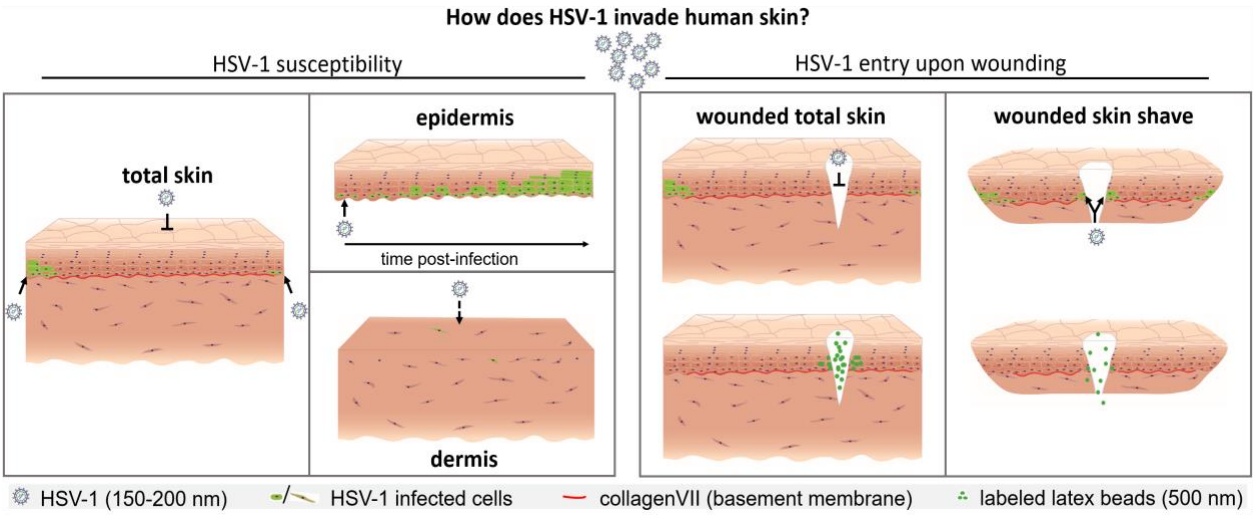

Figure 7. Schematic summary of HSV-1 entry in human skin and upon wounding.
Ex vivo infection of full-thickness (total skin) resulted in infected cells only at the sample edges. Separation of the epidermis from the dermis allows the virus access to basal keratinocytes with spreading to suprabasal layers over time. In the isolated dermis, viral access is limited to single cells of the upper papillary dermis. While wounding of full-thickness skin does not give virus sufficient access to cellular receptors for infection, wounds allow efficient access for latex bead (500 nm) penetration via the apical skin surface as well as via damaged dermal layer in wounded skin shaves. Moreover, basal keratinocytes are infected in wounded skin shaves where the virus most likely gained access via the damaged dermal layer (De La Cruz et al., 2021).

4.2.3 Mimicking pathological phenotypes that allow HSV-1 entry

For successful infection, HSV-1 must bypass epidermal barriers of human skin through epithelial breaks or a pathologically impaired barrier function. While the wounded skin surface allowed particle penetration of latex beads, HSV-1 invasion was surprisingly not permitted after *ex vivo* infection suggesting that further modifications are required for successful invasion. Individuals with the chronic, pruritic inflammatory skin disease atopic dermatitis (AD) can be seriously afflicted by cutaneous viral infections in which the most commonly recognized condition, *eczema herpeticum*, is caused by HSV. As a complex, multifactorial disease with a wide spectrum of clinical phentoypes, AD is associated with skin microbiome imbalance, immune response alterations, and epidermal barrier impairment which could act as predisposing risk factors for the higher susceptibility to HSV-1 (Bussmann et al., 2008; Beck et al., 2009; Damour et al., 2020). Our *ex vivo* infection method allows us to

mainly focus on whether AD-associated dysfunctional epidermal barriers can facilitate the initial steps of HSV-1 invasion. Indeed, in Möckel et al. (2022) we found that HSV-1 can invade lesional AD skin via the apical skin surface to infect cells of the suprabasal layers. The dysfunctional epidermal barriers were confirmed in the skin samples by SC and TJ barrier stainings, although in varying degrees throughout the different AD samples (Möckel et al., 2022).

AD is considered an archetypal type 2 immunity-driven disease and thus Th2 cytokine-driven inflammation are among parameters that could contribute to skin barrier dysfunction (Homey et al., 2006; reviewed in Beck et al., 2022). However, whether the dysregulated immune response is a result of skin barrier abnormalities or rather the trigger that give rise to deficient barriers is not fully understood. Recent studies have shown that the supplementation of Th2 cytokines in human epidermal equivalents induce *in vitro* hallmarks of AD skin on the lipid and protein level (Danso et al., 2014). Thus, in Möckel et al. (2022), we further assessed the parameters that contribute to HSV-1 invasion in AD skin by stimulating nonpathological skin with IL-4 and IL-13 to examine whether Th2 cytokine-driven inflammation can induce sufficient modifications in the skin to drive viral penetration *per se*. Indeed, *ex vivo* HSV-1 infection of IL-4/IL-13-stimulated human skin demonstrated successful viral invasion via the apical skin surface. The vast majority of associated barrier defects described for AD involves components of the SC. In particular, a loss-of-function mutation in the filaggrin gene is a well-known genetic risk factor for AD development (Brown and McLean, 2012; McAleer and Irvine, 2013). Indeed, we found significantly decreased filaggrin stainings in the AD skin samples compared to nonpathological skin (Möckel et al., 2022). However, our initial attempt in Möckel et al. (2022) to visualize putative IL-induced barrier alterations demonstrated no obvious change in filaggrin staining distribution and intensity suggesting that HSV-1 invasion upon IL-stimulation is likely not driven by impairments in the SC.

Apart from SC barrier defects, AD skin also characterized by impairments of the TJ barrier (Brandner et al., 2015; Kobielak and Boddupally, 2014). TJs have historically been considered a secondary epidermal barrier behind the SC, however, more recent evidence have revealed their crucial roles in skin barrier function. Thus, TJ barrier deficiencies could putatively be involved in the facilitated HSV-1 invasion of IL-stimulated skin independent of the SC. Indeed,

while we found no obvious change in filaggrin stainings in Möckel et al. (2022), our most recent findings showed a strong redistribution of the TJ protein claudin-1 upon IL-4/IL-13 induction (De La Cruz et al., to be submitted). The importance of claudin-1 in the mammalian skin barrier has been extensively shown. Claudin-1-deficient mice undergo a dramatic loss of water and die within one week of birth (Furuse et al., 2002). Meanwhile, human individuals who exhibit claudin-1 null mutations suffer from neonatal icthyosis sclerosing cholangitis (NISCH) syndrome and although it is not lethal, patients exhibit icthyosiform skin alterations and develop liver disease (Feldmeyer et al., 2006; Hadj-Rabia et al., 2004). Interestingly, while we found a decrease of claudin-1 in the granular layers coupled with a redistributed increase in the lower epidermal layers of the IL-induced human skin explants, another study using Th2 cytokine-induced human epidermal equivalents found a decrease of claudin-1 in lower epidermal layers (Gruber et al., 2015). This may be reflective of the claudin-1 genetic differences found in distinct AD populations and subgroups (reviewed in Bäsler and Brandner, 2017).

In addition to redistributed claudin-1, occludin and ZO-1 also exhibited changes, as staining of human skin explants after IL-treatment showed more punctate signals in the upper granular layer compared to mock-treated samples. While occludin is dispensible, both ZO-1 and claudin-1 are crucial for the barrier function of TJs. In fact, ZO-1 is required for the polymerization and localization of claudin-1 at TJs (Umeda et al., 2006). Changes in TJ staining distribution in IL-treated skin suggests epidermal barrier impairment which could possibly allow HSV-1 better access to its cellular receptors to initiate infection in the skin.

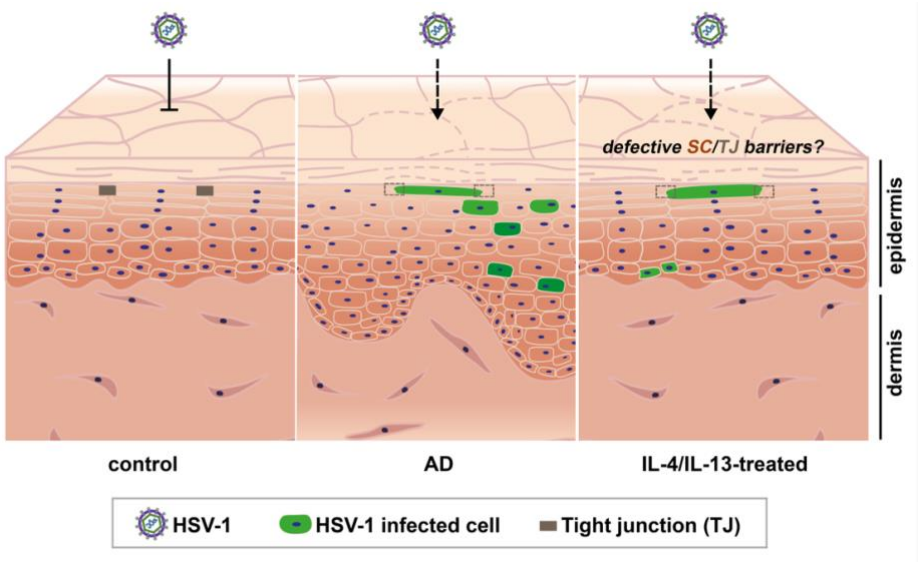

Figure 8. Schematic summary of HSV-1 entry in human skin under pathological conditions
In nonpathological skin conditions, the stratum corneum (SC) and tight junctions (TJ) provide effective barriers to inhibit HSV-1 invasion from the skin surface. Atopic dermatitis (AD) skin, on the other hand, is characterized by epidermal thickening, impaired SC barriers (dotted lines) as well as dysunctional TJ barriers (dotted boxes). IL-4/IL-13 stimulation of healthy, human skin may result in impaired SC and dysfunctional TJ barriers (modified from Möckel et al., 2022).

4.3 Localization of the cellular receptor nectin-1

After overcoming barriers of the human epidermis, the fundamental next step for HSV-1 is to approach and engage a cellular receptor for entry in its target keratinocytes. Previous *ex vivo* infection studies using epidermal sheets from HVEM- or nectin-1-deficient mice have identified nectin-1 as the major receptor while HVEM has a less efficient, more limited role (Petermann et al., 2015b). This is in line with our human skin results in De La Cruz et al. (2021) which demonstrated the presence nectin-1 and HVEM on epidermal keratinocytes, suggesting that both can serve as receptors, with nectin-1 possessing altogether higher levels. As a cell-cell adhesion molecule, nectin-1 is involved in the formation of AJs which should be located just underneath TJs (Takai et al., 2008). A continually intriguing part in skin physiology and pathology is that although TJs and AJs function to prevent viruses from crossing the epithelial barrier, certain viruses (HSV included) remarkably exploit components of these junctional structures as entry receptors. While some viruses developed strategies to directly alter cellular junctions to reach their receptors, HSV-1 is commonly known to opportunistically rely on conditions that lead to barrier defects for facilitated access to its cellular receptors (Torres-Flores and Arias, 2015). Here, we addressed the intriguing question on how HSV-1 is able to approach nectin-1 in tissue and what role functional and impaired epidermal barriers could play in restricting or facilitating this access (De La Cruz et al., to be submitted).

4.3.1 Nectin-1 redistribution during epidermal barrier formation

Studies have shown that the functional assembly and maintenance of TJs are facilitated by formation of AJs (reviewed in Irie et al., 2004). Thus, to relate the localization of nectin-1 and formation of TJs with HSV-1 susceptibility of human epidermis, we employed stratified cultures. Previous studies in our lab using stratified cultures based on HaCaT cells and primary murine keratinocytes have shown that formation of TJs inhibits HSV-1 viral entry (Rahn et al., 2017). To augment these findings and address whether the distribution and accessibility of nectin-1 changes during the process of differentiation, we performed infection studies of stratified cultures based on N/TERT keratinocytes in De La Cruz et al. (to be submitted). In undifferentiated conditions where TJ components occludin and ZO-1 were either absent or

diffused, nectin-1 was found in both the apical and basolateral membranes. This correlated with a high number of infected cells indicating that nectin-1 was readily accessible for HSV-1 in undifferentiated N/TERT keratinocytes. In contrast, after 8 days of differentiation which showed a more continuous distribution of TJs as visualized by staining of the TJ components, only single apical infected cells were found in some areas. Under the same culture conditions, nectin-1 was found enriched in the lateral surfaces of the large apical cells, however, given the low number of infected cells it can be surmised that the presence of mature tight junctions restricted viral access to the receptor. Viral inaccessibility in differentiated keratinocytes gives the first hint that nectin-1 is spatially distributed underneath mature TJs (De La Cruz et al., to be submitted).

To further investigate nectin-1 distribution in relation to HSV-1 susceptibility of various epidermal layers during TJ and SC barrier formation, human epidermal equivalents (3D cultures) were employed in De La Cruz et al. (to be submitted). We first investigated human epidermal equivalents generated with N/TERT cells as they have been reported to be similar to those made using primary human keratinocytes in terms of morphology, SC permeability, and expression of epidermal differentiation markers (Smits et al., 2017). HSV-1 infection studies and penetration of fluorescently-labelled latex beads in N/TERT 3D cultures support a negative correlation between functional barrier formation and viral/particle penetration. A complete block of infection was found after 8 days of exposure to the air-liquid interface which constitutes a fully developed and stratified 3D epidermal culture with functional TJ and SC barriers (De La Cruz et al., to be submitted).

TJs and SC may have a plausible, inter-dependent relationship in the formation and maintenance of a functional epidermal barrier (Haftek et al., 2022). Concomitantly, this makes it difficult to assess the contribution of both barriers in restricting HSV-1 entry. Thus, to dissect the barriers and assess the contribution of TJ formation alone in nectin-1 distribution, we limited our focus on earlier days of 3D culture development which preceded the formation of the SC (De La Cruz et al., to be submitted). In these studies, we sought to more closely resemble *in vivo* epidermal homeostasis and thus generated 3D cultures using primary human keratinocytes. While undifferentiated primary human keratinocytes were well infected prior to lifting to the air-liquid interface (Day 0), we observed a large drop in infection a mere 2

days after which corresponded to emerging TJ formation. The sudden drop in infected cells may be attributed to the localization of nectin-1 in relation to the TJs. While the receptor is very well expressed on the lateral membranes of basal keratinocytes, nectin-1 stainings on suprabasal cells are less distinct and appear to be located underneath lateral claudin-1 stainings. This suggests that early stage TJ formation already provides a barrier against HSV-1 invasion, although the barrier is still leaky as infection is not fully prevented. The earliest indication of SC formation found at Day 4 is accompanied by even less infected cells. However, since Day 4 is also accompanied by more mature TJs which may therefore further inhibit access to nectin-1, it is more likely that functional TJs play a larger role in restricting HSV-1 invasion than the SC at this time point. This is additionally supported by the results of the infection studies in stratified cultures since, while these models lack the capability of producing a SC, susceptibility to HSV-1 is prevented by TJ formation alone (De La Cruz et al., to be submitted).

Fully developed epidermal 3D cultures (Day 8) revealed that while nectin-1 colocalizes with E-cadherin at AJs in the epidermal layers, nectin-1 also colocalizes with claudin-1 in the granular layers except for the uppermost SG1 layer where only the TJ was detected (De La Cruz et al., to be submitted). This indicates that while nectin-1 is present on keratinocytes throughout the epidermis, HSV-1 is prevented by the presence of functional TJs (and perhaps the SC) from accessing the receptor. As this most likely represents *in vivo* conditions in nonpathological skin, the question arises as to how pathological skin conditions characterized by epidermal barrier defects influence the localization and accessibility of nectin-1 for the virus.

4.3.2 Nectin-1 accessibility under pathological skin conditions

In De La Cruz et al. (to be submitted), nectin-1 distribution and accessibility is addressed under pathological skin conditions. Previously, in Möckel et al. (2022) we found that Th2 cytokine-induced modifications in human skin after stimulation with IL-4 and IL-13 facilitated HSV-1 penetration. While stainings of the SC component filaggrin did not exhibit obvious changes, stainings of the TJ proteins claudin-1, occludin, and ZO-1 were all either redistributed or diffused in IL-stimulated compared to mock-treated samples. A previous study found that IL-

4 and IL-13-treatment of human epidermal equivalents induced an AD-like phenotype in the 3D cultures (Kamsteeg et al., 2011). Thus, in De La Cruz et al. (to be submitted) we explored whether IL-stimulation of epidermal 3D cultures during barrier development would result in changes to the epidermal barrier that could enhance HSV-1 invasion. While IL-induced N/TERT 3D cultures (Day 8) demonstrated weaker stainings of SC and TJ barrier components and facilitated penetration of latex beads, HSV-1 invasion was only very rarely found in the basal layer. As nectin-1 staining pattern after IL-stimulation led to a more punctate staining suggesting some IL-induced effects on intercellular junctions, it is unclear whether IL-stimulation rendered the receptor unusable or if epidermal barrier changes in the fully developed 3D cultures were simply not sufficient for HSV-1 invasion. When IL-stimulation and HSV-1 infection was restricted to the early days of 3D culture development of primary human keratinocytes, we observed enhanced infection of IL-treated samples only while cornification was still absent. This suggests that the Th2 cytokines mostly target the TJs rather than the SC barrier which is in agreement with our results of IL-induced human skin explants.

Since TJ barrier function may be linked to AJ formation, we analyzed the distribution of both junctional structures in human skin after IL-induction in De La Cruz et al. (to be submitted). AJs can be found at the dermoepidermal junction (DEJ) as well as in cell-cell contact regions in all viable layers of the epidermis albeit in varying degrees (Kaiser et al., 1993; Tunggal et al., 2005). TJ proteins colocalize at functional barrier-forming TJ structures in the upper granular layer, however, they are not restricted to this area and can even be found in other epidermal layers indicating that the proteins play other roles in the epidermis (reviewed in Bäsler and Brandner, 2017). AJ stainings of IL-induced skin in De La Cruz et al. (to be submitted) revealed that while E-cadherin remained evenly distributed throughout the epidermal layers, nectin-1 was more strongly expressed in the suprabasal and granular layers. As TJs are also redistributed after IL-induction, this suggests a putative role for nectin-1 in modulating TJ formation. While nectin-1 remained localized underneath ZO-1 in both IL- and mock-treated skin, co-staining of nectin-1 and claudin-1 in the upper granular layers demonstrated an increase in colocalization as well as more punctate staining after IL-treatment. Studies have demonstrated that TJ proteins can be involved in proliferation, differentiation, adhesion, and apoptosis depending on which epidermal layer it is expressed (reviewed in Kirschner and Brandner, 2012). In fact, TJ remnants of claudin-1 can be detected

on lateral membranes of lower SC layers and are suggested to form a barrier against degrading enzymes to protect corneodesmosomes from degradation (Haftek et al., 2011; Igawa et al., 2011). Whether the more punctated stainings of claudin-1 and nectin-1 found after IL-induction correspond to SC impairment and thus better access to nectin-1 is still speculative. Nevertheless, redistributed TJ stainings upon IL-induction of skin suggest an impaired TJ barrier which could grant HSV-1 better access to nectin-1 in underlying layers.

As we have previously demonstrated in Möckel et al. (2022) that lesional AD skin characterized by impaired barrier functions predisposes the epidermis for HSV-1 invasion, we examined nectin-1 distribution and localization in AD skin samples and further analyzed whether TJ redistribution influences the accessibility of the receptor (De La Cruz et al., to be submitted). The dysfunctional skin barrier of AD skin is associated with epidermal growth and differentiation defects (Guttman-Yassky et al., 2009). Thus, in De La Cruz et al. (to be submitted) we investigated whether alterations in epidermal differentiation influences the distribution of AJs in the characteristically thickened epidermis of AD skin. Studies have shown that nectin-1 is involved in the formation of cadherin-based AJs in keratinocytes (Tanaka et al., 2003). While evidence for a direct linkage between nectin-1 and E-cadherin themselves have been found, interactions between their cytoplasmic binding partners afadin and α-catenin have been described (Hoshino et al., 2005). Indeed E-cadherin and nectin-1 demonstrated colocalized stainings and were evenly distributed throughout the epidermal layers of both control skin and AD skin samples. While the receptor was found throughout the epidermal layers, variations in nectin-1 staining intensity between the AD samples was observed which is reflective of variable nectin-1 transcript levels previously described in Möckel et al. (2022). Whether less intense stainings of nectin-1 corresponds to disturbed AJ formation is still speculative. As AJ assembly may be linked to functional TJ, we next explored how the impaired TJ barriers of AD skin might influence nectin-1 distribution. In nonpathological skin, we found nectin-1 distinctly underneath ZO-1 indicating that the functional TJ barrier inhibits HSV-1 invasion from the skin surface. Indeed, analysis of the two AD skin samples exhibit a marked redistribution of ZO-1 while nectin-1 remained present throughout the epidermal layers. In contrast to the results from IL-induced skin, increased redistribution of nectin-1 to the granular layers was not found in AD skin which suggests that IL-induced redistribution of nectin-1 does not mimic the receptor's localization in AD skin.

Indeed, dysfunctional epidermal barriers in AD skin is grounded on many different factors (Czarnowicki et al., 2017; Nakatsuji et al., 2017; De Benedetto et al., 2011). Still, regardless of which factor(s) lead to barrier impairments of the lesional AD skin samples, our results suggest that the dysfunctional barriers enable virus access to nectin-1. Taken together, our findings reveal that functional TJs restrict HSV-1 access to nectin-1 in epidermal keratinocytes while barrier impairment in pathological skin conditions enable easier access for HSV-1 in skin invasion.

References

Aberle H, Schwartz H, Kemler R. 1996. Cadherin-catenin complex: protein interactions and their implications for cadherin function. J Cell Biochem 61 (4):514-523.

Armengot-Carbo M, Hernández-Martín Á, Torrelo A. 2015. The role of filaggrin in the skin barrier and disease development. Actas Dermosifiliogr 106 (2):86-95.

Bäsler K, Brandner JM. Tight junctions in skin inflammation. 2017. Pflugers Arch 469(1):3-14.

Brady RC, Bernstein DI. 2004. Treatment of herpes simplex virus infections. Antivir Res 61 (2):73–81.

Brandner JM, Zorn-Kruppa M, Yoshida T, Moll I, Beck LA, De Benedetto A. 2015. Epidermal tight junctions in health and disease. Tissue Barriers 3 (1-2):e974451.

Beck LA, Boguniewicz M, Hata T, Schneider LC, Hanifin J, Gallo R, Paller AS, Lieff S, Reese J, Zaccaro D, Milgrom H, Barnes KC, Leung DYM. 2009. Phenotype of atopic dermatitis subjects with a history of eczema herpeticum. J Allergy Clin Immunol 124 (2):260-269.e2697.

Beck LA, Cork MJ, Amagai M, De Benedetto A, Kabashima K, Hamilton JD, Rossi AB. 2022. Type 2 Inflammation Contributes to Skin Barrier Dysfunction in Atopic Dermatitis. JID Innov 2 (5):100131.

Becker TM. 1992. Herpes gladiatorum: a growing problem in sports medicine. Cutis 50 (2):150–152.

Brown SJ, McLean WH. One remarkable molecule: filaggrin. 2012. J Invest Dermatol 132 (3 Pt 2):751-762.

Bussmann C, Peng WM, Bieber T, Novak N. 2008. Molecular pathogenesis and clinical implications of eczema herpeticum. *Expert Rev Mol Med* 10:e21.

Campadelli-Fiume G, Arsenakis M, Farabegoli F, Roizman B. 1988. Entry of herpes simplex virus 1 in BJ cells that constitutively express viral glycoprotein D is by endocytosis and results in degradation of the virus. J Virol 62:159–167.

Campadelli-Fiume G, Menotti L. 2007. Human Herpesviruses: Biology, Therapy, and Immuniphrophylaxis: Entry of alphaherpesviruses into the cell. Cambridge University Press, Cambridge.

Clement C, Tiwari V, Scanlan PM, Valyi-Nagy T, Yue BYJT, Shukla D. 2006. A novel role for phagocytosis-like uptake in herpes simplex virus entry. J Cell Biol 174:1009–1021.

Clements JB, Watson RJ, Wilkie NM. 1977. Temporal regulation of herpes simplex virus type 1 transcription: location of transcripts on the viral genome. Cell 12 (1):75–285.

Cocchi F, Lopez M, Dubreuil P, Campadelli Fiume G, Menotti L. 2001. Chimeric nectin1-poliovirus receptor molecules identify a nectin1 region functional in herpes simplex virus entry. J Virol 75(17):7987-94.

Commisso C, Flinn RJ, Bar-Sagi D. 2014. Determining the macropinocytic index of cells through a quantitative image-based assay. Nat Protoc 9:182–192.

Connolly SA, Jardetzky TS, Longnecker R. 2021. The structural basis of herpesvirus entry. Nat. Rev. Microbiol 19:10–121.

Czarnowicki T, Krueger JG, Guttman-Yassky E. 2017. Novel concepts of prevention and treatment of atopic dermatitis through barrier and immune manipulations with implications for the atopic march. The Journal of allergy and clinical immunology 139 (6):1723–1734.

Damour A, Garcia M, Seneschal J, Lévêque N, Bodet C. 2020. Eczema Herpeticum: Clinical and Pathophysiological Aspects. Clin Rev Allergy Immunol 59(1):1-18.

Danso MO, van Drongelen V, Mulder A, van Esch J, Scott H, van Smeden J, El Ghalbzouri A, Bouwstra JA. 2014. TNF-α and Th2 cytokines induce atopic dermatitis-like features on epidermal differentiation proteins and stratum corneum lipids in human skin equivalents. J Invest Dermatol 134:1941-1950.

De Benedetto A, Rafaels NM, McGirt LY, Ivanov AI, Georas SN, Cheadle C, Berger AE, Zhang K, Vidyasagar S, Yoshida T, Boguniewicz M, Hata T, Schneider LC, Hanifin JM, Gallo RL, Novak N, Weidinger S, Beaty TH, Leung DY, Barnes KC, Beck LA. 2011. Tight junction defects in patients with atopic dermatitis. The Journal of allergy and clinical immunology 127 (3):773-86.e1-7.

De La Cruz N, Knebel-Mörsdorf D. 2020. Endocytic Internalization of Herpes Simplex Virus 1 in Human Keratinocytes at Low Temperature. J Virol 95 (4):e02195-20.

De La Cruz NC, Möckel M, Wirtz L, Sunaoglu K, Malter W, Zinser M, Knebel-Mörsdorf D. 2021. *Ex Vivo* Infection of Human Skin with Herpes Simplex Virus 1 Reveals Mechanical Wounds as Insufficient Entry Portals via the Skin Surface. J Virol 95(21):e0133821.

De La Cruz NC, Möckel M, Wirtz L, Knebel-Mörsdorf D. 2022. Ex vivo Human Skin Infection with Herpes Simplex Virus 1. Bio Protoc 12 (9):e4411.

Devadas D, Koithan T, Diestel R, Prank U, Sodeik B, D.hner K. 2014. Herpes simplex virus internalization into epithelial cells requires Na/H exchangers and p21-activated kinases but neither clathrin- nor caveolin-mediated endocytosis. J Virol 88:13378 –13395.

Di Giovine P, Settembre EC, Bhargava AK, Luftig MA, Lou H, Cohen GH, Eisenberg RJ, Krummenacher C, Carfi A. 2011. Structure of Herpes Simplex Virus Glycoprotein D Bound to the Human Receptor Nectin-1. PLOS Pathogens 7(9): e1002277.

Driskell RR, Lichtenberger BM, Hoste E, Kretzschmar K, Simons BD, Charalambous M, Ferron SR, Herault Y, Pavlovic G, Ferguson-Smith AC, Watt FM. 2013. Distinct fibroblast lineages determine dermal architecture in skin development and repair. Nature 504 (7479):277-281.

Eberlé F, Dubreuil P, Mattei MG, Devilard E, Lopez M. 1995. The human PRR2 gene, related to the human poliovirus receptor gene (PVR), is the true homolog of the murine MPH gene. Gene 159:267–72

Eckert RL, Sturniolo MT, Broome AM, Ruse M, Rorke EA. 2005. Transglutaminase function in epidermis. J Invest Dermatol 124(3):481-492.

Eisenberg RJ, Atanasiu D, Cairns TM, Gallagher JR, Krummenacher C, Cohen GH. 2012. Herpes Virus Fusion and Entry: A Story with Many Characters. Viruses 4 (5):800-832.

Elias PM. 1983. Epidermal lipids, barrier function, and desquamation. The Journal of investigative dermatology 80:44s-9s.

Epstein MA, Hummeler K, Berkaloff A. 1964. The entry and distribution of herpes virus and colloidal gold in HeLa cells after contact in suspension. J Exp Med 119:291–301.

Everett RD, Freeman P, Saitoh H, Dasso M, Orr A, Kathoria M, and Parkinson J. 1998. The disruption of ND10 during herpes simplex virus infection correlates with the Vmw110- and proteasome-dependent loss of several PML isoforms. J Virol 72:6581–6591.

Fatahzadeh M, Schwartz RA. 2007. Human herpes simplex virus infections: epidemiology, pathogenesis, symptomatology, diagnosis, and management. J Am Acad Dermatol 57 (5):737–766

Feldmeyer L, Huber M, Fellmann F, Beckmann JS, Frenk E, Hohl D. 2006. Confirmation of the origin of NISCH syndrome. Hum Mutat 27 (5):408-410.

Foley FD, Greenawald KA, Nash G, Pruitt BA. 1970. Herpesvirus infection in burned patients. The New England journal of medicine 282 (12):652–656.

Fuchs E. 2008. Skin stem cells: rising to the surface. J Cell Biol 180:273–284.

Fuchs E, Cleveland DW. 1998. A structural scaffolding of intermediate filaments in health and disease. Science 279 (5350):514–519.

Furuse M, Fujita K, Hiiragi T, Fujimoto K, Tsukita S. 1998. Claudin-1 and -2: novel integral membrane proteins localizing at tight junctions with no sequence similarity to occludin. J Cell Biol 141 (7):1539-50.

Furuse M, Hirase T, Itoh M, Nagafuchi A, Yonemura S, Tsukita S, Tuskita S. 1993. Occludin: a novel integral membrane protein localizing at tight junctions. J Cell Biol 123 (6 Pt 2):1777-1788.

Furuse M, Hata M, Furuse K, Yoshida Y, Haratake A, Sugitani Y, Noda T, Kubo A, Tsukita S. 2002. Claudin-based tight junctions are crucial for the mammalian epidermal barrier: a lesson from claudin-1-deficient mice. J Cell Biol 156 (6):1099-1111.

Geraghty RJ, Krummenacher C, Cohen GH, Eisenberg RJ, Spear PG. 1998. Entry of alphaherpesviruses mediated by poliovirus receptor-related protein 1 and poliovirus receptor. Science 280:1618–20

Gianni T, Campadelli-Fiume G, Menotti L. 2004. Entry of herpes simplex virus mediated by chimeric forms of nectin1 retargeted to endosomes or to lipid rafts occurs through acidic endosomes. J Virol 78 (22):12268–12276.

Giustizieri ML, Mascia F, Frezzolini A, De Pità O, Chinni LM, Giannett A, Girolomoni G, Pastore S. 2001. Keratinocytes from patients with atopic dermatitis and psoriasis show a distinct chemokine production profile in response to T cell-derived cytokines. J Allergy Clin Immunol 107 (5):871-877.

Gruber R, Bornchen C, Rose K, Daubmann A, Volksdorf T, Wladykowski E, Vidal YSS, Peters EM, Danso M, Bouwstra JA, Hennies HC, Moll I, Schmuth M, Brandner JM. 2015. Diverse regulation of claudin-1 and claudin-4 in atopic dermatitis. Am J Pathol 185:2777–2789

Grünewald K, Desai P, Winkler DC, Heymann JB, Belnap DM, Baumeister W, Steven AC. 2003. Three-dimensional structure of herpes simplex virus from cryo-electron tomography. Science 302:1396–1398.

Guttman-Yassky E, Suárez-Fariñas M, Chiricozzi A, Nograles KE, Shemer A, Fuentes-Duculan J, Cardinale I, Lin P, Bergman R, Bowcock AM, Krueger JG. 2009. Broad defects in epidermal cornification in atopic dermatitis identified through genomic analysis. J Allergy Clin Immunol 124:1235-1244.e58.

Hadj-Rabia S, Baala L, Vabres P, Hamel-Teillac D, Jacquemin E, Fabre M, Lyonnet S, De Prost Y, Munnich A, Hadchouel M, Smahi A. 2004. Claudin-1 gene mutations in neonatal sclerosing cholangitis

associated with ichthyosis: a tight junction disease [published correction appears in Gastroenterology. 2005. Feb 128(2):524]. Gastroenterology 127 (5):1386-1390.

Haftek M, Callejon S, Sandjeu Y, Padois K, Falson F, Pirot F, Portes P, Demarne F, Jannin V. 2011. Compartmentalization of the human stratum corneum by persistent tight junction-like structures. Exp Dermatol 20 (8):617-621.

Haftek M, Oji V, Feldmeyer L, Hohl D, Hadj-Rabia S, Abdayem R. 2022. The Fate of Epidermal Tight Junctions in the stratum corneum: Their Involvement in the Regulation of Desquamation and Phenotypic Expression of Certain Skin Conditions. Int J Mol Sci 23 (13):7486.

Harn HI, Ogawa R, Hsu CK, Hughes MW, Tang MJ, Chuong CM. 2019. The tension biology of wound healing. Exp Dermatol 28 (4):464-471.

Hamid Q, Naseer T, Minshall EM, Song YL, Boguniewicz M, Leung DY. 1996. In vivo expression of IL-12 and IL-13 in atopic dermatitis. J Allergy Clin Immunol 98(1):225-231.

Heming JD, Conway JF, Homa FL. Herpesvirus Capsid Assembly and DNA Packaging. 2017. Adv Anat Embryol Cell Biol 223:119-142.

Herold BC, Visalli RJ, Susmarski N, Brandt CR, Spear PG. 1994. Glycoprotein C-independent binding of herpes simplex virus to cells requires cell surface heparan sulphate and glycoprotein B. J Gen Virol 75:1211–1222.

Hilterbrand AT, Heldwein EE. 2019. Go go gadget glycoprotein!: HSV-1 draws on its sizeable glycoprotein tool kit to customize its diverse entry routes. PLoS Pathog. 15:e1007660.

Holmes IH, Watson DH. 1963. An electron microscope study of the attachment and penetration of herpes virus in BHK21 cells. Virology 21: 112–123.

Homey B, Steinhoff M, Ruzicka T, Leung DY. 2006. Cytokines and chemokines orchestrate atopic skin inflammation. J Allergy Clin Immunol 118 (1):178-189.

Honess RW, Roizman B. 1974. Regulation of herpesvirus macromolecular synthesis. I. Cascade regulation of the synthesis of three groups of viral proteins. J Virol 14 (1):8–19.

Hönzke S, Wallmeyer L, Ostrowski A, Radbruch M, Mundhenk L, Schäfer-Korting M, Hedtrich S. 2016. Influence of Th2 Cytokines on the Cornified Envelope, Tight Junction Proteins, and ß-Defensins in Filaggrin-Deficient Skin Equivalents. J Invest Dermatol 136 (3):631-639.

Hoshino T, Sakisaka T, Baba T, Yamada T, Kimura T, Takai Y. 2005. Regulation of E-cadherin endocytosis by nectin through afadin, Rap1, and p120ctn. J Biol Chem 280 (25):24095-24103.

Huber MT, Wisner TW, Hegde NR, Goldsmith KA, Rauch DA, Roller RJ, Krummenacher C, Eisenberg RJ, Cohen GH, Johnson DC. 2001. Herpes Simplex Virus with Highly Reduced gD Levels Can Efficiently Enter and Spread between Human Keratinocytes. J Virol 75: 10309–10318.

Igawa S, Kishibe M, Murakami M, Honma M, Takahashi H, Iizuka H, Ishida-Yamamoto A. 2011. Tight junctions in the stratum corneum explain spatial differences in corneodesmosome degradation. *Exp Dermatol* 20 (1):53-57.

Irie K, Shimizu K, Sakisaka T, Ikeda W, Takai Y. 2004. Roles and modes of action of nectins in cell-cell adhesion. Semin Cell Dev Biol 15(6):643-656.

Johnson DC, Huber MT. Directed egress of animal viruses promotes cell-to-cell spread. 2002. J Virol 76 (1):1–8.

Kaiser HW, Ness W, Jungblut I, Briggaman RA, Kreysel HW, O'Keefe EJ. 1993. Adherens junctions: demonstration in human epidermis. J Invest Dermatol 100 (2):180-185.

Kamsteeg M, Bergers M, de Boer R, Zeeuwen PLJM, Hato SV, Schalkwijk J, Tjabringa GS. 2011. Type 2 helper T-cell cytokines induce morphologic and molecular characteristics of atopic dermatitis in human skin equivalent. The American journal of pathology 178 (5):2091–2099.

Karasneh GA, Shukla D. 2011. Herpes simplex virus infects most cell types in vitro: Clues to its success. J Virol 8:481.

Kiehart DP. 1999. Wound healing: The power of the purse string. Curr Biol 9 (16):R602-R605. doi:10.1016/s0960-9822(99)80384-4

Kirschner N, Brandner JM. 2012. Barriers and more: functions of tight junction proteins in the skin. Ann N Y Acad Sci 1257:158-166.

Kobielak A, Boddupally K. 2014. Junctions and inflammation in the skin. Cell Commun Adhes 21 (3):141-147.

Koyama AH, Uchida T. 1987. The mode of entry of herpes simplex virustype 1 into Vero cells. Microbiol Immunol 31:123–130.

Krummenacher C, Baribaud F, Ponce De Leon M, Baribaud I, Whitbeck JC, Xu R, Cohen GH, Eisenberg RJ. 2004. Comparative usage of herpesvirus entry mediator A and nectin-1 by laboratory strains and clinical isolates of herpes simplex virus. Virology 322:286–299.

Krummenacher C, Carfí A, Eisenberg RJ, Cohen GH. 2013. Entry of herpesviruses into cells: the enigma variations. Adv Exp Med Biol 790:178-195.

Langan SM, Williams HC. 2019. Clinical Features and Diagnostic Criteria of Atopic Dermatitis. In: Peter Hoeger, Veronica Kinsler, Albert Yan, John Harper, Arnold Oranje, Christine Bodemer et al. (editors): Harper's Textbook of Pediatric Dermatology: Wiley. pp193–211.

Larrick JW, Enns C, Raubitschek A, Weintraub H. 1985. Receptor mediated endocytosis of human transferrin and its cell surface receptor. J Cell Physiol 124:283–287.

Lavker RM. 1976. Membrane coating granules: The fate of the discharged lamellae. Journal of Ultrastructure Research 55 (1):79–86.

Lippincott-Schwartz J, Roberts TH, Hirschberg K. 2000. Secretory protein trafficking and organelle dynamics in living cells. Annu Rev Cell Dev Biol 16:557–589.

Lycke E, Hamark B, Johansson M, Krotochwil A, Lycke J, Svennerholm B. 1988. Herpes simplex virus infection of the human sensory neuron. Anelectron microscopy study. Arch Virol 101:87–104.

Mateo M, Generous A, Sinn PL, Cattaneo R. 2015. Connections matter--how viruses use cell–cell adhesion components. J Cell Sci 128 (3):431-439.

Matsui T, Amagai M. 2015. Dissecting the formation, structure and barrier function of the stratum corneum [published correction appears in Int Immunol. 2017 May 1;29(5):243-244]. Int Immunol 27 (6):269-280.

May RC, Machesky LM. 2001. Phagocytosis and the actin cytoskeleton. J Cell Sci 114:1061–1077.

Mayor S, Pagano RE. 2007. Pathways of clathrin-independent endocytosis. Nat Rev Mol Cell Biol 8 (8):603-12.

McAleer MA, Irvine AD. 2013. The multifunctional role of filaggrin in allergic skin disease. J Allergy Clin Immunol 131 (2):280-291.

Mehrel T, Hohl D, Rothnagel JA, Longley MA, Bundman D, Cheng C, Lichti U, Bisher ME, Steven AC, Steinert PM, Yuspa SH, Roop DR. 1990. Identification of a major keratinocyte cell envelope protein, loricrin. Cell 61: 1103–1112.

Milne RSB, Nicola AV, Whitbeck JC, Eisenberg RJ, Cohen GH. 2005. Glycoprotein D receptor-dependent, low-pH-independent endocytic entry of herpes simplex virus type 1. J Virol 79 (11):6655–6663.

Modrow S, Falke D, Truyen U. 1997. Molekulare Virologie. Eine Einführung für Biologen und Mediziner. Spektrum Akademischer Verlag, Heidelberg, DE.

Möckel M, De La Cruz NC, Rübsam M, Wirtz L, Tantcheva-Poor I, Malter W, Zinser M, Bieber T, Knebel-Mörsdorf D. 2022. Herpes Simplex Virus 1 Can Bypass Impaired Epidermal Barriers upon *Ex Vivo* Infection of Skin from Atopic Dermatitis Patients. J Virol 96 (17):e0086422.

Morgan C, Rose HM, Mednis B. 1968. Electron microscopy of herpessimplex virus. I. Entry. J Virol 2:507–516.29.

Morrison ME, Racaniello VR. 1992. Molecular cloning and expression of a murine homolog of the human poliovirus receptor gene. J Virol 66:2807–13

Nakatsuji T, Chen TH, Narala S, Chun KA, Two AM, Yun T, Shafiq F, Kotol PF, Bouslimani A, Melnik AV, Latif H, Kim JN, Lockhart A, Artis K, David G, Taylor P, Streib J, Dorrestein PC, Grier A, Gill SR, Zengler K, Hata TR, Leung DYM, Gallo RL. 2017. Antimicrobials from human skin commensal bacteria protect against Staphylococcus aureus and are deficient in atopic dermatitis. Science translational medicine 9 (378).

Nicola AV, Straus SE. 2004. Cellular and viral requirements for rapid endocytic entry of herpes simplex virus. J Virol 78:7508-7517.

Nicola AV, Hou J, Major EO, Straus SE. 2005. Herpes simplex virus type 1 enters human epidermal keratinocytes, but not neurons, via a pH-dependent endocytic pathway. J Virol 79:7609–7616.

Niessen CM. 2007. Tight junctions/adherens junctions: basic structure and function. J Invest Dermatol 127(11):2525-2532.

Oh MJ, Akhtar J, Desai P, Shukla D. 2010. A role for heparan sulfate in viral surfing. *Biochemical and biophysical research communications* 391 (1):176–181.

Ojala PM, Sodeik B, Ebersold MW, Kutay U, Helenius A. 2000. Herpes simplex virus type 1 entry into host cells: reconstitution of capsid binding and uncoating at the nuclear pore complex in vitro. Molecular and cellular biology 20 (13):4922–4931.

Paladino P, Collins SE, Mossman KL. 2010. Cellular localization of the herpes simplex virus ICP0 protein dictates its ability to block IRF3-mediated innate immune responses. PloS One 5:e10428.

Petermann P, Haase I, Knebel-Mörsdorf D. 2009. Impact of Rac1 and Cdc42 signaling during early herpes simplex virus type 1 infection of keratinocytes. J Virol 83:9759 –9772.

Petermann P, Rahn E, Thier K, Hsu MJ, Rixon FJ, Kopp SJ, Knebel-Mörsdorf D. 2015a. Role of Nectin-1 and Herpesvirus Entry Mediator as Cellular Receptors for Herpes Simplex Virus 1 on Primary Murine Dermal Fibroblasts. Journal Virol 89 (18):9407–9416.

Petermann P, Thier K, Rahn E, Rixon FJ, Bloch W, Özcelik S, Krummenacher C, Barron MJ, Dixon MJ, Scheu S, Pfeffer K, KnebelMörsdorf D. 2015b. Entry mechanisms of herpes simplex virus 1 into murine epidermis: involvement of nectin-1 and herpesvirus entry mediator as cellular receptors. J Virol 89 (1):262–274.

Pilling A, Rosenberg MF, Willis SH, Jäger J, Cohen GH, Eisenberg RJ, Meredith DM, Holzenburg A. 1999. Three-dimensional structure of herpes simplex virus type 1 glycoprotein D at 2.4-nanometer resolution. Journal of virology, 73(9), 7830–7834.Dermal Fibroblasts. Journal of virology 89 (18):9407–9416.

Proksch E, Brandner JM, Jensen JM. 2008. The skin: an indispensable barrier. Experimental dermatology 17 (12):1063–1072.

Rahn E, Petermann P, Hsu MJ, Rixon FJ, Knebel-Mörsdorf D. 2011. Entry pathways of herpes simplex virus type 1 into human keratinocytes are dynamin- and cholesterol-dependent. PloS one 6 (10):e25464.

Rahn E, Thier K, Petermann P, Knebel-Mörsdorf D. 2015a. Ex vivo infection of murine epidermis with herpes simplex virus type 1. J Vis Exp 102: e53046

Rahn E, Petermann P, Thier K, Bloch W, Morgner J, Wickström SA, Knebel-Mörsdorf D. 2015b. Invasion of herpes simplex virus type 1 into murine epidermis: an ex vivo infection study. J Invest Dermatol 135:3009–3016.

Rahn E, Thier K, Petermann P, Rübsam M, Staeheli P, Iden S, Niessen CM, Knebel-Mörsdorf D. 2017. Epithelial Barriers in Murine Skin during Herpes Simplex Virus 1 Infection: The Role of Tight Junction Formation. The Journal of investigative dermatology 137 (4):884–893.

Rice RH, Green H. 1979. Presence in human epidermal cells of a soluble protein precursor of the cross-linked envelope: Activation of the cross-linking by calcium ions. Cell 18: 681–694.

Richards S, Scott IR, Harding CR, Liddell JE, Powell GM, Curtis CG. 1988. Evidence for filaggrin as a component of the cell envelope of the newborn rat. Biochem. J. 253, 153-160.

Roizman B, Sears AE. 1993. Herpes simplex viruses and their replication, pp.11-68. In Roizman B, Whitley RJ, Lopez C. (ed), The Human Herpesviruses, Raven, New York.

Roizman B, Whitley RJ. 2013. An inquiry into the molecular basis of HSV latency and reactivation. Annu Rev Microbiol 67:355-374.

Sayers CL, Elliott G. 2016. Herpes simplex virus 1 enters human keratinocytes by a nectin-1-dependent, rapid plasma membrane fusion pathway that functions at low temperature. J Virol 90:10379–10389.

Samanta D, Almo SC. 2015. Nectin family of cell-adhesion molecules: structural and molecular aspects of function and specificity. Cell Mol Life Sci 72 (4):645-658.

Schelhaas M, Jansen M, Haase I, Knebel-Mörsdorf D. 2003. Herpes simplex virus type 1 exhibits a tropism for basal entry in polarized epithelial cells. The Journal of general virology 84 (9):2473–2484.

Schneeberger EE, Lynch RD. 2004. The tight junction: a multifunctional complex. Am J Physiol Cell Physiol 286(6):C1213-C1228.

Shenoy R, Mostow E, Cain G. 2015. Eczema herpeticum in a wrestler. Clinical journal of sport medicine: official journal of the Canadian Academy of Sport Medicine 25 (1):e18-9.

Sieczkarski SB, Whittaker GR. 2002. Dissecting virus entry via endocytosis. J. Gen. Virol.83:1535-1545.

Simpson SA, Manchak MD, Hager EJ, Krummenacher C, Whitbeck JC, Levin MJ, Freed CR, Wilcox CL, Cohen GH, Eisenberg RJ, Pizer LI. 2005. Nectin-1/HveC Mediates herpes simplex virus type 1 entry into primary human sensory neurons and fibroblasts. J Neurovirol 11: 208–218.

Simpson CL, Patel DM, Green KJ. 2011. Deconstructing the skin: cytoarchitectural determinants of epidermal morphogenesis. *Nature reviews. Molecular cell biology* 12 (9):565–580.

Singh M, Goodyear HM, Breuer J. 2020. Herpes simplex infections. In Hoeger P, Kinsler V, Yan A, Harper J, Oranje A, Bodemer C et al. (editors) 2020. Harper's Textbook of Pediatric Dermatology: Wiley.

Smith JD, de Harven E. 1974. Herpes simplex virus and humancytomegalovirus replication in WI-38 cells. II. An ultrastructural studyof viral penetration. J Virol 14:945–956.

Smith JS, Robinson NJ. 2002. Age-specific prevalence of infection with herpes simplex virus types 2 and 1: a global review. J Infect Dis 186(Supplement 1):S3–S28.

Smith MC, Boutell C, Davido DJ. 2011. HSV-1 ICP0: paving the way for viral replication. Future Virol 6:421– 429.

Smits JPH, Niehues H, Rikken G, van Vlijmen-Willems IMJJ, van de Zande GWHJF, Zeeuwen PLJM, Schalkwijk J, van den Bogaard EH. 2017. Immortalized N/TERT keratinocytes as an alternative cell source in 3D human epidermal models. Scientific reports 7 (1):11838.

Sodeik B, Ebersold MW, Helenius A. 1997. Microtubule-mediated transport of incoming herpes simplex virus 1 capsids to the nucleus. J Cell Biol 136(5):1007-21.

Sorrell JM, Caplan AI. Fibroblast heterogeneity: more than skin deep. 2004. J Cell Sci 117 (5):667-675.

Stenn KS, Link R, Moellmann G, Madri J, Kuklinska E. 1989. Dispase, a neutral protease from Bacillus polymyxa, is a powerful fibronectinase and type IV collagenase. J Invest Dermatol 93 (2):287-290.

Stern S, Herr W. 1991. The herpes simplex virus trans-activator VP16 recognizes the Oct-1 homeodomain: evidence for a homeodomain recognition subdomain. Genes Dev 5:2555–2566.

Steven AC, Steinert PM. 1994. Protein composition of cornified cell envelopes of epidermal keratinocytes. J Cell Sci 107 (Pt 2):693-700

Tachibana K, Nakanishi H, Mandai K, Ozaki K, Ikeda W, Yamamoto Y, Nagafuchi A, Tsukita S, Takai Y. 2000. Two cell adhesion molecules, nectin and cadherin, interact through their cytoplasmic domain-associated proteins. J Cell Biol 150(5):1161-1176.

Tajpara P, Mildner M, Schmidt R, Vierhapper M, Matiasek J, Popow-Kraupp T, Schuster C, Elbe-Bürger A. 2019. A preclinical model for studying herpes simplex virus infection. J Invest Dermatol 139:673–682.

Takahashi K, Nakanishi H, Miyahara M, Mandai K, Satoh K, Nishioka H, Aoki J, Nomoto A, Mizoguchi A, Takai Y. 1999. Nectin/PRR: an immunoglobulin-like cell adhesion molecule recruited to cadherin-based adherens junctions through interaction with afadin, a PDZ domain-containing protein. J. Cell Biol. 145:539–49

Takai Y, Nakanishi H. 2003. Nectin and afadin: novel organizers of intercellular junctions. J. Cell Sci.116:17-27.

Takai Y, Ikeda W, Ogita H, Rikitake Y. 2008. The immunoglobulin-like cell adhesion molecule nectin and its associated protein afadin. Annual review of cell and developmental biology 24:309–342.

Tanaka, Y., Nakanishi, H., Kakunaga, S., Okabe, N., Kawakatsu, T., Shimizu, K., & Takai, Y. 2003. Role of nectin in formation of E-cadherin-based adherens junctions in keratinocytes: analysis with the N-cadherin dominant negative mutant. Molecular biology of the cell, 14(4), 1597–1609.

Torres-Flores JM, Arias CF. 2015. Tight Junctions Go Viral! Viruses 7 (9):5145-54.

Tsukita S, Furuse M, Itoh M. 2001. Multifunctional strands in tight junctions Nat Rev Mol Cell Biol 4:285-293

Tunggal, J. A., Helfrich, I., Schmitz, A., Schwarz, H., Günzel, D., Fromm, M., Kemler, R., Krieg, T., & Niessen, C. M. 2005. E-cadherin is essential for in vivo epidermal barrier function by regulating tight junctions. The EMBO journal 24 (6):1146–1156.

Umeda K, Ikenouchi J, Katahira-Tayama S, Furuse K, Sasaki H, Nakayama M, Matsui T, Tsukita S, Furuse M, Tsukita S. 2006. ZO-1 and ZO-2 independently determine where claudins are polymerized in tight-junction strand formation. Cell 126 (4):741-754.

Warner MS, Geraghty RJ, Martinez WM, Montgomery RI, Whitbeck JC, Xu R, Eisenberg RJ, Cohen GH, Spear PG. 1998. A cell surface protein with herpesvirus entry activity (HveB) confers susceptibility to infection by mutants of herpes simplex virus type 1, herpes simplex virus type 2, and pseudorabies virus. Virology 246 (1):179–189.

Weeks BS, Ramchandran RS, Hopkins JJ, Friedman HM. 2000. Herpes simplex virus type-1 and -2 pathogenesis is restricted by the epidermal basement membrane. *Archives of virology* 145 (2):385–396.

Whitley RJ, Kimberlin DW, Roizman B. 1998. Herpes simplex viruses. Clin Infect *Dis* 26:541-555.

Wilson EK, Deweber K, Berry JW, Wilckens JH. 2013. Cutaneous infections in wrestlers. Sports health 5 (5):423–437.

Wirtz L, De La Cruz NC, Möckel M, Knebel-Mörsdorf D. 2022. Susceptibility of Human and Murine Dermal Fibroblasts to Herpes Simplex Virus 1 in the Absence and Presence of Extracellular Matrix. J Virol 96 (4):e0206821.

Wirtz L, Möckel M, Knebel-Mörsdorf D. 2020. Invasion of herpes simplex virus 1 into murine dermis: role of nectin-1 and herpesvirus entry mediator as cellular receptors during aging. J Virol 94:e02046-19.

WuDunn D, Spear PG. 1989. Initial interaction of herpes simplex virus with cells is binding to heparan sulfate. J Virol 63:52–58.

Zhang N, Yan J, Lu G, Guo Z, Fan Z, Wang J, Shi Y, Qi J, Gao GF. 2011. Binding of herpes simplex virus glycoprotein D to nectin-1 exploits host cell adhesion. Nat Commun 2:577

Abbreviations

°C	degree Celsius
3D	three-dimensional
AD	Atopic dermatitis
AJ	adherens junction
BHK-21	Baby hamster kidney fibroblasts
Ca^{2+}	calcium
CAM	cell adhesion molecule
CHO	Chinese hamster ovary
cldn-1	claudin-1
CPE	cytopathic effect
DEJ	dermoepidermal junction
DNA	deoxyribonucleic acid
E	early
e-cad	E-cadherin
ECM	extracellular matrix
EM	electron microscopy
et al.	et alia (and others)
F-actin	filamentous actin
Fig.	figure
FITC	fluorescein isothiocyanate
gC	glycoprotein C
gB	glycoprotein B
gD	glycoprotein D
gH	glycoprotein H
gL	glycoprotein L
HFFF2	Human Fetal Foreskin Fibroblast 2
HSV	herpes simplex virus
HSV-1	herpes simplex virus 1
HSV-2	herpes simplex virus 2
HveB	herpesvirus entry mediator B
HveC	herpesvirus entry mediator C
HVEM	herpesvirus entry mediator
ICP0	infected cell protein 0
IE	immediate-early
Ig	immunoglobulin

IHC	immunohistochemistry
IL	interleukin
IL-4	interleukin-4
IL-13	interleukin-13
IRF3	interferon regulatory factor 3
K	keratin
K1	keratin 1
K5	keratin 5
K10	keratin 10
K14	keratin 14
KO	knockout
L	late
nm	nanometer
NPC	nuclear pore complex
ocln	occludin
PDZ	post synaptic density protein, Drosophila disc large tumor suppressor, and zonula occludens-1 protein
PI	phosphoinositide
PM	plasma membrane
PML	promyelocytic leukemia
PRR	poliovirus receptor-related
RNA	ribonucleic acid
RNAP II	RNA polymerase II
SC	stratum corneum
TEM	transmission electron microscopy
Th2	T helper type 2
TJ	tight junction
UV	ultraviolet
ZO-1	zonula occludens 1
ZO-2	zonula occludens 2
α	alpha
β	beta

Acknowledgements

I would like to express my gratitude to my thesis supervisor, Prof. Dr. Dagmar Mörsdorf for the wonderful PhD project. I appreciate all the helpful advice, constructive criticism, and discussions that led me to grow as a researcher.

I would also like to thank Prof. Dr. Niels Gehring who has generously accepted the role of being my second advisor and reviewer of whom I am very appreciative for comments regarding my thesis.

Thank you to my former group members—Lisa Wirtz and Maureen Möckel for the fun memories in and outside the lab! I would also like to acknowledge my colleagues at the Center of Biochemistry as well as in Dermatology for input at our seminars.

Finally, I would like to thank my family—Mom and Dad, my sister Cristina, and my grandparents Papa and Mama for their loving encouragement from all the way across the world! And thank you to Arndt.

Erklärung

Hiermit versichere ich an Eides statt, dass ich die vorliegende Dissertation selbstständig und ohne die Benutzung anderer als der angegebenen Hilfsmittel und Literatur angefertigt habe. Alle Stellen, die wörtlich oder sinngemäß aus veröffentlichten und nicht veröffentlichten Werken dem Wortlaut oder dem Sinn nach entnommen wurden, sind als solche kenntlich gemacht. Ich versichere an Eides statt, dass diese Dissertation noch keiner anderen Fakultät oder Universität zur Prüfung vorgelegen hat; dass sie - abgesehen von unten angegebenen Teilpublikationen und eingebundenen Artikeln und Manuskripten - noch nicht veröffentlicht worden ist sowie, dass ich eine Veröffentlichung der Dissertation vor Abschluss der Promotion nicht ohne Genehmigung des Promotionsausschusses vornehmen werde. Die Bestimmungen dieser Ordnung sind mir bekannt. Darüber hinaus erkläre ich hiermit, dass ich die Ordnung zur Sicherung guter wissenschaftlicher Praxis und zum Umgang mit wissenschaftlichem Fehlverhalten der Universität zu Köln gelesen und sie bei der Durchführung der Dissertation zugrundeliegenden Arbeiten und der schriftlich verfassten Dissertation beachtet habe und verpflichte mich hiermit, die dort genannten Vorgaben bei allen wissenschaftlichen Tätigkeiten zu beachten und umzusetzen. Ich versichere, dass die eingereichte elektronische Fassung der eingereichten Druckfassung vollständig entspricht.

Teilpublikationen:

De La Cruz N, Knebel-Mörsdorf D. Endocytic Internalization of Herpes Simplex Virus 1 in Human Keratinocytes at Low Temperature. *J Virol*. 2020;95(4):e02195-20. doi:10.1128/JVI.02195-20

De La Cruz NC, Möckel M, Wirtz L, Sunaoglu K, Malter W, Zinser M, Knebel-Mörsdorf D. *Ex Vivo* Infection of Human Skin with Herpes Simplex Virus 1 Reveals Mechanical Wounds as Insufficient Entry Portals via the Skin Surface. *J Virol*. 2021;95(21):e0133821. doi:10.1128/JVI.01338-21

Möckel M, De La Cruz NC, Rübsam M, Wirtz L, Tantcheva-Poor I, Malter W, Zinser M, Bieber T, Knebel-Mörsdorf D. Herpes Simplex Virus 1 Can Bypass Impaired Epidermal Barriers upon *Ex Vivo* Infection of Skin from Atopic Dermatitis Patients. *J Virol*. 2022;96(17):e0086422. doi:10.1128/jvi.00864-22

De La Cruz NC, Möckel M, Niehues H, et al. *Ex Vivo* Infection of Human Skin Models with Herpes Simplex Virus 1: Accessibility of the Receptor Nectin-1 during Formation or Impairment of Epidermal Barriers Is Restricted by Tight Junctions. *J Virol*. 2023;97(6):e0026223. doi:10.1128/jvi.00262-23

Wirtz L, De La Cruz NC, Möckel M, Knebel-Mörsdorf D. Susceptibility of Human and Murine Dermal Fibroblasts to Herpes Simplex Virus 1 in the Absence and Presence of Extracellular Matrix. *J Virol*. 2022;96(4):e0206821. doi:10.1128/JVI.02068-21

De La Cruz NC, Möckel M, Wirtz L, Knebel-Mörsdorf D. *Ex vivo* Human Skin Infection with Herpes Simplex Virus 1. *Bio Protoc*. 2022;12(9):e4411. Published 2022 May 5. doi:10.21769/BioProtoc.4411

Köln, den 25.09.2023

Nydia Camille De La Cruz